UNIVERSITY OF OKLAHOMA

GRADUATE COLLEGE

TOTAL WATER LEVEL MODELING IN THE NORTH CAROLINA COASTAL PLAIN: COMPARING ADCIRC AND HEC-RAS

A THESIS

SUBMITTED TO THE GRADUATE FACULTY

in partial fulfillment of the requirements for the

Degree of

MASTER OF SCIENCE IN ENVIRONMENTAL ENGINEERING

By

SAMUEL BUSH
Norman, Oklahoma
2017

TOTAL WATER LEVEL MODELING IN THE NORTH CAROLINA COASTAL PLAIN: COMPARING ADCIRC AND HEC-RAS

A THESIS APPROVED FOR THE
SCHOOL OF CIVIL ENGINEERING AND ENVIRONMENTAL SCIENCE

BY

_____
Dr. Randall Kolar, Chair

_____
Dr. Kendra Dresback

_____
Dr. Yang Hong

ACKNOWLEDGEMENTS

I would like to express my gratitude to my committee for their patience, constructive criticism, and valuable advice in the development of this research. Special thanks are due to Dr. Dresback and Dr. Kolar for their assistance in understanding and using the ADCIRC model, and to Dr. Humberto Vergara for his guidance with HL-RDHM. I'd also like to thank my family for their constant love and support. Mom, your example is a guiding star. Finally, I thank CIMMS for their support, particularly Kodi Berry, and Kevin Kelleher, whose advice I tried my best not to forget.

TABLE OF CONTENTS

ACKNOWLEDGEMENTS ..... **IV**
TABLE OF CONTENTS ..... **V**
LIST OF TABLES ..... **VIII**
LIST OF FIGURES ..... **IX**
ABSTRACT ..... **XIII**
1. MOTIVATION FOR STUDY **1**
2. RATIONALE FOR THIS RESEARCH **4**
3. LITERATURE REVIEW **6**
FUNCTIONALITY OF ADCIRC 6
POTENTIAL OF HEC-RAS 7
PAIRED MODELS 9
4. HYPOTHESIS, OBJECTIVES, & GOAL **13**
HYPOTHESES 13
Hypothesis 1 ..... *13*
Hypothesis 2 ..... *13*
Hypothesis 3 ..... *13*
OBJECTIVES 14
GOALS 15
5. THEORY & GENERAL METHODS **16**
WHAT IS A MODEL? 16
HL-RDHM 17
SAC-SMA *17*
Channel Routing *18*
HL-RDHM in the Tar River Basin *22*
ADCIRC 24
General description of ADCIRC *24*
HEC-RAS 27
General Description of HEC-RAS *27*
COUPLINGS 31
Purpose of Coupling Schemes *34*
Hypothesis 1 –HEC-RAS Model Is As Accurate As ADCIRC Model *34*
Hypothesis 2A – HEC-RAS Accuracy Not Affected By ADCIRC Resolution *35*
Hypothesis 3 – HEC-RAS and Coarse ADCIRC Provides Results as Accurate as Fine ADCIRC *35*
COMPARISON METHODS 35
Nash-Sutcliffe Efficiency *35*
Standard Comparison Hydrograph *36*
6. SELECTING APPROPRIATE BOUNDARY CONDITIONS **39**
Nomenclature *39*
Upstream Boundary Conditions *39*
Downstream Boundary Conditions *40*
Initial reduction of redundant BC types *40*
Alternate Labels *42*
Performance at USGS Gauges *43*
Conclusions *49*
Future work *49*
7. HURRICANE IRENE **50**
FORCING AND VALIDATION STRATEGY 52
Boundary Conditions *52*
Upstream Boundary Condition – Tar River at Tarboro, NC *53*
Downstream Boundary Condition – Pamlico Sound at Washington, NC *54*
RIVER DOMAIN RESULTS 54

Gauge Station Results *55*
Gauge Peak Accuracy by Model *57*
Comparison of Results at Gauge Sites *60*
Comparison to High Water Marks *60*
Inundated Area *62*
Inundation Depth *65*
INUNDATION DEPTH COMPARISON – ADCIRC VS HEC-RAS 65
Area 1 – Upstream of NC 222 ..... *66*
Area 2 – Unnamed Meander Downstream of NC 222 ..... *67*
Area 3 – Greenville, West of Pitt-Greenville Airport *69*
Area 4 – Greenville Bridges *70*
Area 5 – Greenville Boulevard NE Crossing *72*
Area 6 – Downstream of Greenville *73*
Summary of HEC-RAS and ADCIRC Inundation Differences *74*
Comparison of Inundation Depths – HEC-RAS Forced with ADCIRC *75*
Summary of River vs. Riverless BCs *76*
Summary of Model Comparisons for Irene *76*

8. HURRICANE FLOYD 78
STORM DESCRIPTION 78
Pre-Storm Conditions *78*
Hurricane Track & Winds *79*
FORCING AND VALIDATION STRATEGY 79
Boundary Conditions *80*
Upstream Boundary Condition – Tar River at Tarboro, NC *80*
Downstream Boundary Condition – Pamlico Sound at Washington, NC *81*
RIVER DOMAIN RESULTS 81
Gauge Station Results *82*
Gauge Peak Accuracy by Model *82*
Inundated Area *85*
Summary of Model Comparisons for Floyd *89*

9. APRIL 2003 RAINFALL EVENT 90
STORM DESCRIPTION 90
Event Conditions *90*
FORCING AND VALIDATION STRATEGY 92
Boundary Conditions *93*
Upstream Boundary Condition – Tar River at Tarboro, NC *94*
Downstream Boundary Condition – Pamlico Sound at Washington, NC *94*
RIVER DOMAIN RESULTS 95
Gauge Station Results *95*
Gauge Peak Accuracy by Model *96*
Inundated Area *99*
SUMMARY OF MODEL COMPARISONS FOR APRIL, 2003 103

10. TIMING ADVANTAGES OF RIVERLESS VS. RIVER ADCIRC 104
INTRODUCTION 104
METHODS 104
Meshes used *104*
Coarse Mesh Description *104*
Fine Mesh Description *104*
Determination of Stable Timestep *105*
RESULTS & CONCLUSIONS 105

11. DISCUSSIONS AND FUTURE WORK 107
DISCUSSION OF HYPOTHESES 107
Hypothesis 1 - Is HEC-RAS more accurate than ADCIRC in the Tar River? *107*

Hypothesis 2 – What are the costs/benefits associated with incorporating rivers in an ADCIRC model? *110*
Hypothesis 2A *110*
Hypothesis 2B *112*
Hypothesis 2 – Combined *112*
Hypothesis 3 ..... *112*
RECOMMENDATIONS 114
Operational Implications *114*
Possible Future Studies *114*
Radius of Impact of Downstream BC Errors *114*
Boundary Condition Development *115*
Cost-Benefit Quantification *115*
Improved River Resolution *115*

WORKS CITED **116**
APPENDIX A – MAPS OF NODAL ATTRIBUTES **124**
FINE MESH PARAMETER MAPS 125
Fine Mesh Horizontal Eddy Viscosity *125*
Fine Mesh Initial River Elevation *126*
Fine Mesh Manning's n at Sea Floor *127*
Fine Mesh Primitive Weighting in Continuity Equation (Tau0) *128*
Fine Mesh Surface Canopy Coefficient *129*
Fine Mesh Bathymetry *130*
Fine Mesh Node Spacing *131*
COARSE MESH PARAMETER MAPS 131
Coarse Mesh Horizontal Eddy Viscosity *132*
Coarse Mesh Manning's n at Sea Floor *133*
Coarse Mesh Primitive Weighting in Continuity Equation (Tau0) *134*
Coarse Mesh Surface Canopy Coefficient *135*
Coarse Mesh Bathymetry *136*
Coarse Mesh Node Spacing *137*

APPENDIX B – HL-RDHM MODEL VALIDATION **138**
HURRICANE ISABEL 138
HURRICANE FLOYD 142
APRIL, 2003 146

APPENDIX C – OCEANIC MODEL VALIDATION **151**
GAUGE LOCATIONS 151
APRIL, 2003 VALIDATION 152
Beaufort *152*
Duck Pier *152*
Oregon Inlet *153*
HURRICANE FLOYD VALIDATION 154
Beaufort *154*
Duck Pier *154*
Oregon Inlet *155*
HURRICANE IRENE 156
Beaufort *156*
Duck Pier *156*
Oregon Inlet *157*

12. APPENDIX D – INUNDATION MAPPING METHODS **158**
INUNDATED AREA IN TARGET DOMAIN – ADCIRC NATIVE 158
INUNDATED AREA IN HEC-RAS DOMAIN – HEC-RAS PARALLEL 160

LIST OF TABLES

TABLE 7-1 - BOUNDARY CONDITIONS 42
TABLE 8-1 - HURRICANE IRENE FORCING AND VALIDATION DATASETS 52
TABLE 8-2 - HIGH WATER MARK ERRORS 61
TABLE 9-1 - HURRICANE FLOYD FORCING AND VALIDATION DATASETS 79
TABLE 10-1 - FORCING AND VALIDATION DATASETS - APRIL, 2003 93
TABLE 11-1 - MAXIMUM STABLE TIMESTEPS BY GRID 106
TABLE 12-1 - PEAK PREDICTION ERROR FACTORS, HEC-RAS/ADCIRC 109
TABLE 12-2 - PEAK PREDICTION ERROR FACTORS, HEC-RAS (RDHM UPSTREAM), RIVERS/NO RIVERS 111
TABLE 12-3 - PEAK PREDICTION ERROR FACTORS, HEC-RAS (ADCIRC UPSTREAM), RIVERS/NO RIVERS 111
TABLE 12-4 - PEAK PREDICTION ERROR FACTORS, HEC-RAS/ADCIRC 113
TABLE B-5- SELECTED "BEST" RDHM MEMBER PROPERTIES 142

LIST OF FIGURES

FIGURE 1-1 LEFT - POPULATION CHANGE IN U.S. COASTAL WATERSHED COUNTIES (1970-2010) (MELILLO, ET AL., 2014). RIGHT – COASTAL AREAS OUTSIDE RIVER FORECAST ZONES (MASHRIQUI, ET AL., 2014) 1
FIGURE 5-1 SIMPLE GRIDCELL CONNECTIVITY. THIS 6-CELL MODEL WOULD CONSIST OF THREE WATERSHED SUB-BASINS A, B, AND C. 19
FIGURE 5-2 TAR RIVER REPRESENTATION IN HEC-RAS 28
FIGURE 5-3 EXAMPLE HEC-RAS CROSS SECTION, INCLUDING A BRIDGE CROSSING OF HIGHWAY 264 OVER THE TAR RIVER 29
FIGURE 5-4 COUPLING 1 – "EXISTING SYSTEM" 31
FIGURE 5-5 COUPLING 2 – COUPLED SYSTEM USING FINE ADCIRC 32
FIGURE 5-6 COUPLING SCHEME 3 –HEC-RAS USING FINE ADCIRC'S FORCINGS 33
FIGURE 5-7 COUPLING 4 – COUPLED SYSTEM USING COARSE ADCIRC 33
FIGURE 5-8 COUPLING SCHEME 5 – HEC-RAS, FINE ADCIRC UPSTREAM, COARSE ADCIRC DOWNSTREAM 34
FIGURE 5-9 EXAMPLE COMPARISON HYDROGRAPH 37
FIGURE 5-10 HOW TO READ COMPARISON HYDROGRAPH 38
FIGURE 6-1 HEC-RAS INPUT AND OUTPUT FLOWS (IN COMBINED BC) 41
FIGURE 6-2 HEC-RAS INPUT AND OUTPUT STAGES (IN COMBINED BC) 41
FIGURE 6-3 HEC-RAS RESPONSE AT GREENVILLE, NC USING ADCIRC FLOW UPSTREAM AND DOWNSTREAM. MODEL RESULTS IN RED, OBSERVATIONS IN BLACK. 42
FIGURE 6-4 USGS GAUGE LOCATIONS. IMAGERY COURTESY GOOGLE EARTH 43
FIGURE 6-5 STAGE ERROR VS. BOUNDARY CONDITION CONFIGURATION, ROCK SPRING, NC. MODEL RESULTS IN RED, OBSERVATIONS IN BLACK. 44
FIGURE 6-6 BOUNDARY CONDITION COMPARISON - FLOW AT GREENVILLE, NC 45
FIGURE 6-7 BOUNDARY CONDITION COMPARISON - STAGE AT GREENVILLE, NC 46
FIGURE 6-8 BOUNDARY CONDITION COMPARISON - FLOW AT GRIMESLAND, NC 48
FIGURE 7-1 SOIL MOISTURE CONDITIONS TWO DAYS PRIOR TO HURRICANE IRENE'S NC LANDFALL (NOAA, 2012) 50
FIGURE 7-2 - TAR RIVER AT TARBORO, NC. ADCIRC RESULTS IN GREEN, ADCIRC RESULTS INTERPRETED BY HEC-RAS IN RED, STAGE SOLVED FROM HL-RDHM FLOWS IN BLUE, OBSERVATIONS IN BLACK. LEFT PANEL FLOW, RIGHT PANEL STAGE 53
FIGURE 7-3 - PAMLICO SOUND AT WASHINGTON - ADCIRC WITH RIVERS ON IN RED, ADCIRC WITHOUT RIVERS RESOLVED IN BLUE 54
FIGURE 7-4 TAR RIVER AT ROCK SPRINGS, NC. ADCIRC RESULTS IN GREEN, ADCIRC RESULTS INTERPRETED BY HEC-RAS IN RED, STAGE SOLVED FROM HL-RDHM FLOWS IN BLUE, OBSERVATIONS IN BLACK 55
FIGURE 7-5 TAR RIVER AT GREENVILLE, NC. ADCIRC RESULTS IN GREEN, ADCIRC RESULTS INTERPRETED BY HEC-RAS IN RED, STAGE SOLVED FROM HL-RDHM FLOWS IN BLUE, OBSERVATIONS IN BLACK. LEFT PANEL FLOW, RIGHT PANEL STAGE 55
FIGURE 7-6 TAR RIVER AT GRIMESLAND, NC. ADCIRC RESULTS IN GREEN, ADCIRC RESULTS INTERPRETED BY HEC-RAS IN RED, STAGE SOLVED FROM HL-RDHM FLOWS IN BLUE, OBSERVATIONS IN BLACK 56
FIGURE 7-7 PEAK TIMING ERROR BY DISTANCE UPSTREAM. ADCIRC RESULTS IN GREEN, ADCIRC RESULTS INTERPRETED BY HEC-RAS IN RED, STAGE SOLVED FROM HL-RDHM FLOWS IN BLUE, OBSERVATIONS IN BLACK 58

FIGURE 7-8 PEAK STAGE ERROR BY DISTANCE UPSTREAM. ADCIRC RESULTS IN GREEN, ADCIRC RESULTS INTERPRETED BY HEC-RAS IN RED, STAGE SOLVED FROM HL-RDHM FLOWS IN BLUE, OBSERVATIONS IN BLACK 58
FIGURE 7-9 PEAK FLOW ERROR BY DISTANCE UPSTREAM. ADCIRC RESULTS IN GREEN, ADCIRC RESULTS INTERPRETED BY HEC-RAS IN RED, STAGE SOLVED FROM HL-RDHM FLOWS IN BLUE, OBSERVATIONS IN BLACK 59
FIGURE 7-10 USGS HIGH WATER MARK LOCATIONS 61
FIGURE 7-11 HURRICANE IRENE INUNDATION AT TARBORO 62
FIGURE 7-12 HURRICANE IRENE INUNDATION AT ROCK SPRING 63
FIGURE 7-13 HURRICANE IRENE INUNDATION AT GREENVILLE 63
FIGURE 7-14 HURRICANE IRENE INUNDATION AT GRIMESLAND 64
FIGURE 7-15 HURRICANE IRENE INUNDATION AT WASHINGTON, NC 64
FIGURE 7-16 ADCIRC INUNDATION DEPTH MINUS HEC-RAS STAGE/STAGE INUNDATION DEPTH. PINK INDICATES HEC-RAS RESULTS ABOVE ADCIRC RESULTS. DARKENING SHADES OF BLUE INDICATE ADCIRC RESULTS ABOVE HEC-RAS RESULTS. 66
FIGURE 7-17 INUNDATION DIFFERENCES UPSTREAM OF NC 222 CROSSING 66
FIGURE 7-18 NC 222 CROSSING 67
FIGURE 7-19 UNNAMED REGION OF POSITIVE HEC-RAS BIAS DOWNSTREAM OF NC 222 68
FIGURE 7-20 HEC-RAS CROSS SECTIONS AT UNNAMED BEND, SOUTH OF NC 222 69
FIGURE 7-21 INUNDATION DIFFERENCES AT AND NEAR MARTIN LUTHER KING JR. HIGHWAY CROSSING 69
FIGURE 7-22 INUNDATION DIFFERENCES DOWNSTREAM OF MEMORIAL DRIVE CROSSING 71
FIGURE 7-23 SPATIAL LOCATION OF BRIDGE SECTIONS IN HEC-RAS MODEL SHOWN IN BLACK 72
FIGURE 7-24 INUNDATION DIFFERENCES BETWEEN ADCIRC AND HEC-RAS NEAR GREENVILLE BLVD NE CROSSING 72
FIGURE 7-25 INUNDATION DIFFERENCES WELL DOWNSTREAM OF GREENVILLE BOULEVARD NE CROSSING 73
FIGURE 7-26 UNPROCESSED NED DEM DOWNSTREAM OF GREENVILLE BOULEVARD NE CROSSING. RED OVAL INDICATES APPROXIMATE REGION OF NEARBY ROADWAY. BLUE POLYGON INDICATES APPROXIMATE EXTENT OF UNEXPECTED MODEL RESULTS. YELLOW DOTS INDICATE HEC-RAS BANK POINTS. 74
FIGURE 7-27 ERROR IN HEC-RAS SOLUTION INDUCED BY RIVERLESS BC – HURRICANE IRENE 76
FIGURE 8-1 HURRICANE DENNIS RAINFALL TOTALS (NEWPORT/MOREHEAD, NC WEATHER FORECAST OFFICE, NWS, N.D.) 78
FIGURE 8-2 HURRICANE FLOYD STORM TRACK & WIND SPEEDS (NEWPORT/MOREHEAD, NC WEATHER FORECAST OFFICE, NWS, N.D.) 79
FIGURE 8-3 TAR RIVER AT TARBORO, NC. ADCIRC RESULTS IN GREEN, ADCIRC RESULTS INTERPRETED BY HEC-RAS IN RED, HL-RDHM FLOWS IN BLUE, OBSERVATIONS IN BLACK. FLOW IN LEFT PANEL, STAGE IN RIGHT PANEL 80
FIGURE 8-4 PAMLICO SOUND AT WASHINGTON. ADCIRC RESULTS IN GREEN, ADCIRC RESULTS INTERPRETED BY HEC-RAS IN RED, HL-RDHM FLOWS IN BLUE, OBSERVATIONS IN BLACK. RIVERLESS ADCIRC FLOWS WERE NOT WELL RESOLVED AND ARE NOT SHOWN. STAGE OBSERVATIONS ARE NOT AVAILABLE AT THIS GAUGE AND TIME PERIOD. FLOW IN LEFT PANEL, STAGE IN RIGHT PANEL 81
FIGURE 8-5 TAR RIVER AT GREENVILLE, NC. ADCIRC RESULTS IN GREEN, ADCIRC RESULTS INTERPRETED BY HEC-RAS IN RED, STAGE SOLVED FROM HL-RDHM FLOWS IN BLUE, OBSERVATIONS IN BLACK. LEFT PANEL FLOW, RIGHT PANEL STAGE. FLOW IN LEFT PANEL, STAGE IN RIGHT PANEL 82

FIGURE 8-6 PEAK TIMING ERROR BY DISTANCE UPSTREAM. ADCIRC RESULTS IN GREEN, ADCIRC RESULTS INTERPRETED BY HEC-RAS IN RED, STAGE SOLVED FROM HL-RDHM FLOWS IN BLUE, OBSERVATIONS IN BLACK 83
FIGURE 8-7 PEAK FLOW ERROR BY DISTANCE UPSTREAM. ADCIRC RESULTS IN GREEN, ADCIRC RESULTS INTERPRETED BY HEC-RAS IN RED, STAGE SOLVED FROM HL-RDHM FLOWS IN BLUE, OBSERVATIONS IN BLACK 83
FIGURE 8-8 PEAK STAGE ERROR BY DISTANCE UPSTREAM. ADCIRC RESULTS IN GREEN, ADCIRC RESULTS INTERPRETED BY HEC-RAS IN RED, STAGE SOLVED FROM HL-RDHM FLOWS IN BLUE, OBSERVATIONS IN BLACK 84
FIGURE 8-9 HURRICANE FLOYD INUNDATION AT TARBORO 85
FIGURE 8-10 HURRICANE FLOYD INUNDATION AT ROCK SPRING 86
FIGURE 8-11 HURRICANE FLOYD INUNDATION AT GREENVILLE 86
FIGURE 8-12 HURRICANE FLOYD INUNDATION AT GRIMESLAND 87
FIGURE 8-13 HURRICANE FLOYD INUNDATION AT WASHINGTON, NC 87
FIGURE 8-14 ERROR IN HEC-RAS SOLUTION INDUCED BY RIVERLESS BC – HURRICANE FLOYD 88
FIGURE 9-1 LOCATION AND WIND SPEED RESULTS AT NBDC 41025 91
FIGURE 9-2 TS ANA TRACK, (THE WEATHER COMPANY, 2017) 92
FIGURE 9-3 TAR RIVER AT TARBORO, NC. ADCIRC RESULTS IN GREEN, ADCIRC RESULTS INTERPRETED BY HEC-RAS IN RED, HL-RDHM FLOWS IN BLUE, OBSERVATIONS IN BLACK. FLOW IN LEFT PANEL, STAGE IN RIGHT PANEL 94
FIGURE 9-4 PAMLICO SOUND AT WASHINGTON - ADCIRC RESULTS IN GREEN, ADCIRC RESULTS INTERPRETED BY HEC-RAS IN RED, HL-RDHM FLOWS IN BLUE, OBSERVATIONS IN BLACK. FLOW IN LEFT PANEL, STAGE IN RIGHT PANEL 94
FIGURE 9-5 TAR RIVER AT GREENVILLE, NC. ADCIRC RESULTS IN GREEN, ADCIRC RESULTS INTERPRETED BY HEC-RAS IN RED, STAGE SOLVED FROM HL-RDHM FLOWS IN BLUE, OBSERVATIONS IN BLACK. LEFT PANEL FLOW, RIGHT PANEL STAGE. FLOW IN LEFT PANEL, STAGE IN RIGHT PANEL 96
FIGURE 9-6 PEAK TIMING ERROR BY DISTANCE UPSTREAM. ADCIRC RESULTS IN GREEN, ADCIRC RESULTS INTERPRETED BY HEC-RAS IN RED, STAGE SOLVED FROM HL-RDHM FLOWS IN BLUE, OBSERVATIONS IN BLACK 97
FIGURE 9-7 PEAK FLOW ERROR BY DISTANCE UPSTREAM. ADCIRC RESULTS IN GREEN, ADCIRC RESULTS INTERPRETED BY HEC-RAS IN RED, STAGE SOLVED FROM HL-RDHM FLOWS IN BLUE, OBSERVATIONS IN BLACK 97
FIGURE 9-8 PEAK STAGE ERROR BY DISTANCE UPSTREAM. ADCIRC RESULTS IN GREEN, ADCIRC RESULTS INTERPRETED BY HEC-RAS IN RED, STAGE SOLVED FROM HL-RDHM FLOWS IN BLUE, OBSERVATIONS IN BLACK 98
FIGURE 9-9 APRIL 2003 RAINFALL EVENT INUNDATION AT TARBORO 99
FIGURE 9-10 APRIL 2003 RAINFALL EVENT INUNDATION AT ROCK SPRING 99
FIGURE 9-11 APRIL 2003 RAINFALL EVENT INUNDATION AT GREENVILLE 100
FIGURE 9-12 APRIL 2003 RAINFALL EVENT INUNDATION AT GRIMESLAND 100
FIGURE 9-13 APRIL 2003 RAINFALL EVENT INUNDATION AT WASHINGTON, NC 101
FIGURE 9-14 ERROR IN HEC-RAS SOLUTION INDUCED BY RIVERLESS BC – APRIL, 2003 102
FIGURE 10-1 BINARY SEARCH ALGORITHM 105
FIGURE B-1 - RDHM ENSEMBLE MEMBERS AT USGS 02083500. CALIBRATED IN RED, *A PRIORI* IN BLUE, OBSERVED IN BLACK 138
FIGURE B-2 - RDHM ENSEMBLE CALIBRATED MEMBERS AT USGS 02083500. MODELLED IN RED, OBSERVED IN BLACK 139
FIGURE B-3 - RDHM ENSEMBLE *A PRIORI* MEMBERS AT USGS 02083500. MODELLED IN RED, OBSERVED IN BLACK 139

FIGURE B-4 - HURRICANE IRENE HL-RDHM ENSEMBLE SKILL SUMMARY, BIN = 0.25 140
FIGURE B-5 - RDHM ENSEMBLE MEMBER 16 AT USGS 02083500 DURING HURRICANE IRENE. MODELLED IN BLUE, OBSERVED IN BLACK 141
FIGURE B-6 - RDHM ENSEMBLE MEMBERS AT USGS 02083500. CALIBRATED IN RED, *A PRIORI* IN BLUE, OBSERVED IN BLACK 143
FIGURE B-7 - RDHM ENSEMBLE CALIBRATED MEMBERS AT USGS 02083500. MODELLED IN RED, OBSERVED IN BLACK 143
FIGURE B-8 - RDHM ENSEMBLE *A PRIORI* MEMBERS AT USGS 02083500. MODELLED IN RED, OBSERVED IN BLACK 144
FIGURE B-9 - HURRICANE FLOYD HL-RDHM ENSEMBLE SKILL SUMMARY, BIN = 0.05 145
FIGURE B-10 - RDHM ENSEMBLE BEST MEMBER AT USGS 02083500 DURING HURRICANE FLOYD. MODELLED IN RED, OBSERVED IN BLACK 146
FIGURE B-11 - RDHM ENSEMBLE MEMBERS AT USGS 02083500. CALIBRATED IN RED, *A PRIORI* IN BLUE, OBSERVED IN BLACK 147
FIGURE B-12 - RDHM ENSEMBLE CALIBRATED MEMBERS AT USGS 02083500. MODELLED IN RED, OBSERVED IN BLACK 148
FIGURE B-13 - RDHM ENSEMBLE *A PRIORI* MEMBERS AT USGS 02083500. MODELLED IN RED, OBSERVED IN BLACK 148
FIGURE B-14 - HURRICANE FLOYD HL-RDHM ENSEMBLE SKILL SUMMARY, BIN = 0.05 149
FIGURE B-15 - RDHM ENSEMBLE BEST MEMBER AT USGS 02083500 DURING APRIL, 2003. MODELLED IN RED, OBSERVED IN BLACK 150
FIGURE C-1 - NOS GAUGE LOCATIONS (NOAA/NOS/CO-OPS, 2013) 151
FIGURE D-1 - INUNDATION OF TAR RIVER ABOVE TAR AT PAMLICO STATION DURING HURRICANE IRENE 159
FIGURE D-2 - IRENE INUNDATION AT GREENVILLE 159
FIGURE D-3 - IRENE INUNDATION AT WASHINGTON 160
FIGURE D-4 - INUNDATION USING GEORAS METHOD 161
FIGURE D-5 - INUNDATION AT GREENVILLE USING GEORAS METHOD 162
FIGURE D-6 - ADCIRC INUNDATION AT WASHINGTON USING GEORAS METHOD 162

ABSTRACT

The purpose of this Master's thesis was to develop and compare an ADCIRC and ADCIRC/HEC-RAS paired model for the purpose of total water level forecasting using the Tar River and Pamlico Sound area as a test case. ADCIRC is a 2D hydrodynamic model widely used for coastal storm impact prediction. HEC-RAS is a 1D hydraulic river and stream modeling system. Both models are capable of simulating river systems, but while some of the differences between ADCIRC and HEC-RAS can be intuited simply by studying their underlying equations, a case-study comparison of each model's ability to accurately and quickly simulate storm impact on a riverine/estuarine system may serve as a valuable tool to forecasters. As part of this project, individual models of the Tar River and Pamlico Sound area in North Carolina were prepared, both in HEC-RAS and in ADCIRC. Pairings of these models were devised to intuit the benefits and drawbacks of using ADCIRC, or pairing ADCIRC with HEC-RAS, to simulate the response of the Tar River and Pamlico Sound during three test events. The results of this study will inform and assist forecasters in selecting and developing similar paired models for coastal river systems across the U.S. and around the globe, as well as improving the body of knowledge about each model's relative performance in riverine and estuarine areas. This should result in more meaningful and accurate predictions, which will save lives and property in coastal, storm-sensitive riverine areas.

1. MOTIVATION FOR STUDY

Coastal areas in the USA are of significant social and economic importance – as much as 3% of the US population lives within zones classified as the 100-year coastal flood hazard area (Crowell, et al., 2010) and populations in coastal watershed counties are generally increasing (Melillo, et al., 2014), as shown in Figure 1-1.

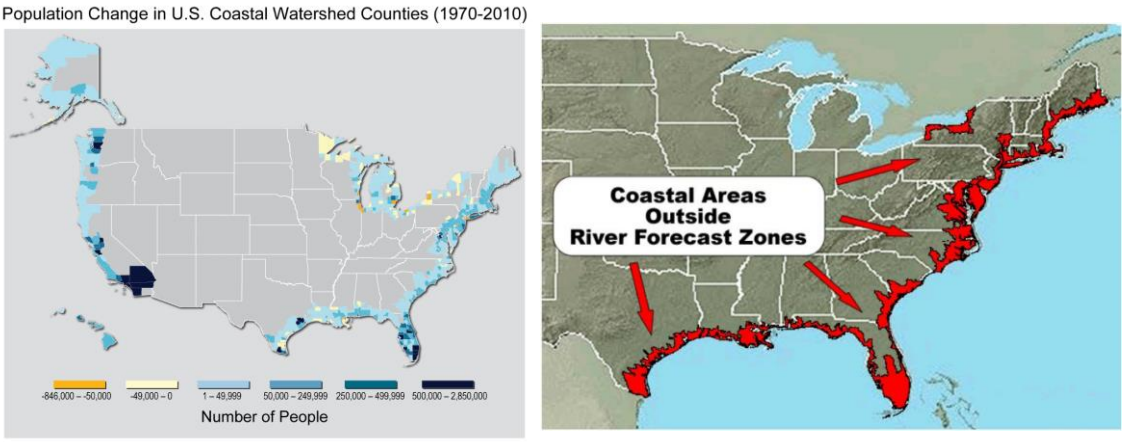

Figure 1-1 Left - Population change in U.S. coastal watershed counties (1970-2010) (Melillo, et al., 2014). Right – Coastal areas outside river forecast zones (Mashriqui, et al., 2014)

The vulnerabilities of coastal regions to storm damage, and the importance of models in mitigating this damage by informing decision makers, have been well established. There are heightened risks to coastal areas due to a growth in population in coastal areas (Van Cooten, et al., 2011), and North Carolina specifically experiences vulnerabilities to coastal storm damage due to the state's geographic and infrastructural features (Mattocks & Forbes, 2008). Total water level modeling of coastal rivers during severe storm events, including estimates of freshwater rainfall runoff, is critical to the accurate prediction of future flooding in coastal cities, specifically as it pertains to long-term risk assessment (Lian et al. 2013).

The US National Weather Service (NWS), which is part of the National Oceanic and Atmospheric Administration (NOAA), is tasked with providing severe weather watches, warnings, and forecasts to the general public. The NWS provides flood stage estimates at over 3500 locations in the United States. However, a significant service gap exists in the riverine-estuarine zone, where freshwater flows are significant but are generally not accounted for in operational model forecasts, as shown in Figure 1-1 (Van Cooten, et al., 2011; Mashriqui, et al., 2014). Numerical prediction of flood stage in these areas, including both freshwater flows as well as oceanic and atmospheric effects ("total water level prediction"), represents a significant numerical challenge due to the presence of multiple significant drivers of flooding.

Multiple research initiatives are underway intended to provide total water level prediction in tidally influenced coastal rivers, including extending existing oceanic models upstream and extending existing riverine models downstream.

Efforts are underway to extend oceanic prediction models further and further into the tidally influenced riverine domain. Oceanic models have been developed using USGS gauge observations to provide freshwater flow boundary conditions, including (among others) NOAA's Tampa Bay, Chesapeake Bay, and Delaware River and Bay Operational Forecast Systems (Wei & Zhang, 2011; Lanerolle, et al., 2011; Schmalz, 2011). One oceanic model, the ADvanced CIRCulation (ADCIRC) model (Leuttich & Westerink, 2004), have been applied in the Tar River (Dresback, et al., 2013; Tromble, 2011), the Mississippi River (Westerink, et al., 2008), and efforts are underway to extend a similar model upland in the Pearl River (McKay & Blain, 2010). Finally, accurate water level

forecasts have been produced in the Washington, D.C. region using the 3D ELCIRC model (Cho, et al., 2012).

As efforts to extend 2D models upland proceed, so too do efforts to extend 1D upland, riverine-models closer to the oceanic boundary by incorporating oceanic forcings. 1D hydraulic models of tidally influenced rivers have been implemented by NOAA in at least five locations (Mashriqui, et al., 2014). Efforts have also been undertaken to supply existing 1D models with downstream boundary conditions, including storm surge and tidal information, such as the Hydrologic Engineering Center's River Analysis System (HEC-RAS) (Christian, et al., 2013). As yet, no upland river model including hydrologic (river network) modelling has been operationally coupled with an oceanic model to produce a prediction of the "total water level" interactions known to exist in tidal estuaries.

As both 1D and higher-dimensional models become available in riverine areas, the question naturally arises, when should a modeler implement a 1D model, instead of a 2D or 3D model? The answer to this question does not have a single answer, as the relative skill and cost of both types of models will depend on the particular morphologies of a particular river (Pappenberger, et al., 2005; Horritt & Bates, 2002). However, studies on these sorts of comparisons on particular domains are relatively uncommon, perhaps due to the significant cost associated with developing such models in the first place.

2. RATIONALE FOR THIS RESEARCH

The Tar River Basin presents a unique and valuable testbed for a direct comparison of 1D and 2D river forecast models for three reasons. First, the river basin is a tidally influenced river of economic importance to the region, including multiple municipal communities that have experienced flooding during extreme storm events, such as Hurricane Floyd (1999) and Hurricane Matthew (2016). Second, NOAA resources have been expended to develop models of this region. Third, the basin represents a river morphology that has not been studied by other comparative coastal river modelling research.

The North Carolina Department of Water Resources (DWR) has this to say about the Tar River Basin:

> *The Tar-Pamlico River Basin is the fourth largest river basin in North Carolina and is one of only four river basins whose boundaries are located entirely within the state. The Tar River originates in north central North Carolina in Person, Granville and Vance counties and flows southeasterly until it reaches tidal waters near Washington and becomes the Pamlico River and empties into the Pamlico Sound. … Development and population growth center around Greenville, Rocky Mount and smaller municipalities. (2014)*

The Tar River basin is studied here, with special attention paid to the region between the Pamlico Sound and the 8m contour, and beyond. In this domain, the Tar River runs within natural banks from that contour to the Pamlico Sound at Washington. At the 8m contour the Tar River is relatively small, with an average width on the order of 30-40m or less during low flows. This width is largely maintained until Grimesland, a town located near the Pamlico Sound.

1D and 2D models of this river basin from Tarboro downstream to Pamlico Sound have already been developed. There is currently a project entitled the Coastal Emergency Risks Assessment (CERA) that provides total water level estimates in multiple tidally influenced watersheds. CERA utilizes a multi-model system consisting of the ADCIRC

surge guidance system (ASGS-STORM) to provide guidance on areas on the east coast including the Tar River Basin, without a 1D river model (Fleming, et al., 2008). ASGS's North Carolina mesh extends a 2D oceanic model (ADCIRC) to the 8m contour within the Tar and Neuse river basins (Dresback, et al., 2013; Tromble, 2011). In addition to the ASGS-STORM project, research funded by NOAA's Office of Hydrologic Development (OHD) has produced a 1D HEC-RAS model of the Tar River Basin extending from Tarboro (located near the 8m contour) well into the tidal zone of the Pamlico River near Washington, NC, calibrated to extreme storm events (Abshire, 2012).

Other research has compared 1D and 2D models in streams (Horritt & Bates, 2002). Compared to prior studies, the Tar River Basin offers a unique opportunity to compare these types of models in a domain featuring a high-elevation handoff, natural river banks, and a narrow river width. Due to these particular features, the availability of operational-ready models, and the imminent need for improved flood prediction in general, a direct skill and timing comparison of 1D and 2D models for use in predicting severe storm flooding in the Tar River is both timely and relevant, and it will be the subject of this research.

3. LITERATURE REVIEW

FUNCTIONALITY OF ADCIRC

ADCIRC has been used as an accurate and effective computational hydrodynamic model for the prediction of severe storm event impacts in coastal regions, including North Carolina (Blanton, et al., 2012; Mattocks & Forbes, 2008; Van Cooten, et al., 2011) and elsewhere. ADCIRC is familiar to NOAA, as it is currently used in the ESTOFS and other forecasting systems within NOAA's operational framework. ADCIRC is operationally used as a 2D or three-dimensional (3-D) model, meaning higher computational resource costs compared to simpler, 1D models. Tanaka, et al. (2011) investigated the scalability of the CG version of ADCIRC. The authors found that the scalability of ADCIRC was high enough to meet the stringent requirements of storm forecasters, namely outputting one day of real time simulation in between 3-7 minutes, but only on tens of thousands of computational cores. There have been some initial steps towards running ADCIRC in an "ensemble" modeling regime (Ramakrishnan, et al., 2006), but it remains to be seen whether low-computation-cost ADCIRC modeling regimes (e.g. models featuring coarser grids) can exhibit similar accuracies. One trend in the ADCIRC community is towards the more generally stable Discontinuous Galerkin (DG) formulation, which boasts improved modeling of "dam-break" style inundation and finely resolved, discontinuous topographies (Dawson, et al., 2011). This method may improve modelling of rivers in ADCIRC, but increases computational cost – Dawson, et al. observed a roughly 4x increase in cost in using a DG formulation compared to CG ADCIRC (2011). It is therefore desirable to evaluate possible alternative modeling configurations that might

lead to a reduction in computational resources required, while preserving model accuracies.

POTENTIAL OF HEC-RAS

The Hydrologic Engineering Center River Analysis System (HEC-RAS) is a popular model for the prediction of river flooding that shows promise for incorporation in the modeling scheme proposed above. It has been used extensively throughout the United States and abroad for assessing the behavior of rivers during high-flow events, and has been used to produce total water level predictions in coastal areas by acting as "middleware" for larger modeling schemes (Lian, et al., 2013; Ray, et al., 2011; Mejia & Reed, 2011). Still, the accuracy of HEC-RAS in comparison with 2D ADCIRC has not been assessed. Therefore, a scheme incorporating HEC-RAS as middleware between a hydrologic model and ADCIRC for total water level prediction in coastal areas is both a promising and an unproven modeling regime, and the study of such a scheme is both timely and relevant.

Horritt and Bates (2002) compared the skill and accuracy of three models of a 60-km stretch of the Severn River in the UK. The three models included HEC-RAS, as well as two 2D models: LISFLOOD-FP, a raster-based inundation model that uses 1D channel flow and 2D floodplain flow, and TELEMAC-2D, a model which uses Galerkin's method of weighted residuals to solve the 2D shallow water (Saint-Venant) equations of free surface flow over an unstructured mesh. The authors were surprised to find that for their river morphology, and given a sufficiently resolved DEM raster onto which HEC-RAS results might be projected, the 1D HEC-RAS model proved a more robust and accurate predictor of flood flowrates than both 2D models. Specifically, their methodology

included calibrating the models' channel and floodplain roughness, once using flood wave travel times and once using flood inundation gathered from satellite imagery. HEC-RAS was the model which showed the greatest agreement between both calibrations' roughness values, and thus was deemed the most insensitive to methods and the most reliable. They suggest that this is due in part to the limited calibration scope and in part to the channel morphology. Specifically, their model domain consisted of a river with steep, well-defined channel sides. This means that, even at times when water levels rapidly rise or fall, the channel sides prevent significant lateral flows. They expect that, given a more spatially variable descriptor of 2D flow and/or in the case of a stream of different morphology, the 2D models might prove more accurate.

This is highly relevant to the problem of incorporating HEC-RAS or any 1D model as an intermediate model for river flood prediction in coastal areas. If 1D or 2D models were proven to always be more accurate at predicting river behaviors, regardless of morphology or modelling methodology, the question of what model to use in a particular area would be as simple as determining the lowest cost method that exhibited adequate accuracy. However, their findings suggest that each river to be modeled should be examined with respect to morphology and expected flow conditions in order to determine whether a 1D or a 2D modelling approach is appropriate. Horritt and Bates showed that a 1D model is more accurate in a domain with steep sidewalls. However, in a relatively flat river, at the confluence of multiple rivers, or as a river nears its mouth, lateral flows may be more significant and 2D models may be more accurate.

Pappenberger et al. (2004) approach the problem of describing the uncertainty of models such as HEC-RAS. They identify possible sources of uncertainty in numerical parameter

selection (e.g. timestep, time weighting), physical parameter selection (topographic measurements and roughness estimates), and boundary conditions (input and output hydrographs). They then use an automated assessment method to describe the response surface of the model to these variables in a combined fashion. The assessment was performed for two different river stretches, which showed differing sensitivities. Their findings confirm some conventional wisdom, namely that distributed model parameter information leads to more accurate modeling of river response. However, the authors demonstrate that this uncertainty problem is inherently more tractable with a 1D model. They suggest that, since uncertainty is always present in any description of the real world, a more detailed model of a river (i.e. a 2D or 3D model) will not necessarily be more reliable than a simpler one, and that instead modelers must take into account the reliability of their data and the origins of their parameter estimates in order to determine whether a particular model is ideal.

PAIRED MODELS

One coupled model used by multiple agencies (Including NOAA, DHS, and an interagency effort known as CI-FLOW) is what's known as the ADCIRC Surge Guidance System - Scalable, Terrestrial, Ocean, River, Meteorologic (ASGS-STORM) (Van Cooten, et al., 2011; Tromble, 2011; Dresback, et al., 2013).

During development of ASGS-STORM, two approaches were considered to couple the hydrologic model (HL-RDHM) to the hydrodynamic model (ADCIRC). Two couplings were suggested for incorporating hydrologic information into the hydrodynamic model. First, a river model could be used as middleware to solve for two-way tidal or storm surge flow at a boundary well below the surge zone. Alternately, the hydrodynamic model could

be extended well upstream of the surge zone to a point where a two-way coupling would not be necessary due to a lack of backwater effects. The decision was made to extend ADCIRC's domain to a contour (8 meters) above the historical surge zone in this region (6 meters), however this approach is known to have tradeoffs – for example, this approach may result in increased computational cost, and may lose accuracy if severe events result in backwater impacts at this handoff location, or if the river is insufficiently resolved (Van Cooten, et al., 2011).

It is for this reason that there are efforts underway to evaluate and improve the coupling between the hydrologic and hydrodynamic models to provide a more robust estimate of storm surge in upland areas. The ideal handoff method will be simple, stable, and computationally cheap, while maintaining accuracy.

A skill assessment of the ASGS-STORM system was performed by Dresback, et al. (2013) who found that the system had the capability to convert accurate forcing predictions (rainfall, winds) into accurate forecasts of storm impacts in the Pamlico Sound and the barrier islands. The study found agreements between High Water Marks in lowland areas of the Pamlico and Tar Rivers, and generally found the system to be accurate for tidal buoys as well. However, the study focused on skill within the Pamlico Sound and in the oceanic domain. The skill assessment was also performed in a holistic, predictive fashion, i.e. it simultaneously evaluated the accuracy of the QPE/QPF precipitation estimates, the hydrologic routing, the wind field predictions, the circulation model and the wave model, all in one single study. Each component was subject to its own validation but the combined inundation results were of a simulated operational system, meaning they were subject to the inherited errors from many sources. This is the

ideal method when describing an operational system, as any real model will of course inherit errors from its predecessors, and the study must show how accurate the model will be in a realistic sense. However the authors found that many of the errors in the ASGS-STORM forecast were likely due to errors in the predicted storm track and intensity.

This philosophy, that each model has its own inherent tendencies towards error, which can be evaluated and described separate from the boundary forcing errors, suggests that a study comparing the validity of two similar models ought to use rigorously quality-controlled, best-case hindcast boundary conditions to isolate inaccuracies as much as possible.

Kitzmiller, et al. (2011) assessed a variety of algorithms for processing multisensor data for the purpose of producing rainfall runoff estimates using an *a priori* parameterized HL-RDHM model of the Tar River Basin. They assessed 3 models and SERFC operational recommendations. They found that, unsurprisingly, the accuracy of runoff hydrographs trended strongly with the accuracy of QPE estimates, but did not commit strongly to recommending any one QPE product over another. Also, they found that while the skill (measured by Nash-Sutcliffe Efficiency – see Equation 5) of results forced by every QPE estimation method were positive, i.e. more predictive than the observed mean, the overall bias was towards underestimating runoff, which they attributed in part to the lack of site-specific calibration and in part to the lack of an assumed base flow for each channel.

Their results, which pertain directly to this basin and modeling regime, suggest three relevant courses of action. First, an accurate QPE product must be selected. Second, while there is basis for using *a priori* parameters, there is also room for improvement using

calibrated parameters. Finally, there is probably merit in assuming a base flow for each channel.

Meija & Reed (2011) engaged in a directional and external coupling of HL-RDHM to HEC-RAS, similar in approach to Lian et al (2013) and in some ways similar to the coupling described here. Specifically, Meija & Reed passed data from HL-RDHM to the upstream boundary condition of a HEC-RAS model, which in turn produced a more accurate combined prediction of river behavior than HL-RDHM alone. This study demonstrates the worth of HEC-RAS as a coupling tool through which hydrologic inputs may be converted into hydrodynamic outputs. Furthermore, it shows that a simple, directional coupling regime is useful as a preliminary step in determining whether a (potentially complicated) coupling project will yield substantial improvements in forecast accuracy and reliability.

4. HYPOTHESIS, OBJECTIVES, & GOAL

HYPOTHESES

The effort of this research is to examine the following three hypotheses and to determine if the data indicate their rejection.

HYPOTHESIS 1

First, it is believed that the use of HEC-RAS to model riverine systems, forced with ADCIRC at the downstream boundary, will produce forecasts with reduced simulation time and without reduced accuracy compared to the use of ADCIRC to model the same riverine areas, given the same boundary condition information. The independent variable in this study will be the model configuration, with model performance (accuracy) as the measured, dependent variable.

HYPOTHESIS 2

Second, it is believed that using a more coarsely resolved ADCIRC mesh to develop a downstream boundary condition for a HEC-RAS model will:

(A) not result in a loss of accuracy in the HEC-RAS model

(B) result in a reduction in the computation time required to achieve a stable ADCIRC solution

The independent variable for this model is the mesh resolution in riverine areas, with model performance (accuracy) and CPU time (cost) as the measured, dependent variables.

HYPOTHESIS 3

Third, as a conclusion of the first two hypotheses, it is believed that simply coupling the existing HEC-RAS model to the coarsely resolved ADCIRC model used in this research

will immediately enable river simulations at significant reduction of cost with either improvements or insignificant reductions in model accuracy.

OBJECTIVES

The objectives of this research are threefold.

First, a practical and representative coupling between ADCIRC, HEC-RAS, and currently available forcings is devised. Work related to this objective is presented in Chapters 5 and 6.

Second, the storm response in the lower region of the Tar River is simulated for three storm events exhibiting different typologies. These three hindcasts use both ADCIRC and HEC-RAS, configured in such a way as to give information about the sources of errors between those two methods. Work related to this objective is presented in Chapters 7, 8, and 9.

An estimate of the time savings made possible by substituting HEC-RAS for ADCIRC in the model domain is calculated by finding the maximum stable ADCIRC timestep both with and without the river domain resolved. Work related to this objective is presented in Chapter 10.

GOALS

The goal of this research is to provide guidance to model users who are seeking to forecast storm floods in tidally influenced rivers. The population and economic activity associated with coastal areas is growing (Van Cooten, et al., 2011), and if successful, the results of this research will join a body of knowledge on best practices for severe storm impact prediction for use in protecting coastal communities. By empowering engineers, emergency planners, and other public and private entities to better predict flood response, the ultimate harms of storms in terms of economic losses and loss of life will be reduced.

5. THEORY & GENERAL METHODS

WHAT IS A MODEL?

Fundamentally, models are nothing more than simplified descriptions of systems. In engineering usage specifically, models fill a critical role in the engineer's toolkit by allowing the prediction of behavior of a system under a set of conditions that may not be measurable empirically.

The term "model" can have many meanings, but in subsequent sections of this research, "model" shall refer to a piece of software, relying heavily on numerical methods, that can be used to solve problems about natural systems by combining predictive differential equations derived from theory with information about systems provided by "forcings." The models used in this research are as follows:

- Distributed rainfall runoff model – HL-RDHM
- 2D Ocean/Hydrodynamic model – ADCIRC
- 1D River model – HEC-RAS

The background, theory, and required forcing information for each of these models are described below. Because the nature of specific models is altered by the forcings applied to that model, these sections also include descriptions of the methods used to apply each model in this research.

HL-RDHM

The Hydrology Laboratory – Research Distributed Hydrologic Model (HL-RDHM) was developed by the National Weather Service (NWS) Office of Hydrologic Development (OHD), Hydrology Laboratory (HL), Hydrologic Science and Modeling Branch (HSMB) (Hydrology Laboratory, 2008). HL-RDHM is used to validate modelling techniques before implementing those techniques in operational modelling software.

HL-RDHM is actually a group of related models bundled and distributed together along with extensive *a priori* datasets, joined by built-in data passing algorithms. Each of these models has been designed to function on the Hydrologic Rainfall Analysis Projection (HRAP) grid. Each grid cell is approximately 4km across, with exact grid size depending on latitude. For this thesis, HL-RDHM was used to calculate a soil water balance (SAC-SMA) and a hillslope and channel routing solution at each grid cell. More information on the SAC-SMA and channel routing operations is included below.

SAC-SMA

HL-RDHM uses the Sacramento Soil Moisture Accounting model with a Heat Transfer component (full acronym SAC-SMA-HT). SAC-SMA-HT combines rainfall estimates with a parameterized calculation of soil moisture to determine each grid cell's effective runoff. These runoff estimates are then fed to the routing model to generate total streamflow estimates for each grid cell.

The SAC-SMA model applies parameters to each grid cell. It is a measured-parameter model – *a priori* datasets are calculated directly from observed data (e.g. land coverage), with no calibration necessary. However, with sufficient data, parameters can be adjusted using weighting factors. It is a continuous model, meaning results are available for

extended periods (in this case, years). It is a physics-based model, consisting of equations derived from a simplified picture of relevant physical principles surrounding conservation of mass in a soil column. Finally, it is a deterministic model, meaning each unique set of inputs produces a single unique set of outputs.

SAC-SMA outputs estimates of fast (surface) and slow (subsurface) runoff for each RDHM grid cell. SAC-SMA also calculates a number of internal state variables as well as estimates of evapotranspirative losses from each grid cell.

The SAC-SMA model requires estimates of precipitation and potential evaporation. In HL-RDHM, this information is discretized using gridded rainfall data as an external forcing and using *a priori* estimates of potential evaporation (PE) data. Rainfall estimates used were quantitative precipitation estimates (QPE), with sources varying by storm.

SAC-SMA also requires gridded parameter datasets for each of the 11 spatially-variable descriptive parameters. A mixture of *a priori* and calibrated parameters was used. For more information on what parameter sets were used and when, see Appendix B.

CHANNEL ROUTING

The channel routing model estimates hillslope flow and channel flow quantities and timing using the kinematic wave approximations based on specified rating curves. This routing model uses HL-RDHM's structured grid and an *a priori* connectivity network containing prevailing channel flow directions (conceptually depicted in Figure 5-1) to determine flow quantity and depth at each grid cell and timestep.

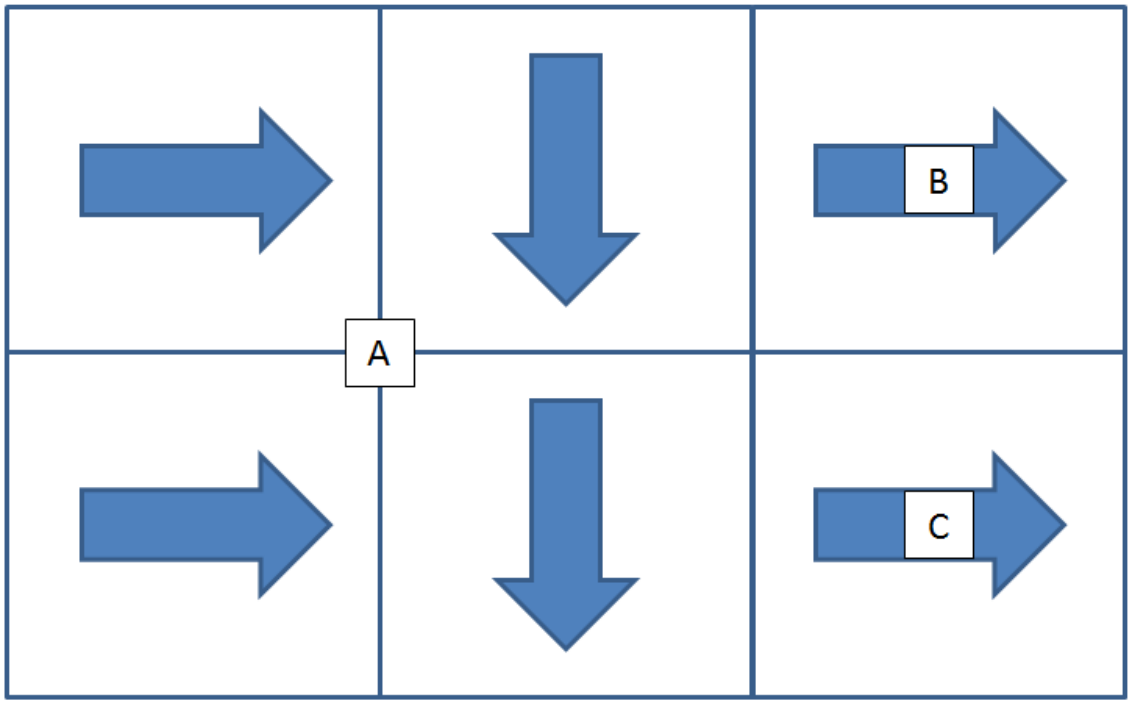

Figure 5-1 Simple Gridcell Connectivity. This 6-cell model would consist of three watershed sub-basins A, B, and C.

The channel routing model uses distributed channel parameters. It is a continuous model, providing time-dependent estimates of flow and depth for the duration of the event, and periods of a year or longer can be simulated. It is a loosely physics-based model, being based on the kinematic wave approximations of open channel flow. The term "loosely" is used here, as kinematic wave approximations are not universally valid for streamflow in natural channels. Each run is solved in a deterministic fashion, however the model can be used with varied parameters to develop a stochastic ensemble. As used herein, it is both a measured-parameter and a fitted-parameter model, as some members of the ensemble use *a priori* datasets and some members of the ensemble use calibrated weighting parameters.

The channel routing model solves the kinematic wave equations for hillslope flow and channel flow. The kinematic wave equations for fluid flow are based on the assumption

that gravity and friction are the only significant forces acting on a water body. These assumptions lead to a momentum equation formulation featuring a consistent stage/discharge or area/discharge relationship, as indicated in Equation 1 and Equation 2.

Equation 1 – Kinematic Wave Momentum Balance, Hillslope Flow (Koren, et al., 2003)

$$q = q_s * h^{\frac{5}{3}}$$

Equation 2 – Kinematic Wave Momentum Balance, Channel Flow (Koren, et al., 2003)

$$Q = Q_0 A^{Q_m}$$

There are only four terms each in Equation 1 and Equation 2. First, there are the dependent variables, representing quantities of flow:

- q in overland, representing flow per unit area
- Q in channel flow, representing total flow (volume per time)

Second, there is a single (constant) parameter representing the channel or hillslope properties:

- q_s in overland, representing a combination of roughness , drainage density (a function of hillslope length), and slope of a hillslope
- Q_0 in channel flow, called the "specific discharge," representing a combination of roughness, slope, and channel shape

Third, there is an independent variable term representing the flow state:

- h in overland, representing depth
- A in channel flow, representing flow area

Finally, there is a flow exponent, a factor of the friction loss and flow shape:

- 5/3 in overland
- Q_m in channel flow (estimated based on channel shape, or calibrated)

The routing model combines these equations with expressions of continuity for both channel and hillslope flow to produce time-variant hydrographs. The equation for continuity (or mass balance) on a hillslope is given as Equation 3.

Equation 3 –Mass Balance, Hillslope Flow (Koren, et al., 2003)

$$\frac{\partial h}{\partial t} + L_h \frac{\partial q}{\partial x} = R_s\,, \qquad 0 < x < L_h$$

Where R_s is the excess runoff from the water balance simulation (SAC-SMA), t is time, L_h is the hillslope length, and x is the distance along the hillslope.

The equation for channel routing is similar in form, with area substituted for depth, and with parameters added to convert the depth-based flow from the hillslope equation into a volumetric basis. It is shown in Equation 4.

Equation 4 –Mass Balance, Channel Flow (Koren, et al., 2003)

$$\frac{\partial A}{\partial t} + \frac{\partial Q}{\partial x} = (q_{Lh} + R_g)\frac{f_c}{L_c}, \qquad 0 < x < L_c$$

Where q_{Lh} is the overland flow (from Equation 3 and Equation 1) and R_g is the estimate of slow runoff/groundwater seepage from the water balance (SAC-SMA). L_c is the channel length within a cell, and f_c is the grid cell area.

The channel routing model requires an estimate of fast and slow subsurface runoff for each grid cell of interest. In practice, these estimates are passed from SAC-SMA continuously during runs, with no user input.

The channel routing model requires, as input, estimates of 7 spatially variable parameters which are used to calculate the independent variables of the above equations: overland slope (Sh), overland roughness (nh), stream channel density (D), channel slope (Sc), channel roughness (nc), channel shape flow parameter (β), and channel top width parameter (α). The specification of these parameters is discussed in the following section.

HL-RDHM IN THE TAR RIVER BASIN

HL-RDHM is used to generate an upstream boundary condition for ADCIRC and HEC-RAS. HL-RDHM is subject to inherent errors. These are mitigated through the use of a 128-member ensemble which includes both *a priori* and calibrated datasets.

The purpose of modelling the Tar River Basin in HL-RDHM was to generate a consistent upstream flow boundary condition for both ADCIRC and HEC-RAS. It is desirable to have a completely error-free boundary condition, so that all errors in each simulation can be associated with their respective modelling schemes, but this is impossible: even if both models' domains terminated at an observation station, many of the storms to be studied resulted in physical damage to the relevant gauges leaving large gaps in the information available. Therefore, HL-RDHM is used to "fill in the gaps" and produce estimates where there are no gauges.

HL-RDHM as used here is an inherently physics-based, measured-parameter model. This type of model is excellent at testing scientific relationships and predictions, but can be subject to errors from multiple sources. Errors in the model can be inherited during initial land property observation, during the conversion of real observed properties to theoretical model parameters via empirical relationships, and finally due to the natural change in the physical state of the basin over time. For example, one might take a LIDAR elevation dataset (subject to measurement inaccuracies from ground properties, or to flaws in the light and detection equipment), process that LIDAR dataset via some empirical metrics to provide an estimate of canopy cover fraction (subject to inaccuracies in identifying trees and vegetation using just shape data, for example mistaking oddly-shaped trees for hills or rivers for roads), only to have those estimates become even less accurate during

and after a severe storm, which might strip large areas of vegetation. Each of the many parameters used by each model is subject to these errors, meaning the overall model inherits errors from potentially hundreds of independent sources. Quantifying and eliminating these errors as they are generated is impossible.

Instead, these errors are mitigated through the use of localizing adjustments and the incorporation of an ensemble. The ensemble members match the weightings developed for use with the ADCIRC Storm Guidance System- Scalable, Terrestrial, Ocean, River, Meteorological (ASGS-STORM):

> *Computational resources allowed for a total of 128 riverine model simulations using HL-RDHM to be performed in real-time for each 6-hour update, corresponding to new QPFs issued by the HPC. These ensemble members were designed to encompass uncertainty in the rainfall forcing (estimated and forecast) and model parameters. The 128 ensemble included four different parameter sets (designated event-based, automatic, multiple basin, and a priori) with three of the parameter sets multiplied by 16 different rainfall multipliers that are uniformly distributed between 0.8 and 1.2. The last parameter set (a priori) was multiplied by 5 different rainfall multipliers, along with 16 channel routing perturbations. Thus, with the first three parameter sets there are 48 members of the ensemble with the last parameter set providing 80 members of the ensemble. (Dresback, et al., 2013)*

The channel routing perturbations in the above quote were applied to the channel routing model (Equation 2) and include four Q_0 factors, varied evenly between 0.6 and 1.2, and four Q_m factors with values of 0.3, 0.5, 0.7, and 1.0. In the ASGS-STORM system, Dresback et al. then combined these estimates with assimilated data to provide forecasts (2013). For this comparison study, a different method was used. The same 128-member ensemble was run, but instead of assimilating data in real-time, the best-performing member was selected by comparing each ensemble member's runoff to observations taken at USGS Station 02083500 Tar River at Tarboro.

Each simulated member's predicted river flow was compared to observed data and weighted using the Nash-Sutcliffe method of quantifying model efficiency, described in Appendix B. The results of these ensemble comparisons are included in Appendix B.

ADCIRC

General description of ADCIRC

ADCIRC is an unstructured mesh finite element hydrodynamic model. It is highly developed, as it has been in use for over 30 years to understand oceanographic circulation phenomena (Blain & Massey, 2007; Dietrich, et al., 2012; Kolar, et al., 2009; Martinez, et al., 1998; Szpilka, et al., 2016).

ADCIRC is a distributed model that solves for state variables over an unstructured mesh using spatially variable parameters. ADCIRC as applied here is a continuous model, designed to predict the behavior of the model domain over an extended period. ADCIRC is a physics-based model solving the shallow water equations. Notably in the model configuration used here, the ADCIRC river model represents a calibrated model, as channel geometries were determined based on observed river behavior (Tromble, 2011). ADCIRC is partially a fitted-parameter model (e.g. roughness, GWCE weighting factor) and partially a measured-parameter model (e.g. bathymetry).

As used here, ADCIRC solves the 2D depth-integrated Generalized Wave Continuity Equation (GWCE) for water surface elevation and the momentum equations for velocity (and flux). The specific formulation of the GWCE is described in the model's theory documentation (Leuttich & Westerink, 2004; Kinnmark, 1986; Kolar, et al., 1994).

ADCIRC requires setup information in the form of bathymetric data and parameter sets, and is forced using meteorological data and boundary conditions.

In addition to extensive surveyed bathymetric data, ADCIRC as used here includes spatially distributed parameter sets for the following parameters:

- Surface directional roughness length
- Surface canopy coefficient (used to reduce wind shear due to covering vegetation)
- Manning's n Roughness
- Weighting in the continuity equation
- Horizontal eddy viscosity with respect to depth

In addition, one initial condition is specified at certain points in the domain:

- Initial water surface elevation

ADCIRC can accept a wide variety of constant, periodic, and non-periodic boundary conditions. As used here, ADCIRC uses the following boundary conditions:

- Internal ("island") and external ("mainland") boundaries – zero normal flux, free tangential slip
- Nonperiodic river inflow boundaries – flux specified by external file, free tangential slip
- Periodic open ocean boundaries – surface elevations specified by calculations on external file
- Meteorological forcings – pressure and velocity fields of varying spatial extent

In this case land boundaries were based on predetermined areas of interest.

There are four nonperiodic river inflow boundaries used in ADCIRC, namely:

- Fishing Creek

- Tar River
- Contentnea Creek
- Neuse River

These river boundary conditions were developed by using a data-adjusted HL-RDHM ensemble run to produce rainfall runoff estimates at each location. These river boundary conditions are discussed in further detail in Appendix B.

Meteorological storm forcings vary based on the event, and are discussed in each event's individual section.

Finally the open ocean boundary was specified using equilibrium M2, S2, N2, K2, K1, O1, P1, and Q1 tidal frequencies drawn from a tidal database (Mukai, et al., 2002).

Two meshes were used, a "coarse" mesh and a "fine" mesh. Both are modified versions of the ADCIRC "v9" mesh developed for use in combined hydrologic and hydraulic flood studies of the Tar and Neuse river basins in North Carolina (Blanton & Luettich, 2008). Each mesh's extent and element resolution are discussed in Appendix B.

Surface roughness, vortex, and computational parameter sets were adopted from prior work (Tromble, 2011) shown to be effective for the "fine" mesh during a detailed hindcast of the basin's response to Hurricane Isabel (Dresback, et al., 2013). Maps showing the spatial variation of each parameter are available as Appendix A.

ADCIRC accepts a wide array of possible internal and external boundary conditions. For this study, constant boundary conditions include internal zero-flux boundaries (representing internal islands) and external zero-flux boundaries (representing external land areas). Non-constant boundary conditions include non-periodic flux specifications at the 8m contour of the Tar and Neuse rivers and Fishing and Contentnea creeks, and an

open ocean boundary to the east covering the Atlantic Ocean. Further details on the non-constant boundary conditions used for each storm are provided in each event's hindcast section.

HEC-RAS

General Description of HEC-RAS

HEC-RAS 4.1.0, the most current version available at the start of this research, is a one-dimensional dynamic wave hydraulic model developed by the Hydraulic Engineering Center (HEC) of the Army Corps of Engineers for use as a River Analysis System (RAS) (Brunner, 2010). HEC-RAS is commonly used to model river behavior for flood inundation mapping, flash flood prediction, and many other applications (Fink, et al., 2006; Astite, et al., 2015; Lian, et al., 2013; Ray, et al., 2011; Mejia & Reed, 2011).

HEC-RAS is a distributed model, which takes inputs of bathymetry and roughness at multiple cross-sections in a river. Unsteady HEC-RAS provides results on a time-dependent basis and can therefore be considered a continuous model. HEC-RAS is based on the combined continuity and momentum equations of fluid flow, also known as the Saint-Venant equations, and is therefore a physics-based model. HEC-RAS is typically calibrated to match observed system behaviors, generally using the Manning's roughness term. HEC-RAS as used here is fully deterministic, with measured bathymetry and calibrated Manning's n roughness. In this case the calibration was performed by Abshire (2012).

HEC-RAS parameters include connectivity information, bathymetry, and roughness. Connectivity information in HEC-RAS consists of the top-down layout of the stream network of interest, weighting parameters quantifying the angle of intersection of each

additional channel beyond the first, and the location and number of each cross-section to be used in calculation. In this simulation there is only one reach included for the Tar River, connected and discretized as shown in Figure 5-2.

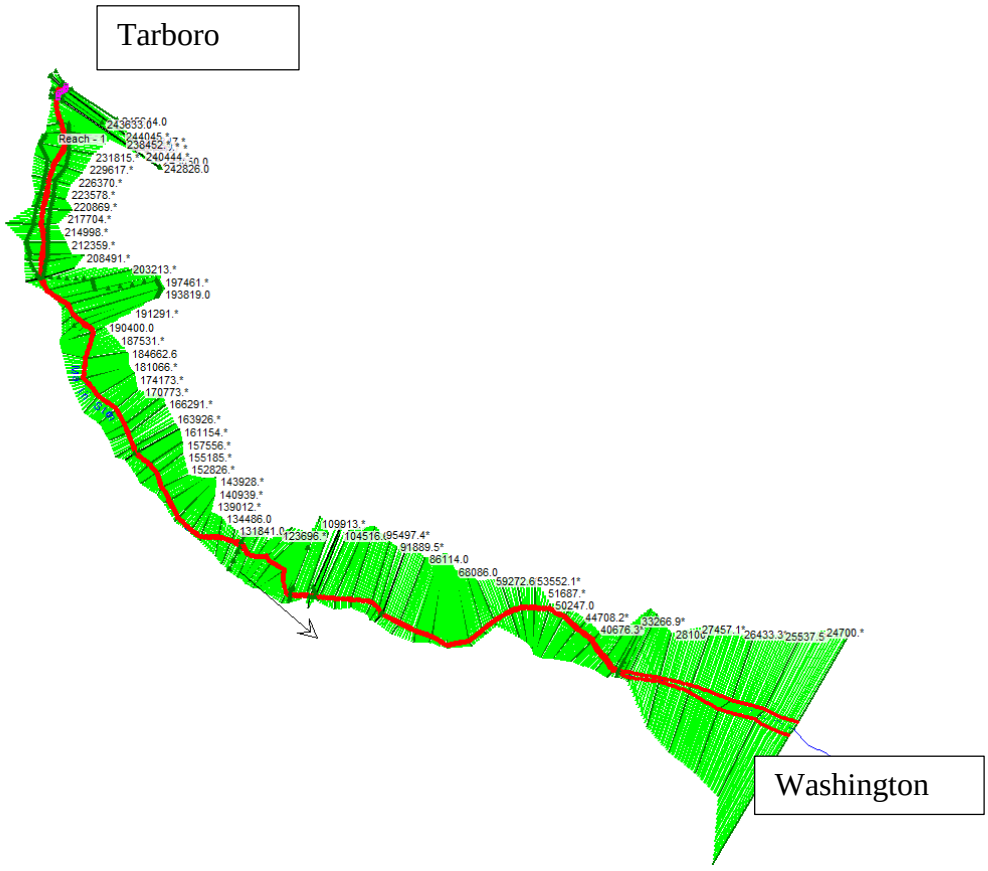

Figure 5-2 Tar River Representation in HEC-RAS

The red line represents the channel, while each green line represents another cross section of interest. Heavy green lines are based on survey data and lighter green lines are interpolated to increase simulation stability. Green shading shows the extent of the floodplains.

Each cross section is parameterized using a defined bottom profile, designated ineffective (or storage) areas, designated bridge sections, and designated Manning's n roughness coefficients. An example of the information used by HEC-RAS at each cross section is shown as Figure 5-3.

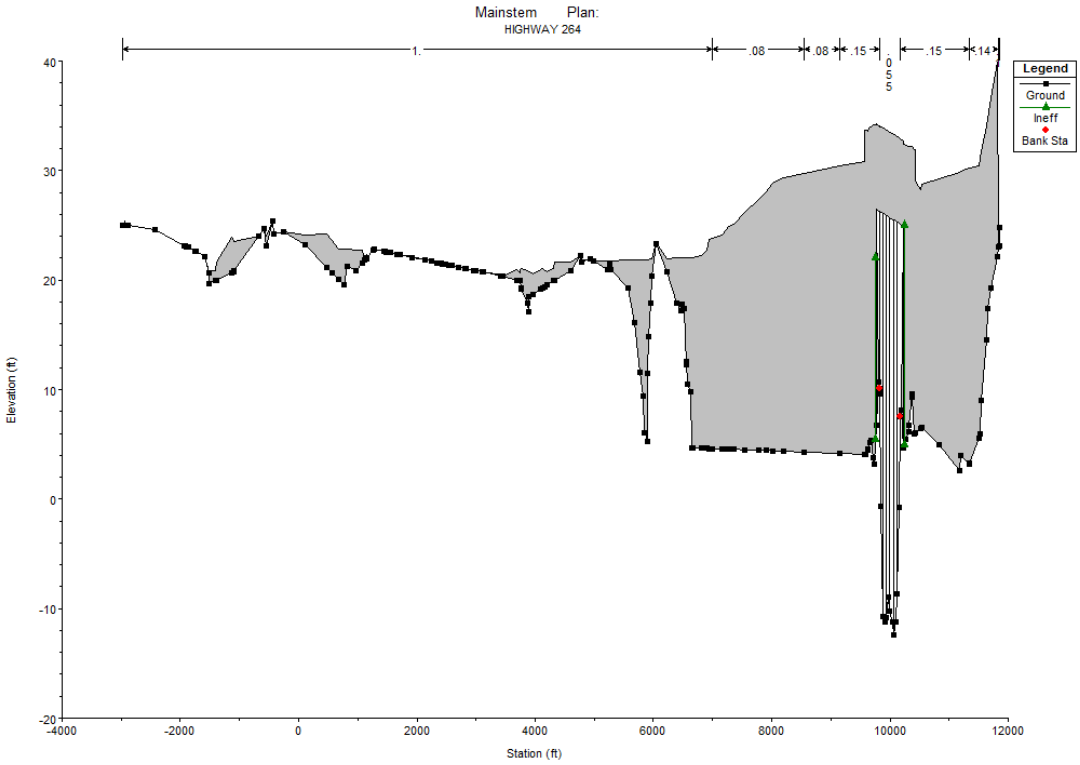

Figure 5-3 Example HEC-RAS Cross Section, Including a Bridge Crossing of Highway 264 Over the Tar River

Cross-sectional information can be input manually using a graphical interface, or it can be generated automatically using GIS software. In practice a combination of both methods is advisable.

HEC-RAS can be operated in a steady (time-invariant) or unsteady (time-dependent) regime. The user must explicitly specify whether the stream reach is subcritical (velocity less than wave celerity), supercritical (velocity greater than wave celerity), or mixed in its flow condition. For an unsteady, mixed flow regime, time-variant boundary conditions are necessary at the upstream and downstream boundaries of each reach. External boundary conditions can be supplied as stage timeseries, flow timeseries, or both. Flow-only boundary conditions also require an initial stage to generate a solution.

HEC-RAS 4.1.0 solves the full 1D form of the Saint-Venant equations, known as the dynamic wave equations, assuming mixed sub- and supercritical flow regimes to provide the incremental change in flow rate (Q) and water surface elevation (z) at each cross section and timestep. Additional information about the formulation of these equations and how they are solved in HEC-RAS software is published by the US Army Corps of Engineering (Brunner, 2010)

Bathymetry, roughness, connectivity, and bridge and ineffective area parameter sets were adapted directly from a model of the Tar River developed by Abshire for evaluating lateral inflows during hurricanes (2012).

For this study, HEC-RAS was run in an unsteady fashion in a mixed flow regime. Run times varied based on event, but computation was performed in 1-hour intervals. Cross sections were interpolated to provide a maximum spacing between sections of 500 feet.

Multiple models were used to develop boundary condition forcings for HEC-RAS. For an explanation of all boundary conditions tested and why the following boundary conditions were selected, see Chapter 6.

COUPLINGS

For the purpose of this research, couplings were implemented in a loose, one-directional fashion. Each model was run independently, with results being passed as manually-inputted boundary forcings for the next model. There are a total of five coupling schemes, summarized below:

- Coupling 1 – Existing System
- Coupling 2 – Coupled System Using Fine ADCIRC
- Coupling 3 – HEC-RAS using Fine ADCIRC's Forcings
- Coupling 4 – Coupled System Using Coarse ADCIRC
- Coupling 5 – HEC-RAS, Fine ADCIRC upstream, Coarse ADCIRC Downstream

Coupling Scheme 1 is shown in Figure 5-4. This is the coupling from HL-RDHM to ADCIRC, where flow from a selected HL-RDHM member is passed to ADCIRC at the river boundaries. This coupling scheme is used to provide a baseline of performance for the existing system, and is used in evaluating Hypotheses 1 and 3.

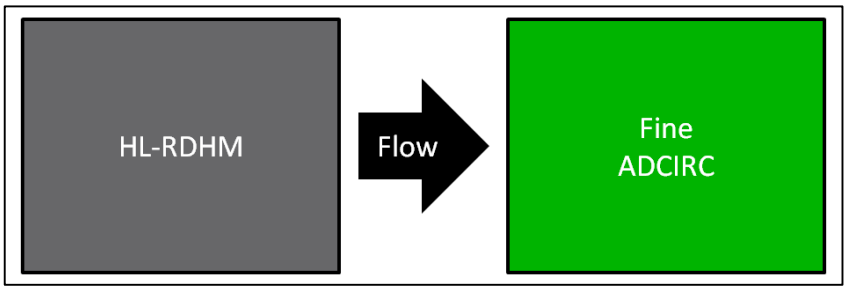

Figure 5-4 Coupling 1 – "Existing System"

Coupling Scheme 2 is diagrammed in Figure 5-5, and consists of the HEC-RAS model, using ADCIRC stage results at the downstream boundary and HL-RDHM flow results at

the upstream boundary. This scheme is used to generate a high-quality downstream boundary condition for use in evaluating Hypothesis 2A.

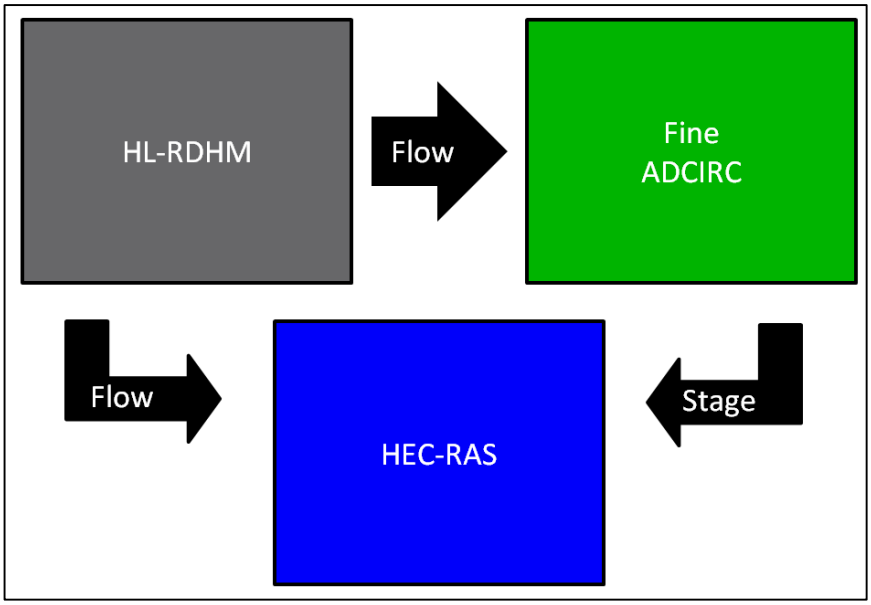

Figure 5-5 Coupling 2 – Coupled System Using Fine ADCIRC

Coupling Scheme 3 is shown in Figure 5-6. This coupling uses results from ADCIRC at the internal boundaries corresponding to the spatial extent of the HEC-RAS river model to provide boundary conditions to that HEC-RAS model. By comparing these results to the results from Coupling Scheme 1, the relative accuracy of ADCIRC and HEC-RAS can be evaluated while isolating the errors at either boundary.

Note that the figure depicts a flow boundary condition at the HEC-RAS upstream boundary – however, in each storm, both flow and stage upstream boundary conditions were tested for suitability and the most accurate boundary condition was chosen, as determined based on comparison to gauge data at the handoff point. This research did not reveal one boundary condition as inherently more accurate.

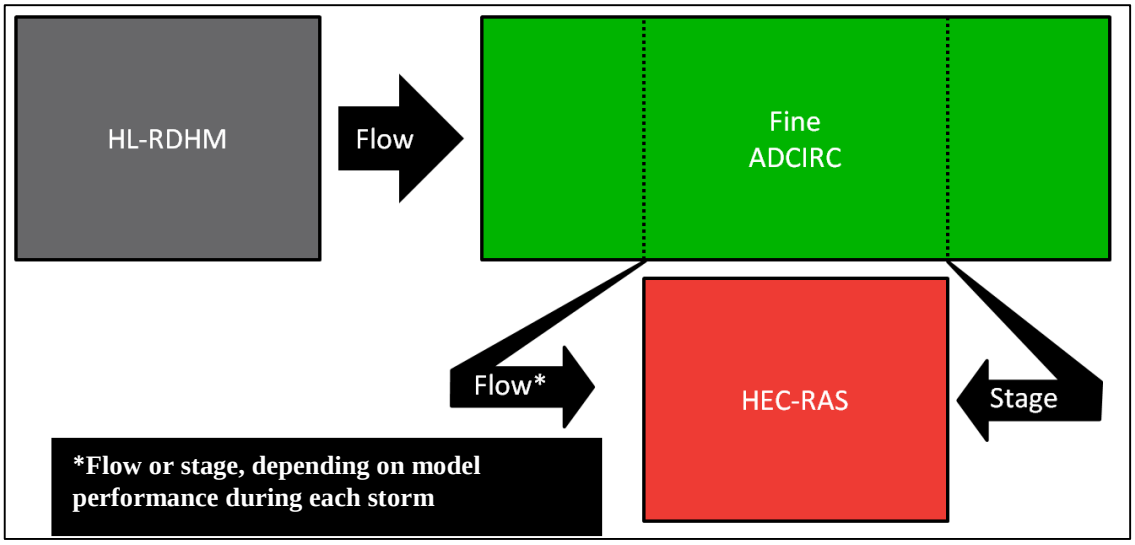

Figure 5-6 Coupling Scheme 3 –HEC-RAS using Fine ADCIRC's Forcings

Finally, two additional couplings were examined (Coupling 4 and Coupling 5), which are conceptually similar to Coupling Schemes 2 and 3, but which use a coarse, riverless version of ADCIRC to provide a downstream stage boundary condition to the HEC-RAS model. These couplings were used to evaluate Hypothesis 2A. They are diagrammed in Figure 5-7 and Figure 5-8.

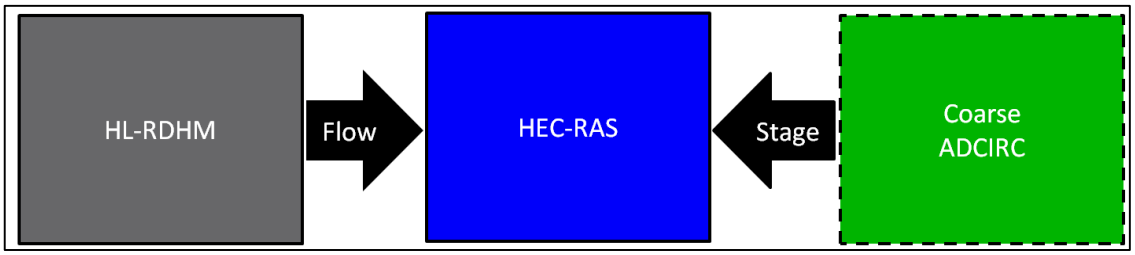

Figure 5-7 Coupling 4 – Coupled System Using Coarse ADCIRC

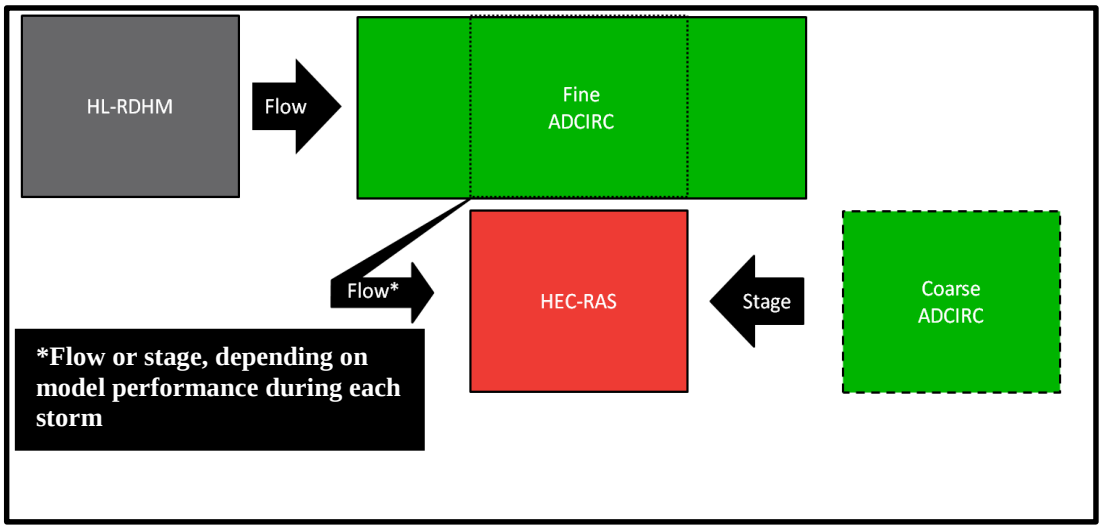

Figure 5-8 Coupling Scheme 5 – HEC-RAS, Fine ADCIRC Upstream, Coarse ADCIRC Downstream

Purpose of Coupling Schemes

Comparisons of model results derived from multiple coupling schemes were used to test the accuracy-related hypotheses as discussed below.

Hypothesis 1 –HEC-RAS Model Is As Accurate As ADCIRC Model

The relative accuracy of HEC-RAS and finely-resolved ADCIRC based on model properties (e.g. resolution, dimensionality, existing parameter sets) is determined in this research by comparing results from Coupling Scheme 1 and Coupling Scheme 3. In these two coupling schemes, both HEC-RAS and the internal, riverine portion of ADCIRC are "forced" with the same information – namely ADCIRC results at the two model internal boundaries.

Note that the results of this hypothesis are only valid for these specific models, with their specific resolutions, calibrations, and forcings.

Hypothesis 2A – HEC-RAS Accuracy Not Affected By ADCIRC Resolution

Whether a river representation is necessary in developing an ADCIRC result for use as a HEC-RAS boundary condition or not is evaluated by comparing model results from Coupling Schemes 2 and 3 to model results from Coupling Schemes 4 and 5.

Hypothesis 3 – HEC-RAS and Coarse ADCIRC Provides Results as Accurate as Fine ADCIRC

While this hypothesis is handled generally in the evaluation of the first two hypotheses, it is of immediate value to answer the question of whether forecasters can or should immediately adopt a coupled HEC-RAS + Coarse ADCIRC scheme instead of a finely resolved ADCIRC scheme for this river basin. To answer this question, the results from Coupling Schemes 1 and 4 should be compared to one another.

Comparison Methods

Model comparisons are discussed in detail in each hindcast's subsection. Reference is made in following sections to Nash-Sutcliffe Efficiency, a statistical measure of model fit, which is described below. Also, for compactness, the results from all coupling methods are plotted on single hydrographs in subsequent sections. A description of how each hydrograph displays information relevant to the hypotheses is also included below.

Nash-Sutcliffe Efficiency

Nash-Sutcliffe Model Efficiency is a statistical measure of the relative correlation of a set of observations at some set of times, compared to a set of model predictions at those times, designed for use with hydrologic datasets (Nash & Sutcliffe, 1970). It is calculated as follows:

Equation 5 - Nash-Sutcliffe Efficiency

$$NSE = 1 - \frac{\sum_{t=1}^{T}(Q_o^t - Q_m^t)^2}{\sum_{t=1}^{T}(Q_o^t - \overline{Q_o})^2}$$

NSE – Nash-Sutcliffe Efficiency

T – total number of timesteps

t – some specific timestep

Q_o – Observed Flow

Q_m – Modelled Flow

NSE values range from 1 to $-\infty$. An NSE of 1 indicates that the model dataset perfectly matches the observed dataset. An NSE of 0 indicates that the model dataset predicts observed data as well as the mean of the observed dataset. A negative NSE means the mean of the observed data is a better predictor of observations than the model being tested. NSE is one of the most widely used skill metrics in hydrology (Gupta & Kling, 2011).

STANDARD COMPARISON HYDROGRAPH

Each event includes hindcast comparisons to gauge data at USGS stations. Results at these stations are plotted in a uniform style for easy legibility. The color and location of results for each coupling scheme are diagrammed below.

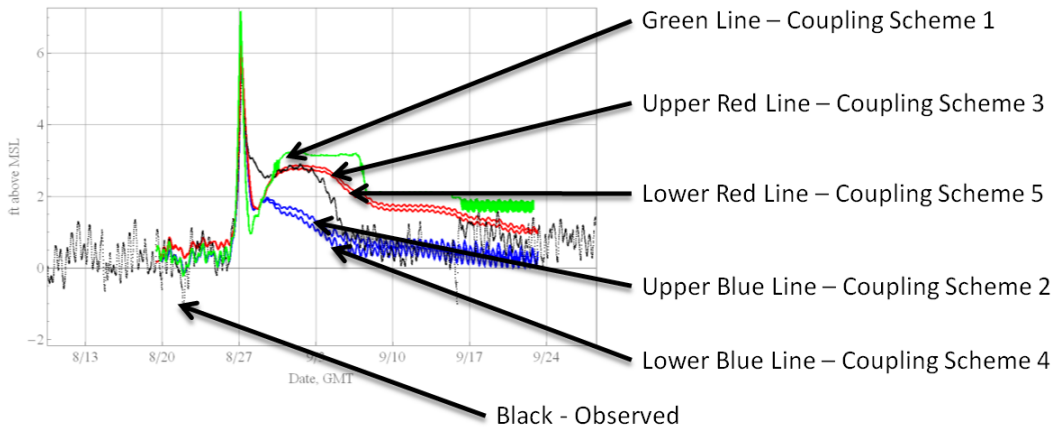

Figure 5-9 Example Comparison Hydrograph

At many gauges, results are dissimilar enough that real conclusions can be drawn simply from visual examination of the hydrographs. The plotting style chosen is designed to allow visible evaluation of all hypotheses (based on the assumption that gauge results are accurate). Figure 5-10 indicates the relevant comparisons the reader is encouraged to make when viewing these hydrographs. First, if the green line shows better agreement to observations than the upper red line, this disagrees with Hypothesis 1. Second, if the red and blue lines show visible separation, the magnitude of this separation is the error in Hypothesis 2A. Finally, if the green line shows better agreement to observations than the lower blue line, this disagrees with Hypothesis 3.

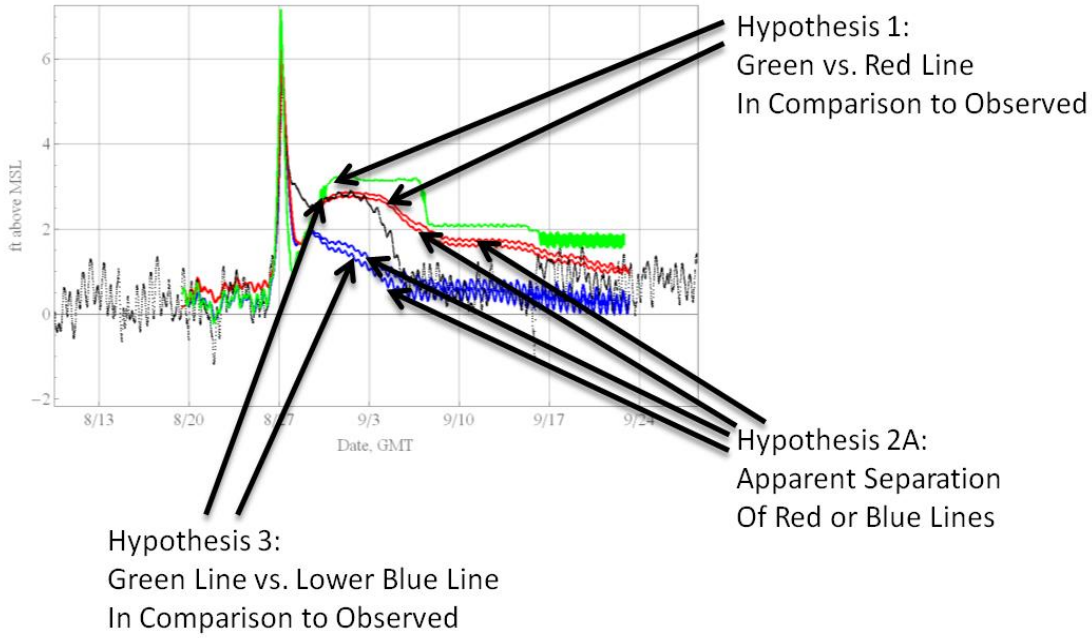

Figure 5-10 How to Read Comparison Hydrograph

6. SELECTING APPROPRIATE BOUNDARY CONDITIONS

Using the results of this modelling effort, there are many boundary conditions possible for implementation as forcings for HEC-RAS. To simplify modelling efforts, the first storm to be studied (Irene) was used as a test case for all possible boundary condition combinations to determine which boundary conditions were most appropriate. This event was selected for this study as it exhibits both significant river flows as well as significant downstream surge.

NOMENCLATURE

For clarity, the following designations are used to refer to boundary conditions. "ADCIRC-Rivers" designates a boundary condition derived from ADCIRC results using a fine grid featuring resolved Tar and Neuse Rivers and forced with HL-RDHM flows for both of those rivers. Similarly "ADCIRC-NoRivers" designates a boundary condition derived from the riverless ADCIRC grid. "RDHM" designates results taken from the HL-RDHM simulation at the HRAP grid cell for the station in question.

UPSTREAM BOUNDARY CONDITIONS

Upstream boundary conditions for the HEC-RAS model were given at the location of USGS Station # 02083500 Tar River at Tarboro. The following four methods were tested for upstream boundary conditions:

- RDHM-Q
- ADCIRC-Rivers-Stage
- ADCIRC-Rivers-Flow
- ADCIRC-Rivers-Stage & Flow

These four were selected for the following reasons. First, the operational model ASGS-STORM uses RDHM runoff estimates at the upstream boundary, so RDHM flows needed to be considered. However, it must be noted that the RDHM runoff information passed to HEC-RAS is from a different location than the RDHM runoff information that is passed to ADCIRC, as the handoff point for the HEC-RAS model (at Tarboro) is approximately 7 miles downstream of the two Tar River Basin RDHM handoff points for ADCIRC. Of note, in that 7 mile span of river, Fishing Creek joins Tar River. This means that the "RDHM-Q" boundary condition uses a 1D kinematic wave model to route waters through that confluence, whereas the ADCIRC boundary conditions use a 2D dynamic wave model to do the same.

Downstream Boundary Conditions

Downstream boundary conditions for the model were given at the location of USGS 02084472 Pamlico Sound at Washington, NC. The following four downstream boundary conditions were tested, yielding a total of 16 possible model configurations.

- ADCIRC-Rivers-Stage
- ADCIRC-Rivers-Flow
- ADCIRC-Rivers-Stage & Flow
- Constant Stage (0 ft above MSL)

Initial reduction of redundant BC types

It was quickly determined that HEC-RAS treats a combined stage/flow hydrograph input as a stage-only hydrograph input. Figure 6-1 and Figure 6-2 show HEC-RAS input and output flows and stages for one of the test scenarios using a combined stage/flow hydrograph at the upstream boundary:

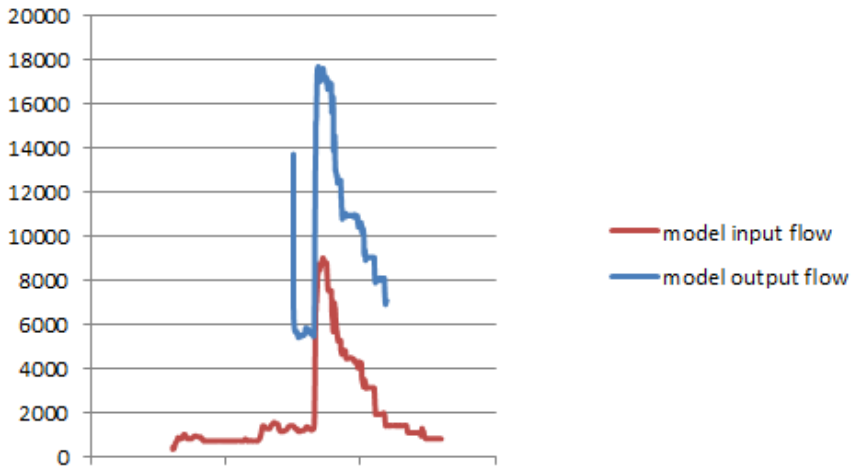

Figure 6-1 HEC-RAS Input And Output Flows (In Combined BC)

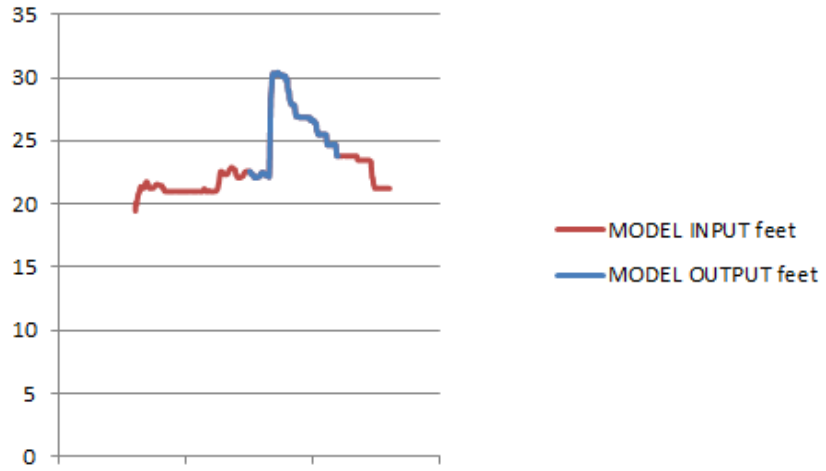

Figure 6-2 HEC-RAS Input and Output Stages (In Combined BC)

These indicate that adding a flow hydrograph to a stage boundary condition does not change model behavior.

It was found that flow-only boundary conditions at the downstream boundary were not sufficient to define the behavior of the river. Flow in the Tar River is typically subcritical, and without a stage downstream boundary, the dynamic wave equation's solution to the resulting water profile is indeterminate. Figure 6-3 shows a typical hydrograph calculated by HEC-RAS using a flow-only downstream boundary condition, in this case in the middle of the river domain at USGS 02083500 Tar River at Greenville, NC:

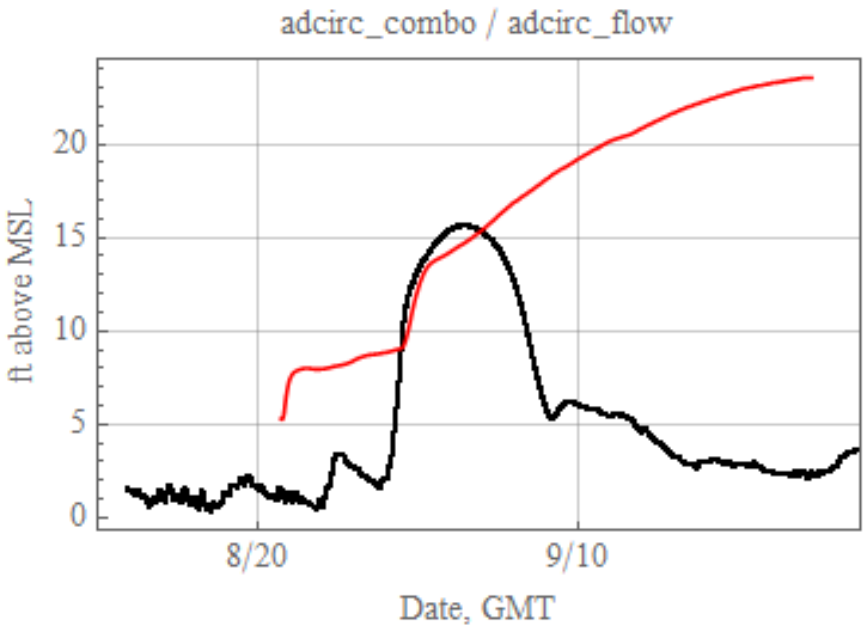

Figure 6-3 HEC-RAS Response At Greenville, NC Using ADCIRC Flow Upstream and Downstream. Model Results in Red, Observations in Black.

It was found that similar behavior (instability at the downstream boundary) was inevitable when a stage boundary condition was not set at the downstream side of the HEC-RAS model. Therefore the original 4x4 set of permutations on the boundary conditions was narrowed to a 3x2 set of boundary conditions listed in Table 6-1.

Table 6-1 - Boundary Conditions

Upstream Boundary Conditions	Downstream Boundary Conditions
RDHM Q	Stage 0
ADCIRC Stage	ADCIRC Stage
ADCIRC Flow	

ALTERNATE LABELS

One of the goals of this research is to perform an "apples-to-apples" comparison of the 1D and 2D models. Towards that end, the two ADCIRC upstream boundary conditions have been labeled "fair" – this is to indicate that, in those cases, both the ADCIRC river domain and the HEC-RAS model were given the same information. The RDHM-Q boundary condition (when coupled with riverless data at the downstream boundary) is

labeled “realistic,” as it best mimics the type of data that would be available during an operational situation.

Performance at USGS Gauges

Skill of each boundary condition combination was quantified by comparing model results to gauge data at each of three USGS stations located within the model domain on the Tar River. These gauges are 02083893 Tar River at US 264 Bypass Near Rock Springs, NC, 02084000 Tar River at Greenville, NC, and 02084173 Tar River at SR 1565 Near Grimesland, NC. These three gauges’ locations, in addition to the location of 02083500 Tar River at Tarboro, NC and 02084472 Pamlico Sound at Washington, NC are shown in Figure 6-4. In subsequent sections, the full gauge numbers and names are abbreviated to include only the city names – “Tarboro”, “Rock Springs”, “Greenville”, “Grimesland”, and “Washington,” as indicated in Figure 6-4.

Figure 6-4 USGS Gauge Locations. Imagery courtesy Google Earth

Stage vs. boundary condition plots of simulations at Rock Springs during Hurricane Irene are shown in Figure 6-5. Flow observations were (and are) not collected at this location.

Flow and Stage results at Greenville during Hurricane Irene are compared to observed values in Figure 6-6 and Figure 6-7.

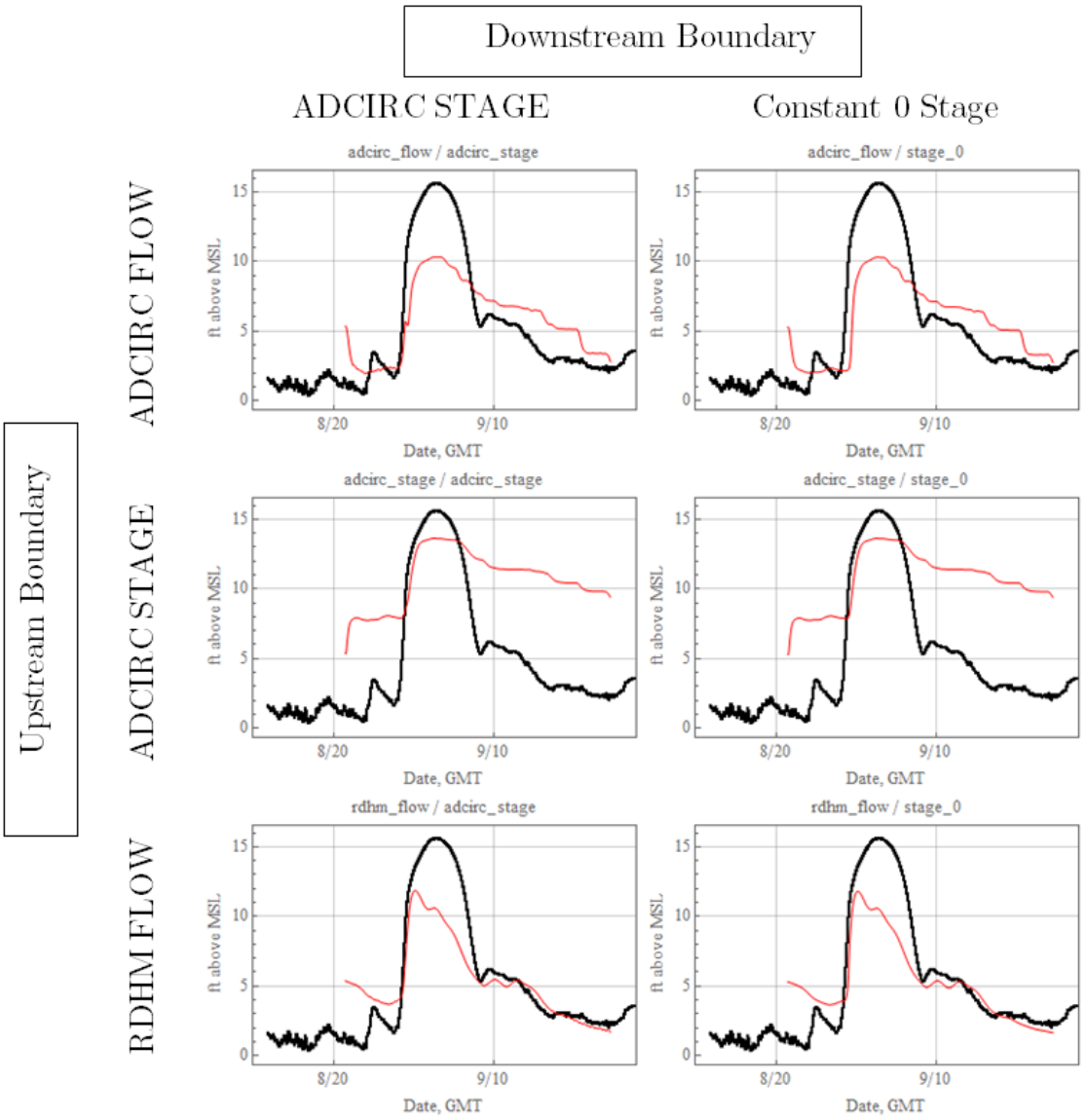

Figure 6-5 Stage Error vs. Boundary Condition Configuration, Rock Spring, NC. Model Results in Red, Observations in Black.

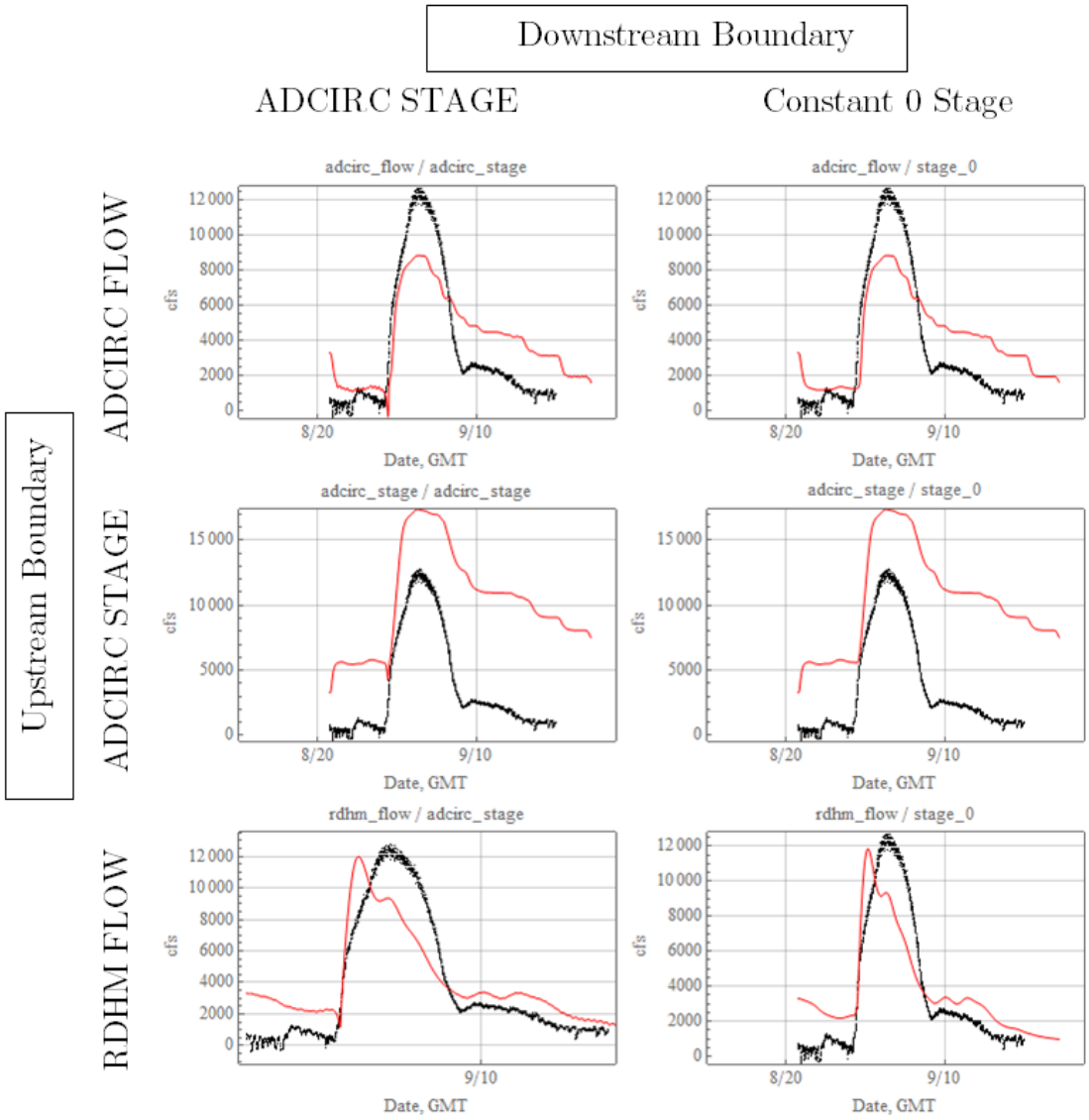

Figure 6-6 Boundary Condition Comparison - Flow at Greenville, NC

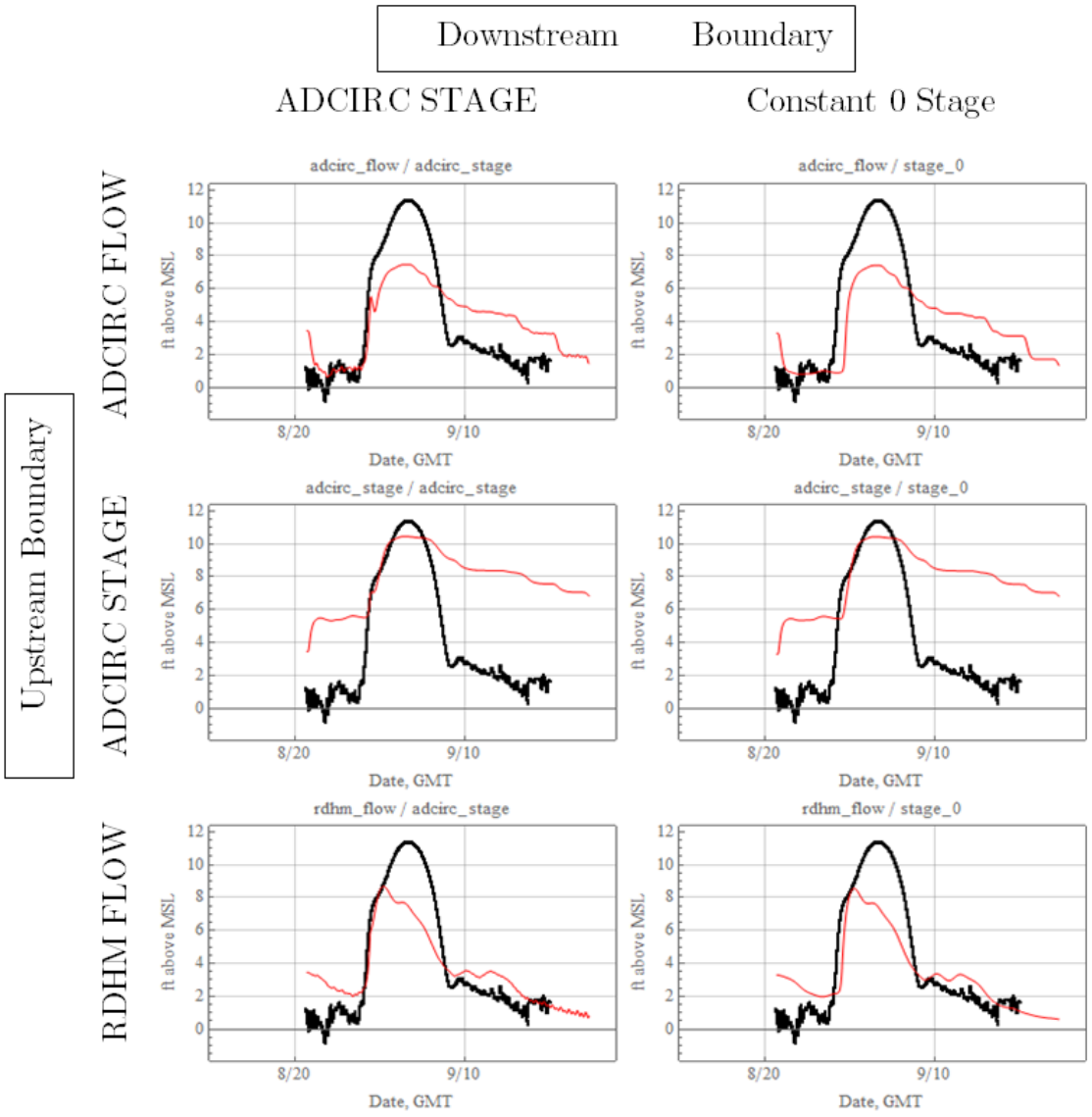

Figure 6-7 Boundary Condition Comparison - Stage at Greenville, NC

Flow results derived from RDHM flow-driven results (Figure 6-6, bottom two graphs) show results closest to peak values as well as values closest to low-flow conditions during the receding limb portion of the event. ADCIRC stage-driven results (Figure 6-6, middle graphs) overestimate flows at all periods of the storm. ADCIRC flow results (Figure 6-6, top two graphs) underestimate peaks while overestimating falling limb flows.

As in Rock Springs, flow-derived peak stage predictions (Figure 6-7, top and bottom rows) do not match the quality of the ADCIRC-stage derived results (Figure 6-7, middle

rows) at this site for any boundary condition combination. And as in Rock Springs, both RDHM-driven models (Figure 6-7, bottom rows) show excellent agreement with observed base flow/low flow conditions on the receding limb.

The last station in the Tar River Basin is located near Grimesland, NC. Only stage data is available from this gauge. HEC-RAS model comparisons to observations during Hurricane Irene at this gauge are shown in Figure 6-8. The two-peaked shape of the hydrograph at Grimesland is particularly illustrative of the impact of storm surge on riverine flooding, with all "0-stage" downstream results (Figure 6-8, right column) showing an absence of a sharp initial storm peak. All models that included ADCIRC results at the downstream boundary (Figure 6-8, left column) overestimated the surge peak. In considering the impact of upstream boundary conditions, the runoff-driven peak (the "broader" peak) results mimic behaviors at upstream gauges – RDHM-driven results (Figure 6-8, bottom row) underestimate peaks, ADCIRC-stage driven results (Figure 6-8, middle row) capture peaks but overestimate falling limb baseflows, and ADCIRC-flow driven results (Figure 6-8, top row) lie somewhere in between, with reasonable representation of falling limb behavior.

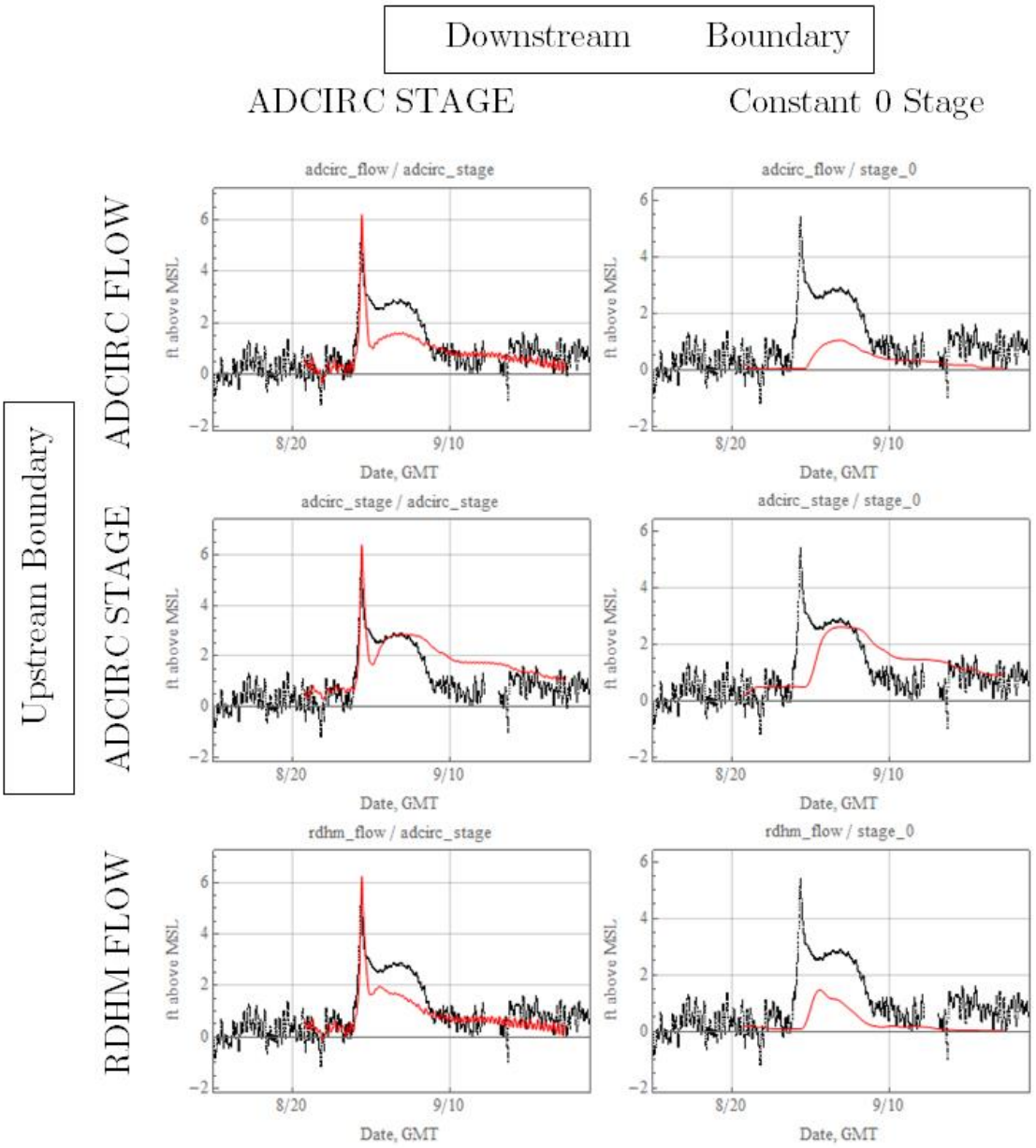

Figure 6-8 Boundary Condition Comparison - Flow at Grimesland, NC

Conclusions

For this comparison, differences between model results and gauge results were striking. All model configurations are driven by conceptual models, yet all models showed fundamentally different river behavior compared to gauge results with regards to stage. The boundary condition set that appears to produce the most "realistic" hydrographs with regards to stage consists of either ADCIRC flows or stages at the upstream boundary with ADCIRC stage at the downstream boundary.

Future work

Both ADCIRC-derived and RDHM-derived upstream boundary conditions are ultimately derived from the same HL-RDHM simulation data. The presence of pre-storm overestimated baseflows in the ADCIRC boundary conditions suggests that baseflow errors may be related to the representation of the confluence zone (between Fishing Creek and the Tar River) between the ADCIRC RDHM handoff point and the HEC-RAS RDHM handoff point.

Receding limb problems may be due to the wetting and drying algorithm in ADCIRC (details of which are discussed by Dietrich (2005)), or due to the coarse resolution of the Tar River ADCIRC mesh used here (discussed by Tromble (2011) and typified by the use of a single-element-wide river). Greater resolution in the ADCIRC model or the inclusion of partial wetting and drying algorithms may produce more realistic falling-limb behavior in stage results derived from ADCIRC results.

7. HURRICANE IRENE

Hurricane Irene serves as the first test case. This section consists of a description of the general storm characteristics, a list of the forcing data used to simulate the event, a discussion of the quality of the generated river model boundary conditions, and a detailed comparison of the resulting river model hindcasts.

Hurricane Irene was a severely damaging event, resulting in multiple fatalities and billions of dollars in damage (NOAA, 2012). Within the model domain, Irene was typified by moderate-to-dry antecedent soil moisture conditions, intense coastal rainfall, and high wind speeds.

Antecedent soil moisture conditions in many areas were saturated, but in the Tar River Basin soil moisture was slightly below typical, as shown in Figure 7-1 courtesy of the NWS.

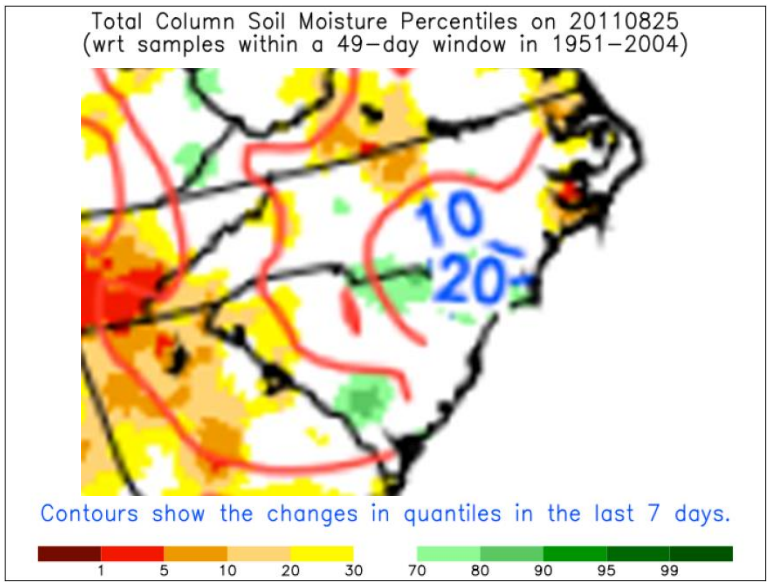

Figure 7-1 Soil Moisture Conditions Two Days Prior to Hurricane Irene's NC Landfall (NOAA, 2012)

Perhaps due to these antecedent conditions, high rainfall totals (exceeding 15 inches (NOAA, 2012)) did not produce significant flooding at Tarboro. At Greenville, river stages exceeded NOAA designated flood stage by two feet, and at Pamlico river stages exceeded flood levels by three feet. This indicates that significant lateral inflows were present in the river system within the model domain. Gauge results at two tributaries of the Tar River, namely Chicod and Town Creeks, support this conclusion. In turn, that means that Irene as a case study will represent model behavior at times when accurate rainfall runoff estimates at the upstream boundary will be significantly below the total flow in the river at the downstream boundary condition due to lateral inflows.

Irene made landfall in North Carolina as a Category 1 hurricane. It struck near Cape Lookout, NC on August 27, 2011 before traversing northwards along the coast and Outer Banks. The strongest sustained winds observed from the system during landfall were experienced just southeast of Pamlico Sound and exceeded 90 mph (NOAA, 2012). For this reason, Irene may prove a valuable "typical" hurricane with respect to wind forcings, in which substantial wind-driven surge ought to be predicted at the downstream end of the modelled river domain.

FORCING AND VALIDATION STRATEGY

Datasets used to force and validate each model are listed in Table 7-1, below:

Table 7-1 - Hurricane Irene Forcing and Validation Datasets

Model	Forcing Datasets	Source(s)	Validation Datasets	Source(s)
Hydrologic Model (HL-RDHM)	Stage IV Multisensor QPE	(NWS NCEP, 2011)	USGS Gauge 02083500 Tar at Tarboro Observed Flow	(USGS, 2015)
Ocean model (ADCIRC)	Hindcast Winds (OWI); Tidal Database	(Oceanweather Inc., 2001); (Mukai, et al., 2002)	Realtime wind speed & direction from NOAA NOS Buoys; coastal tidal gauges	(NOAA, 2015); (NOAA, 2013)
River Models (ADCIRC, HEC-RAS)	Hydrologic and ocean model results		Real time flow and stage measurements (5 sites), high water marks with timings	(USGS, 2015), (McCallum, et al., 2012)

Validation of the hydrologic model is discussed in Appendix B. Validation of the ocean model is discussed in Appendix C. The validation of the two river models under comparison is of prime interest in addressing the questions posed by this research, and is discussed in detail in the following sections.

BOUNDARY CONDITIONS

To achieve an objective comparison of each modelling method, the error types and magnitudes present in boundary conditions should be examined and compared to the model error types and magnitudes within the shared river model domain. To quantify these errors, model results are compared to observed flow and stage timeseries collected at USGS 02083500 Tar River at Tarboro and USGS 02084472 Pamlico Sound at Washington, respectively.

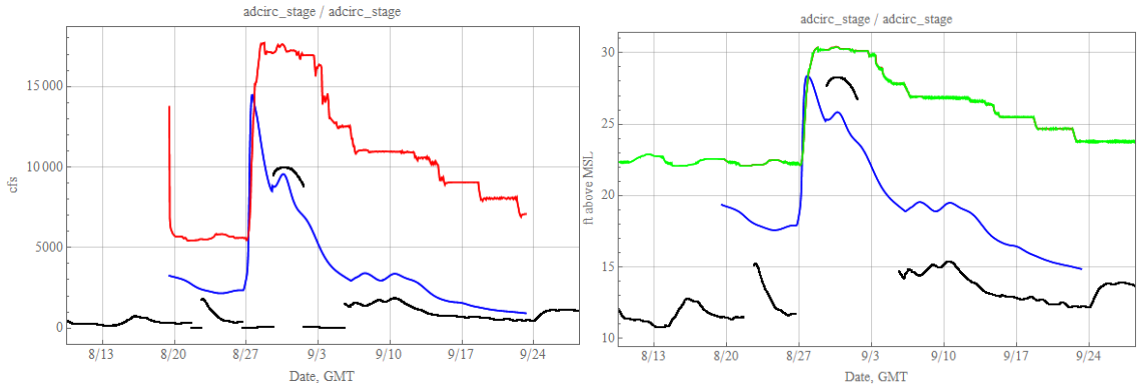

Figure 7-2 - Tar River at Tarboro, NC. ADCIRC results in Green, ADCIRC results interpreted by HEC-RAS in red, stage solved from HL-RDHM Flows in Blue, observations in black. Left panel flow, right panel stage

Figure 7-2 shows the stage results for the two forcing models at the upstream boundary of the river model overlaid with observations taken at USGS 02083500 Tar River at Tarboro. As shown, ADCIRC's internal results (green) and the results from ADCIRC used to provide a forcing to HEC-RAS (red) are virtually identical, and consistently overpredict baseflow and peaks. Peak timing is approximately accurate, but peak duration is extended. HL-RDHM was used to force the HEC-RAS model as well, which resulted in the stage results shown in blue – these results accurately predict peak stages, but estimate that these peaks will occur earlier than was observed.

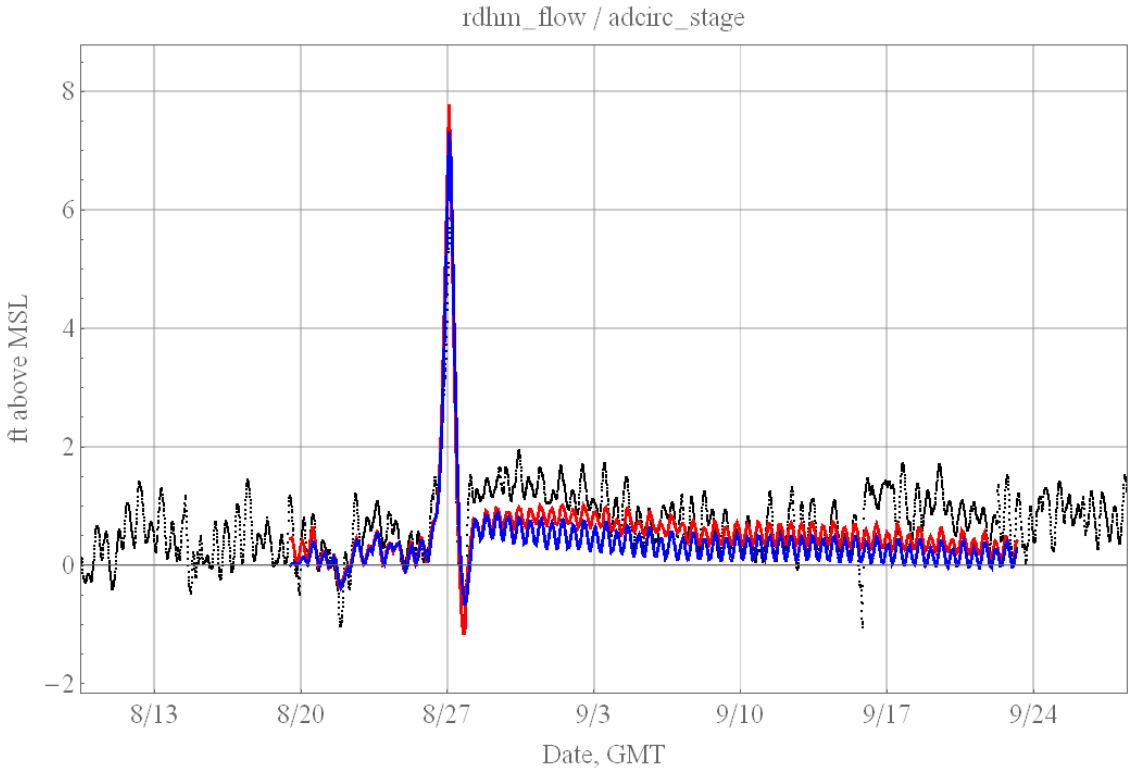

Figure 7-3 - Pamlico Sound at Washington - ADCIRC with rivers on in Red, ADCIRC without rivers resolved in Blue

Figure 7-3 shows forcing model results at the downstream boundary of the river model compared to observations at USGS 02084472 Pamlico Sound at Washington. As expected, the incorporation of rivers in ADCIRC (in Red) resulted in higher overall predicted stages, likely due to the influence of river fluxes. Peak timing is accurate, but both models slightly overpredict the surge peak. As a general note regarding storm form, note that the river peak observed around 9/1 at Tarboro was largely attenuated prior to reaching this downstream location.

RIVER DOMAIN RESULTS

Each model's overall performance in the river domain was evaluated using observations at USGS gauge stations, high water marks, and inundation mapping.

Figure 7-4, Figure 7-5, and Figure 7-6 show modeled and observed stage at three USGS gauges. Flow measurement was not taken at Rock Springs or Grimesland during this event.

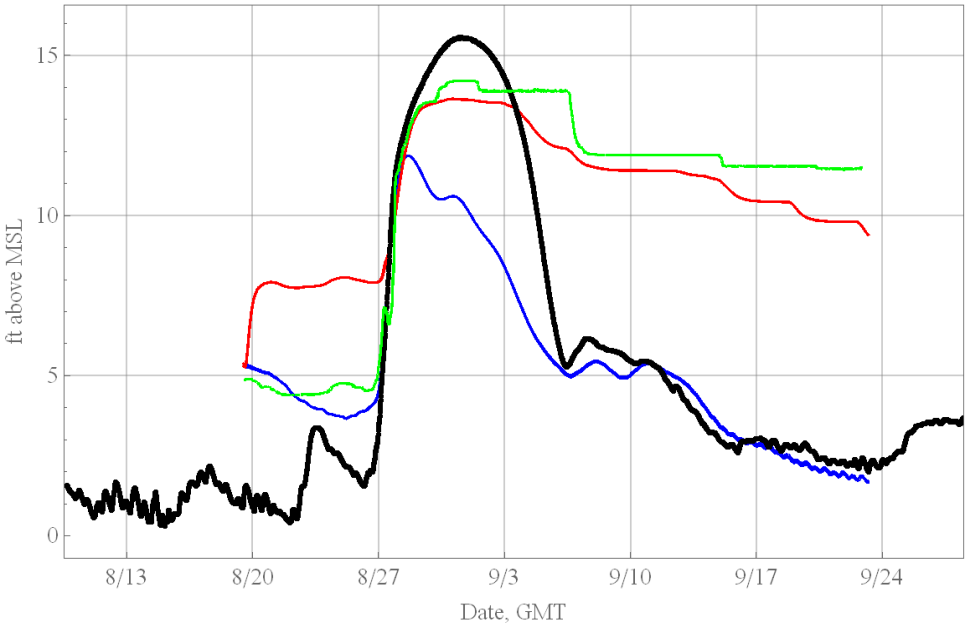

Figure 7-4 Tar River at Rock Springs, NC. ADCIRC results in Green, ADCIRC results interpreted by HEC-RAS in red, stage solved from HL-RDHM Flows in Blue, observations in black

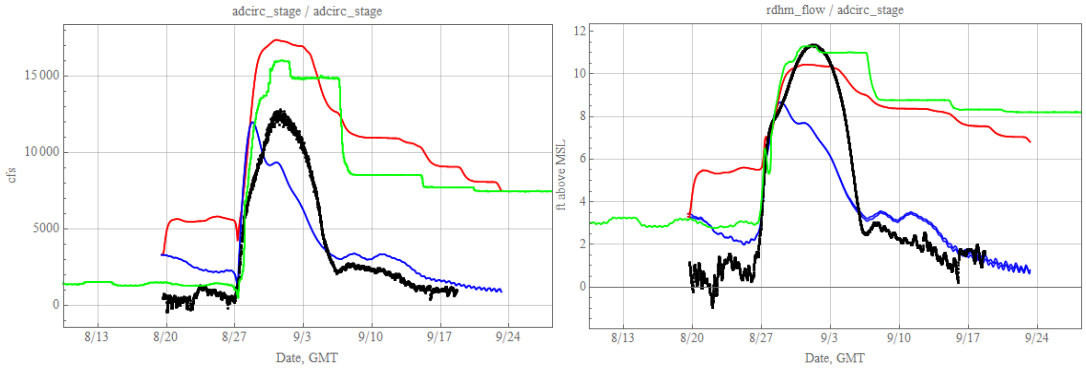

Figure 7-5 Tar River at Greenville, NC. ADCIRC results in Green, ADCIRC results interpreted by HEC-RAS in red, stage solved from HL-RDHM Flows in Blue, observations in black. Left panel flow, right panel stage

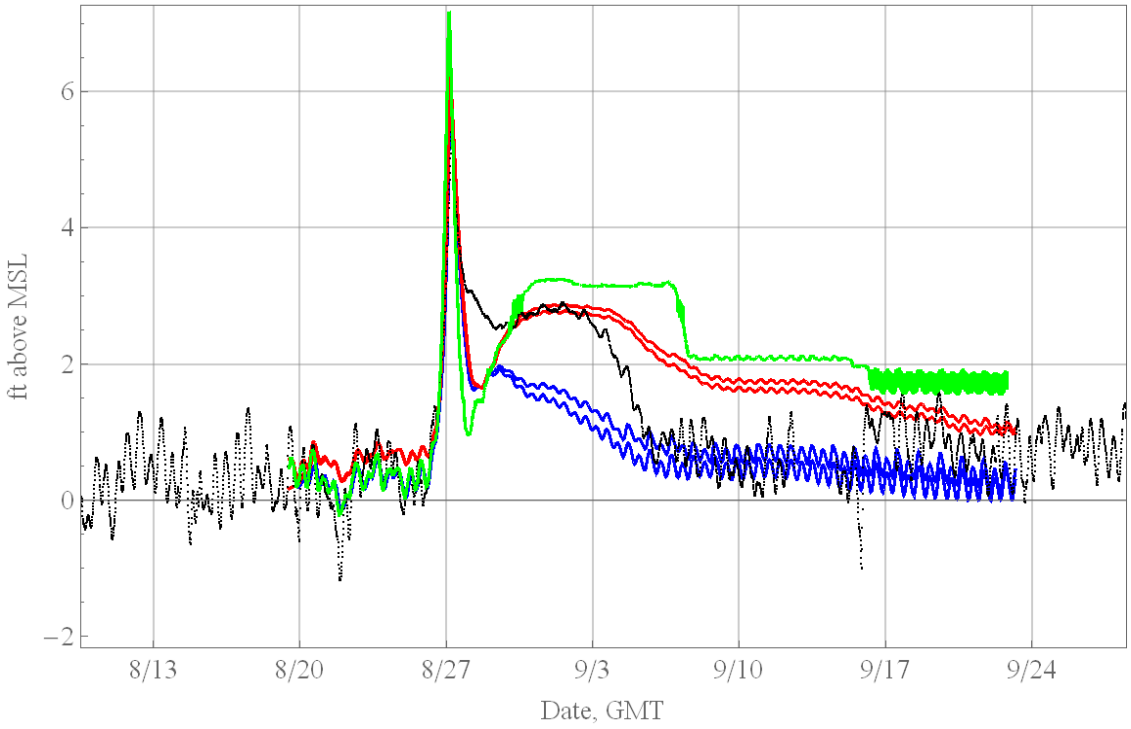

Figure 7-6 Tar River at Grimesland, NC. ADCIRC results in Green, ADCIRC results interpreted by HEC-RAS in red, stage solved from HL-RDHM Flows in Blue, observations in black

Each graph shows observations in black with ADCIRC results in green. HEC-RAS forced with ADCIRC's solution at Tarboro is shown in red. HEC-RAS forced with HL-RDHM flows at Tarboro is shown in blue. Two lines are shown for each HEC-RAS solution based on the downstream forcing. One line is calculated using ADCIRC with rivers resolved, and the other is calculated using ADCIRC with rivers unresolved. The solution without rivers is always below the other, as the riverless solution does not include river flows. Observations from this analysis are discussed below.

First, the general shape of each hydrograph is checked. Relatively speaking, the rising limb for all solutions is well-formed. Initial baseflow is overestimated in ADCIRC-forced results. Rainfall-driven peaks are largely underestimated, with three exceptions: First, ADCIRC correctly captures the rainfall peak at Greenville. Second, ADCIRC

overestimates the rainfall peak at Grimesland, which HEC-RAS (forced with ADCIRC upstream) correctly captures. During the falling limb stage, all models forced with ADCIRC upstream show an artificial "stair-step" pattern and fail to return to baseflow stages.

When comparing the impact of including rivers in the ADCIRC model used as the downstream forcing of a HEC-RAS model, the difference is negligible at Rock Springs and Greenville. The differences between these methods are more significant at Grimesland, but the differences only show a small fraction of total model variation.

When comparing HL-RDHM as an upstream forcing to ADCIRC as an upstream forcing for a HEC-RAS model, HL-RDHM results show timing errors (specifically, early peaks) that are not present in the ADCIRC solution. Furthermore, ADCIRC results are higher overall, and therefore show reduced errors at capturing the peaks (which are generally underpredicted). However, HL-RDHM as an upstream forcing is capable of predicting base- and low-flow conditions, and shows realistic receding limb behavior. ADCIRC as an upstream forcing generates artificial stairstepping which precludes accurate prediction of receding limbs.

When comparing HEC-RAS and ADCIRC as river models, ADCIRC results show a higher prediction. Overall HEC-RAS appears to show higher rate of longitudinal dispersion, which precludes the retention of square- or stepped- waveforms.

Gauge Peak Accuracy by Model

The accuracy of each HEC-RAS simulation with regards to peak timing and stage was calculated. Figure 7-7 shows peak timing errors versus river station, Figure 7-8 shows

peak stage errors versus river station, and Figure 7-9 shows peak flow errors versus river station. River station for each gauge is measured in feet upstream of the model boundary.

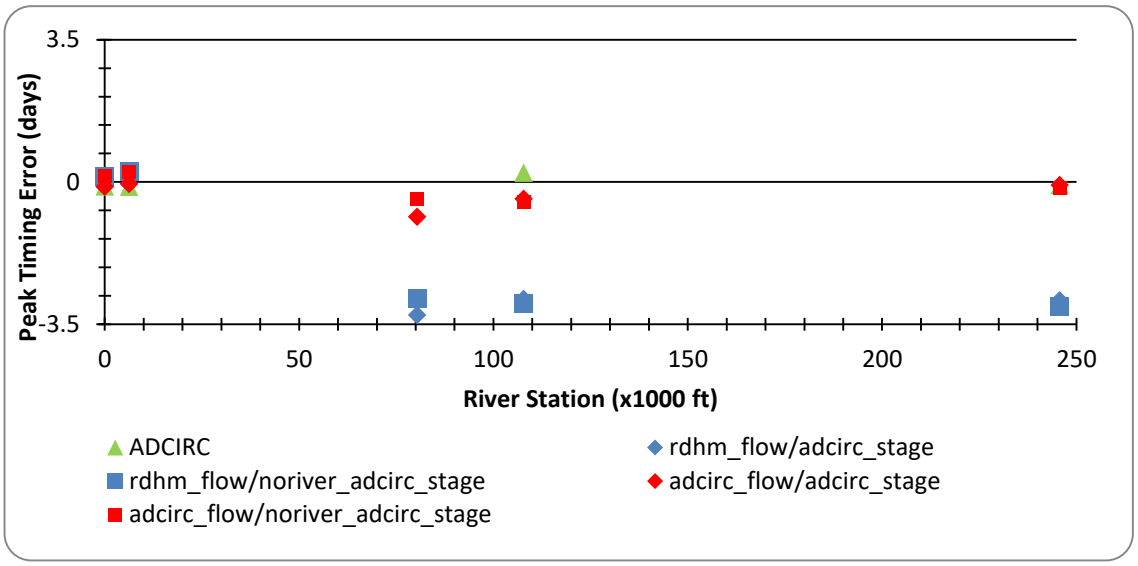

Figure 7-7 Peak Timing Error by Distance Upstream. ADCIRC results in Green, ADCIRC results interpreted by HEC-RAS in red, stage solved from HL-RDHM Flows in Blue, observations in black

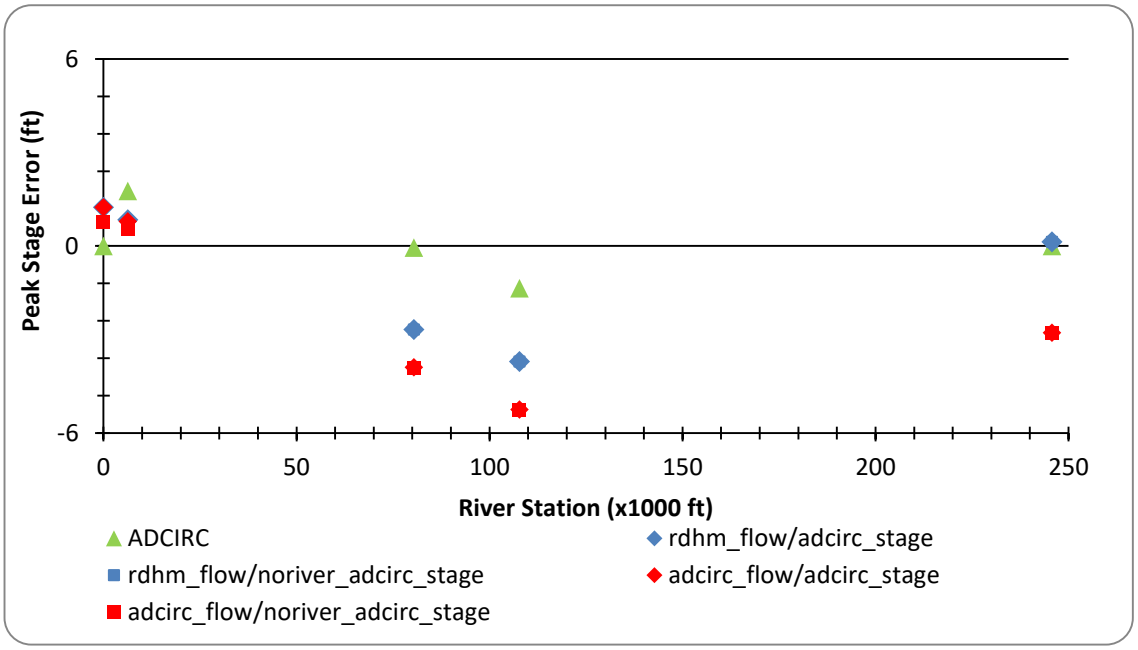

Figure 7-8 Peak Stage Error by Distance Upstream. ADCIRC results in Green, ADCIRC results interpreted by HEC-RAS in red, stage solved from HL-RDHM Flows in Blue, observations in black

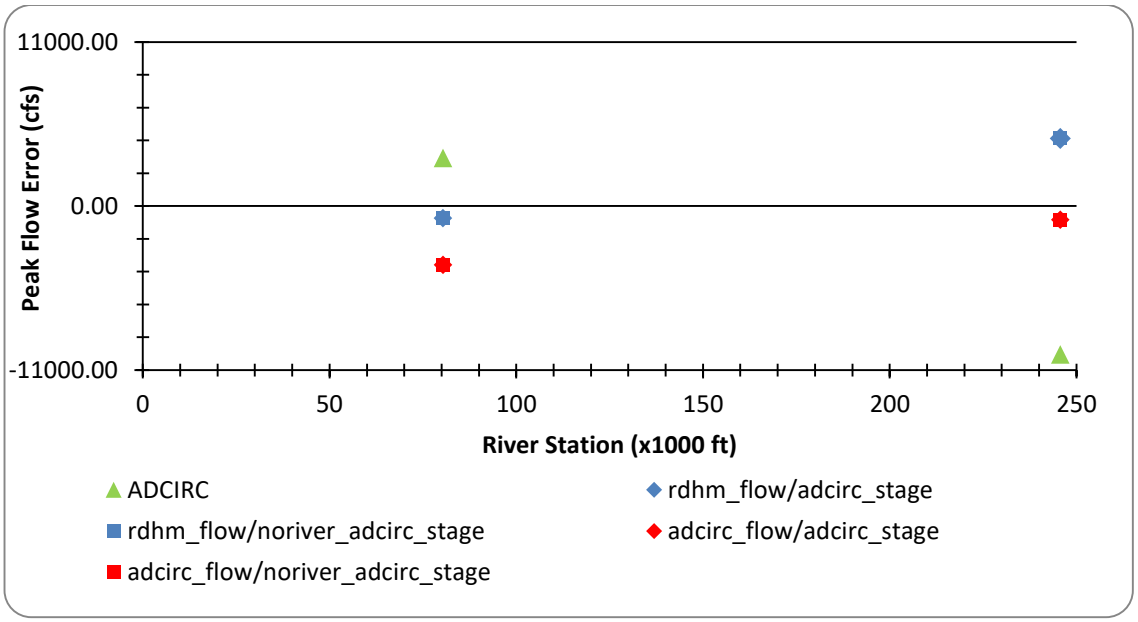

Figure 7-9 Peak Flow Error by Distance Upstream. ADCIRC results in Green, ADCIRC results interpreted by HEC-RAS in red, stage solved from HL-RDHM Flows in Blue, observations in black

As both models use ADCIRC stage at the downstream boundary and ADCIRC peak errors in the open ocean domain are relatively small, HEC-RAS peak errors near the downstream boundary are also small. There are significant peak timing errors at the upstream boundary when using RDHM-upstream boundary conditions, and significant peak stage errors at the upstream boundary when using ADCIRC-upstream boundary conditions.

This suggests that flooding during Irene at the confluence of the Tar River and Fishing Creek, when modeled using HL-RDHM, produces early estimates of flood peaks. This may be explained by HL-RDHM's use of the kinematic wave equation, which cannot capture the backwater effects, for rainfall-runoff routing in the upland hydrology model. Alternately, when ADCIRC is used to model that area, results are inconsistent – stage results are too high and flow results are too low. These errors may arise from the use of

ADCIRC to model the river confluence, or they may be attributed to the handoff of information between HL-RDHM and ADCIRC.

Comparison of Results at Gauge Sites

Overall, ADCIRC alone appears better suited to predicting peak stages above the tidally influenced zone, whereas ADCIRC-stage-forced HEC-RAS shows the best rainfall peak prediction and comparable quality in surge peak prediction in the tidally-influenced zone. Only RDHM-forced HEC-RAS models realistically capture baseflow conditions following the flood wave.

Comparison to High Water Marks

A total of 146 high water marks were collected following Hurricane Irene, however priority was placed on coastal flooding over riverine flooding.

As Figure 7-10 shows, most of the high water marks were collected in areas outside the river model domain (shown in pink). Only two high water marks were collected within the model domain, and both were at the extreme downstream side.

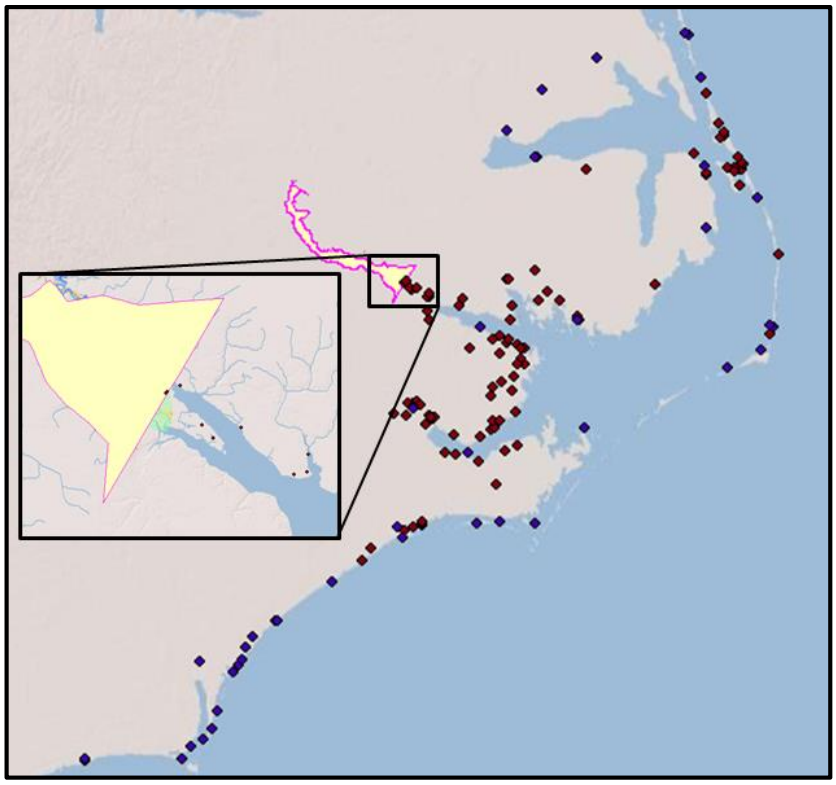

Figure 7-10 USGS High Water Mark Locations

Both high water marks were taken at the low-lying area between Pamlico Sound and Chocowinty Bay. Error at each location was calculated as shown in Equation 6 and are listed in Table 7-2.

Equation 6 - High Water Mark Error Formula

$$Error = Xmodel - Xobserved$$

Table 7-2 - High Water Mark Errors

Site Name	ADCIRC Error (Feet)	HEC-RAS Error (Feet)
HWM-NC-BEA-601	7.811-6.64 = +1.171’	7.758-6.64 = +1.118’
HWM-NC-BEA-602	7.811-6.6 = +1.211’	7.74-6.6 = +1.14’

Error for both models was similar, which is expected, given that both models are forced to agree at the downstream boundary and given that the high water marks are in close proximity to that boundary. Results at the downstream boundary were slightly overestimated, which carried through to these sites. In all, more high water mark data

would be necessary to draw meaningful conclusions beyond those determined from the stage hydrographs predicted at USGS gauges.

INUNDATED AREA

To provide a comparison between inundation extents from models of differing formats, the water surface elevation maps from the peak elevations recorded both by ADCIRC and by the two versions of the HEC-RAS model were converted into inundation rasters using the methods described in Appendix D. These maps are shown in Figure 7-11 through Figure 7-15. Each inundation map was trimmed to the space shared by both models, indicated in yellow. Note that the colored areal extents of inundation are ordered to display all three model results – however, in many maps, the difference between the extent of ADCIRC-forced HEC-RAS results (red) and the extent of the ADCIRC results themselves (green) is only visible as a few pixels.

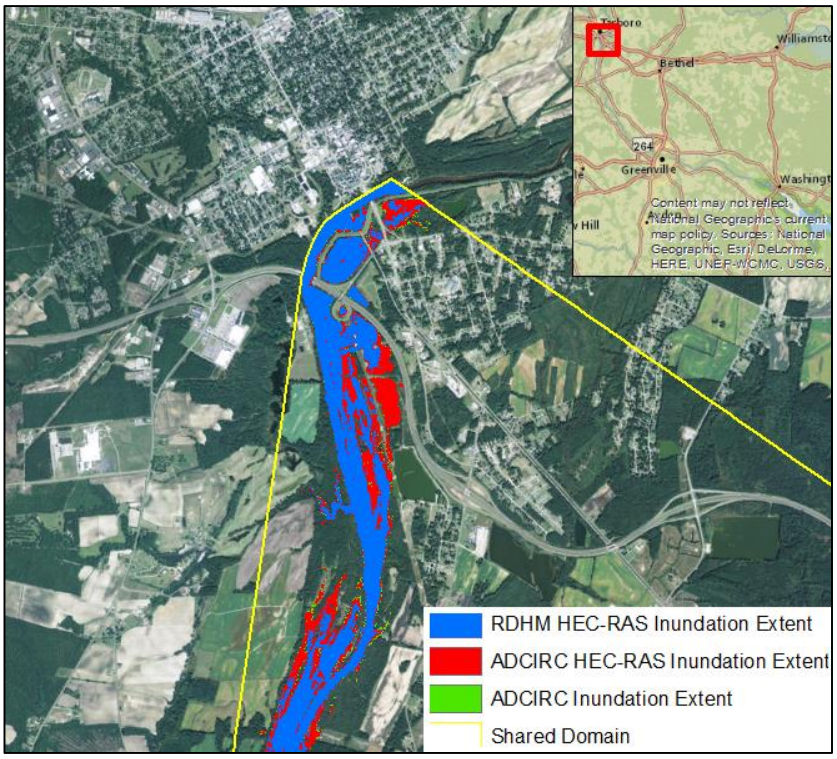

Figure 7-11 Hurricane Irene Inundation at Tarboro

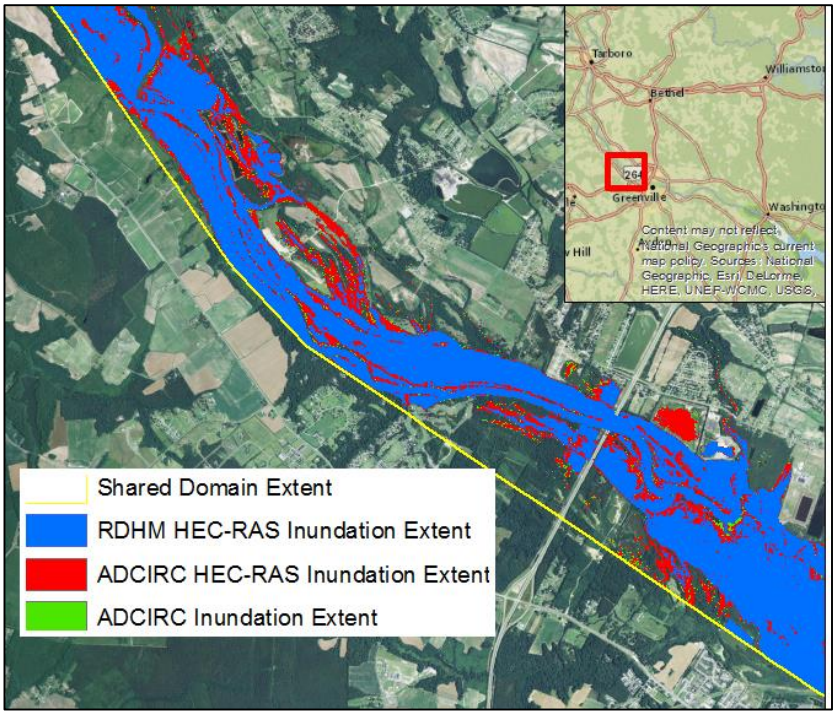

Figure 7-12 Hurricane Irene Inundation at Rock Spring

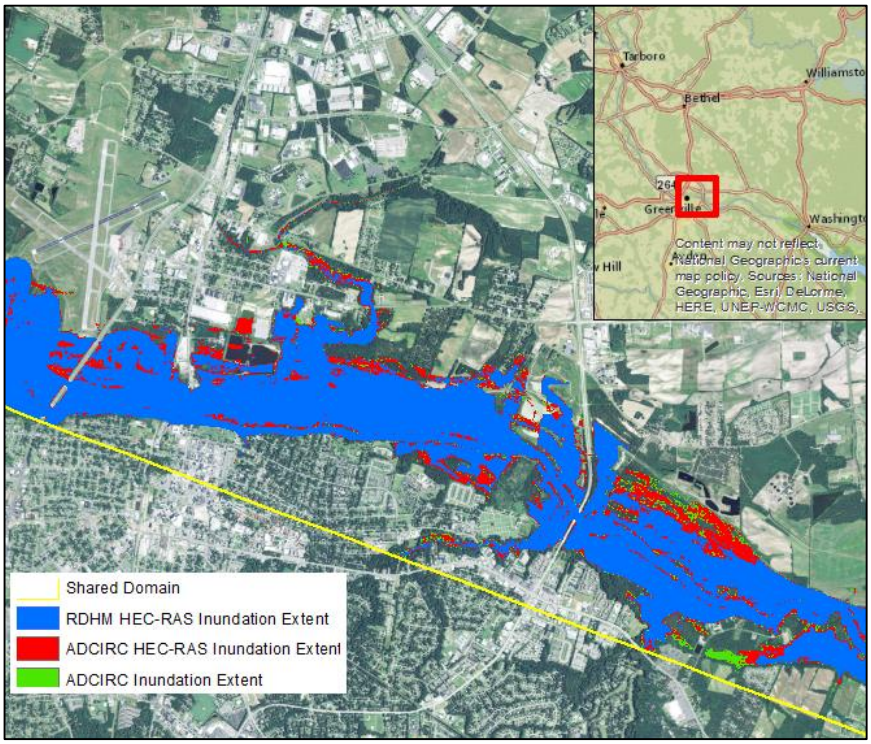

Figure 7-13 Hurricane Irene Inundation at Greenville

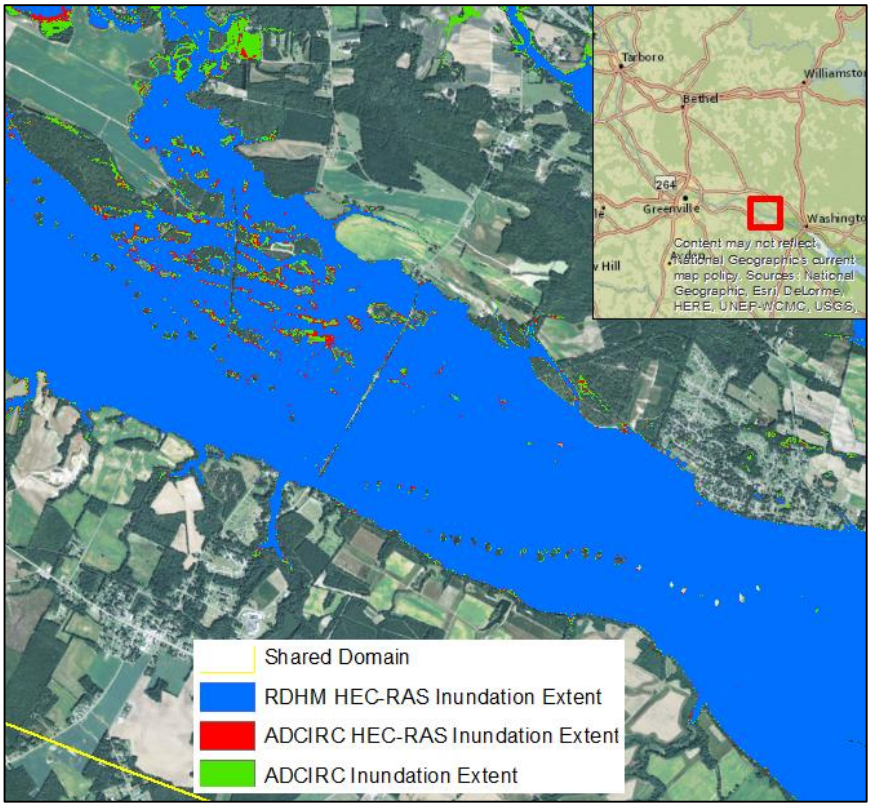

Figure 7-14 Hurricane Irene Inundation at Grimesland

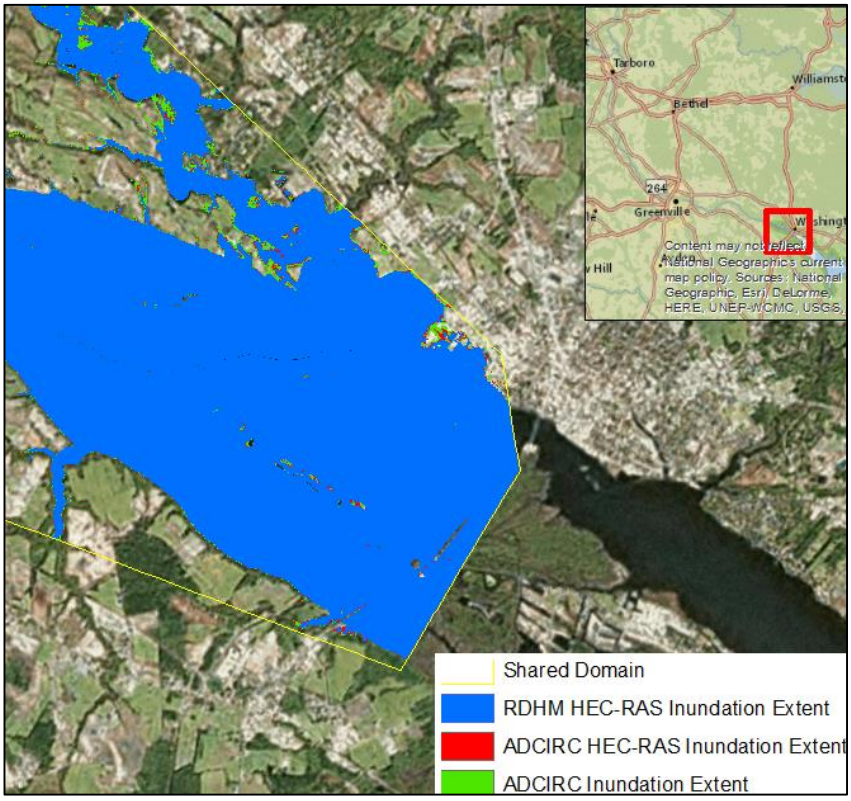

Figure 7-15 Hurricane Irene Inundation at Washington, NC

Differences in inundation extent follow the patterns observed at gauges – at the upstream boundary, ADCIRC results match HEC-RAS forced with ADCIRC, while HEC-RAS forced with HL-RDHM predicts less severe flooding. At the downstream boundary, all models predict approximately the same flooding extent, with slightly more severe inundation being predicted by ADCIRC as compared to HEC-RAS.

Inundation Depth

Two comparisons of inundation depth are presented below. First, the prevailing pattern of ADCIRC producing deeper flood estimates (discussed above) is further clarified by discussing regions where this pattern does not hold. Second, the differences between two HEC-RAS model configurations are discussed in order to provide insight into the spatial variation of errors resulting from using a riverless version of ADCIRC.

Inundation Depth Comparison – ADCIRC vs HEC-RAS

Based on inundation extent and results at gauges, it might appear initially that ADCIRC uniformly predicts more severe flooding than HEC-RAS. However, a comparison of inundation depth between ADCIRC's peak results and the most severe HEC-RAS result (with ADCIRC upstream and ADCIRC with rivers downstream) for Hurricane Irene showed a handful of areas where this trend does not hold, shown in pink in Figure 7-16.

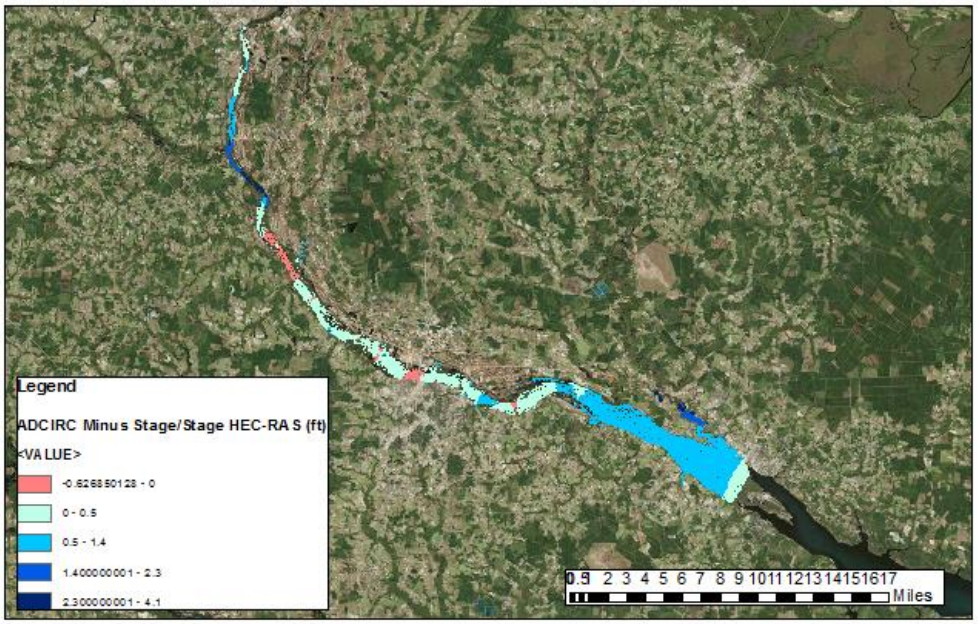

Figure 7-16 ADCIRC inundation depth minus HEC-RAS Stage/Stage Inundation Depth. Pink indicates HEC-RAS results above ADCIRC results. Darkening shades of blue indicate ADCIRC results above HEC-RAS results.

All pink-colored regions in that map, indicating regions where HEC-RAS results are greater than ADCIRC results, are discussed here, sorted into six areas.

AREA 1 – UPSTREAM OF NC 222

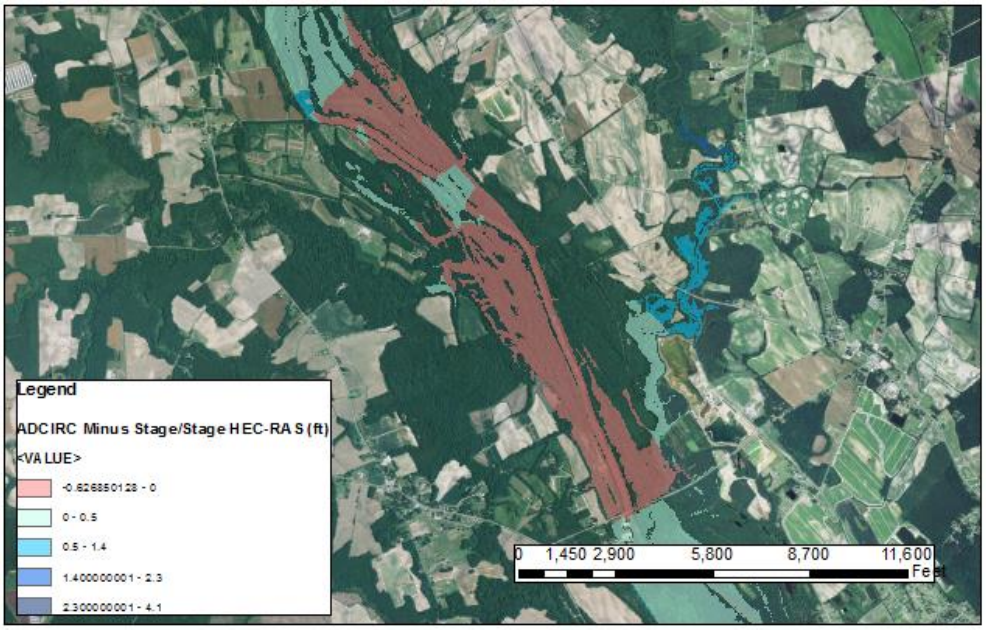

Figure 7-17 Inundation differences upstream of NC 222 crossing

The first section of upward bias appears above the crossing of NC 222, north of Greenville, shown in Figure 7-17. The bridge crossing's representation in HEC-RAS is shown in Figure 7-18 – clearly the bridge is resolved and accounted for. However, in ADCIRC, all bridges were removed from the DEM before preparation of river bathymetries. One possible explanation for this bias is that in this "upstream influence" area, HEC-RAS accounts for flow restriction at NC 222 while ADCIRC does not. The subsequent retention of water causes HEC-RAS's results to overcome the natural negative bias in the model and predict higher flooding in that area. Flow in the region is generally subcritical so this sort of backwater effect is well understood.

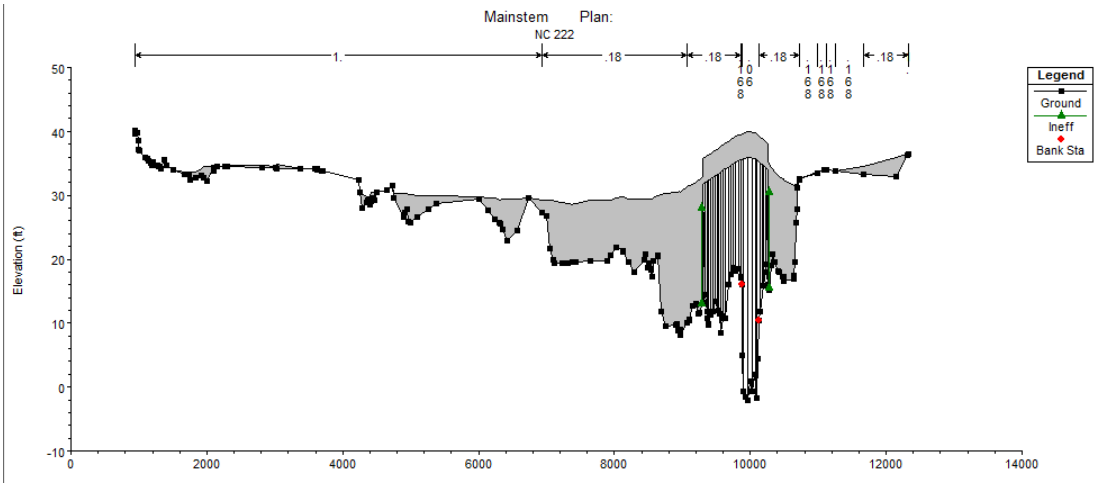

Figure 7-18 NC 222 Crossing

AREA 2 – UNNAMED MEANDER DOWNSTREAM OF NC 222

The second section showing a pink and therefore upward bias is at an unnamed, sharp bend in the Tar River downstream of NC 222, shown in Figure 7-19.

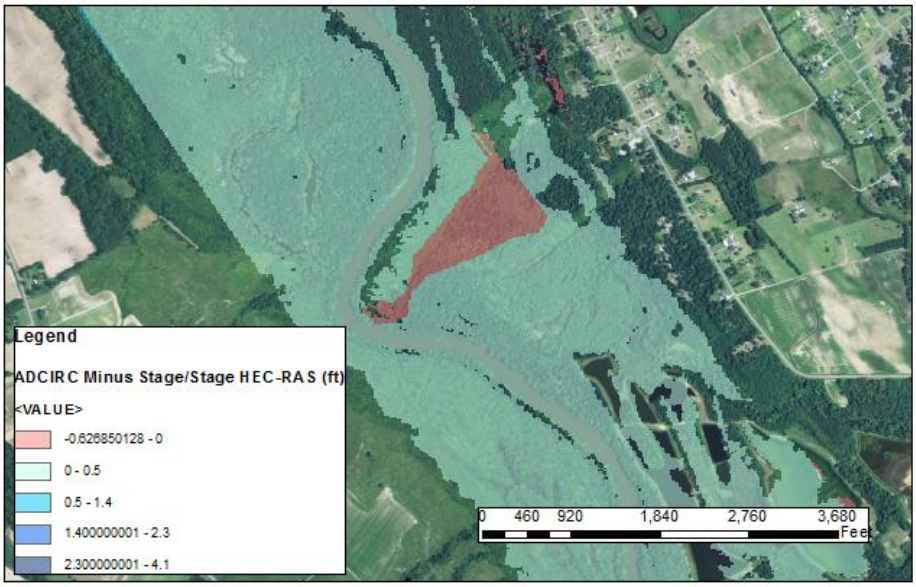

Figure 7-19 Unnamed Region of Positive HEC-RAS Bias Downstream of NC 222

This type of sharp deviation from a straight path is particularly difficult to resolve in a 1D model. Figure 7-20 shows the layout of HEC-RAS cross sections, with yellow dots indicating the model's "bank points," overlaid with ADCIRC mesh nodes shown in red. One explanation is that both models are expected to predict a gradient of water surface elevation, running from high WSE upstream and low WSE downstream. Since HEC-RAS's interpretation of "upstream" is to the northwest, whereas ADCIRC's interpretation of "upstream" is to the northeast, it is easy to see how model results would diverge. However, while this is the only meander showing "pink", this is not the only meander with this difference in model representation, and this theory does not explain why this difference is not seen in other sinuous parts of the river. It is possible that this is simply the only meander where this effect is large enough to outweigh the overall bias trend between the models. However, it is also possible that this difference might be the result between differences in survey points used and may not represent any systematic difference between the models.

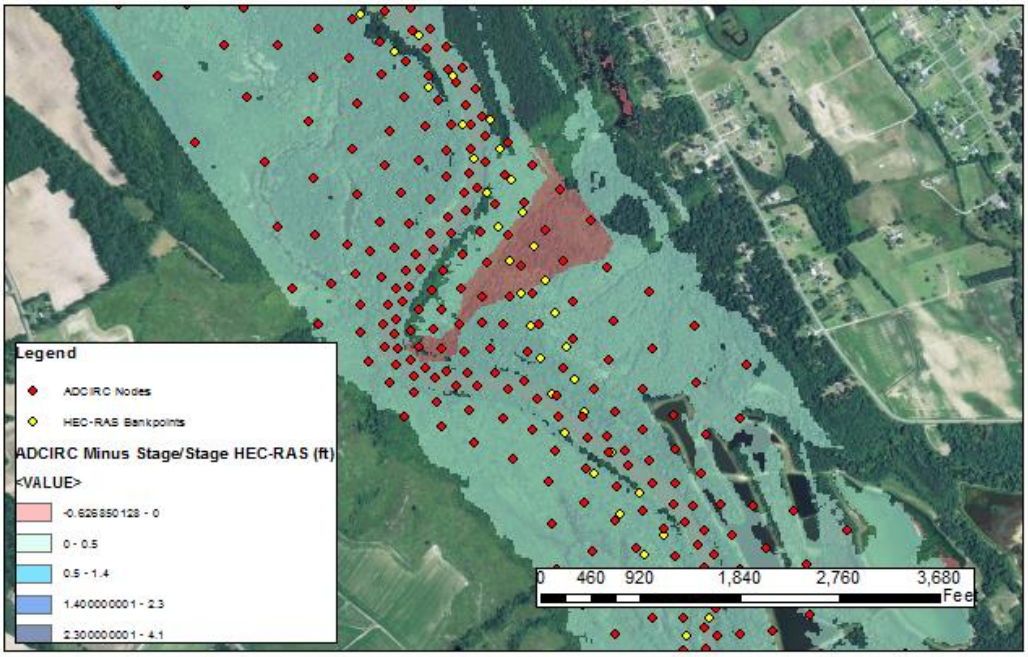

Figure 7-20 HEC-RAS Cross Sections at Unnamed Bend, South of NC 222

AREA 3 – GREENVILLE, WEST OF PITT-GREENVILLE AIRPORT

The third area to discuss is a small stretch of river west of the Pitt-Greenville airport, shown in Figure 7-21.

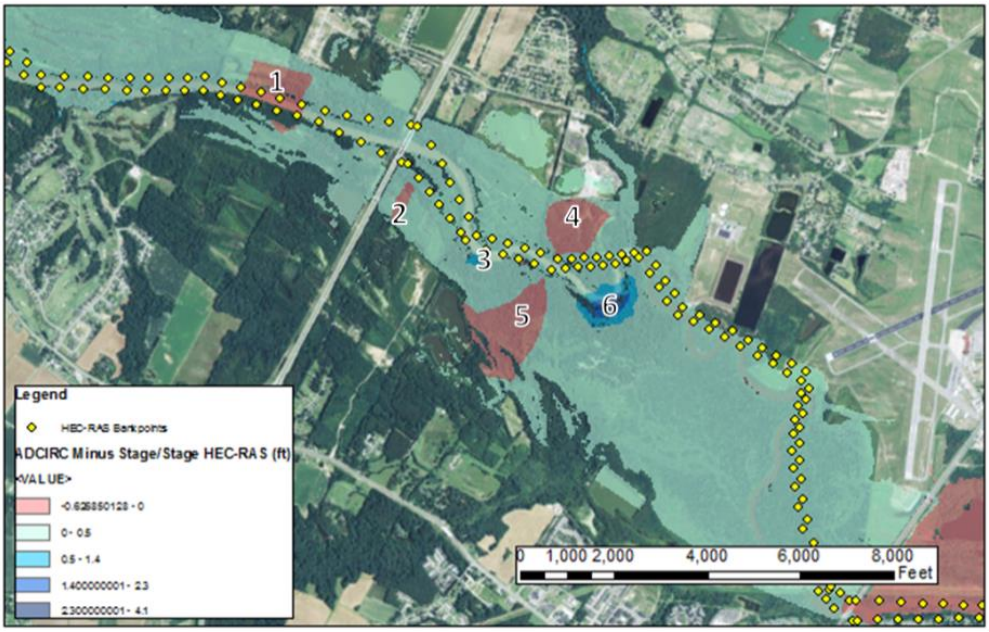

Figure 7-21 Inundation Differences at and near Martin Luther King Jr. Highway Crossing

This area shows wide variation between the models in a relatively short area. The first region of model divergence (1) is upstream of a bridge section, but not immediately upstream. A reasonable explanation of this divergence was not found.

Four regions (2, 3, 5, and 6) between the bridge crossing and the airport are associated with meanders. This somewhat matches the behavior in the previous example, if the explanation is a higher HEC-RAS result inside curved sections and a lower result outside curved sections (or the reverse bias in ADCIRC). However that does not explain region 4, a region with higher HEC-RAS results on the outside of a meander. This explanation leaves much to be desired, not only because it fails to explain region 4 but also because the form of regions 5 and 2 do not appear to conform to the meanders as well as the region discussed in the prior section.

A section of pink is visible in at the far downstream corner of Figure 7-21 – this section is discussed in detail as "Area 4", below.

Area 4 – Greenville Bridges

The next area of divergence occurs between and below four bridge crossings – west to east, they are North Memorial Drive, a railway crossing, North Pitt Street, and South Greene Street. The difference plot for all four crossings is shown in Figure 7-22. Note that, of the four crossings, the North Pitt Street crossing is not included in the HEC-RAS model.

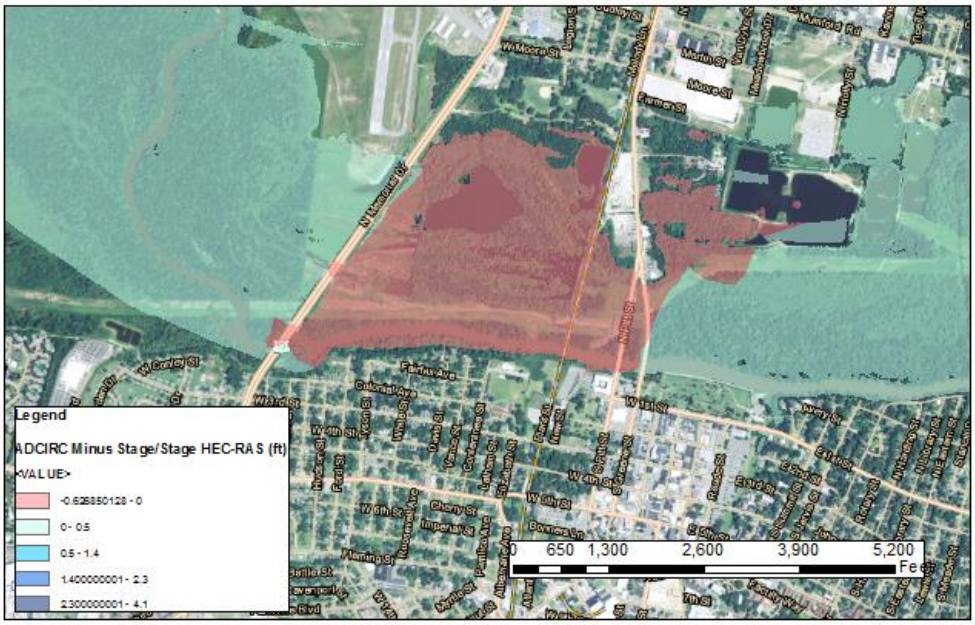

Figure 7-22 Inundation differences downstream of Memorial Drive crossing

It is reasonable to expect high differences around bridges. It is curious to note that this divergence is not observed upstream of North Memorial Drive bridge (farthest west bridge in Figure 7-22), but this may simply indicate that this particular bridge is not hydraulically significant for this event.

Figure 7-23 shows the location of resolved bridges in HEC-RAS – this indicates that much of the area of divergence northeast of the bridge can be explained by the eastward slant of HEC-RAS sections. This does not appear to explain the very northeast section, but that area of difference may still be due to the impact of bridges, and merely extends downstream of the bridge section due to the inundation maps procedure for interpolating between model mesh points.

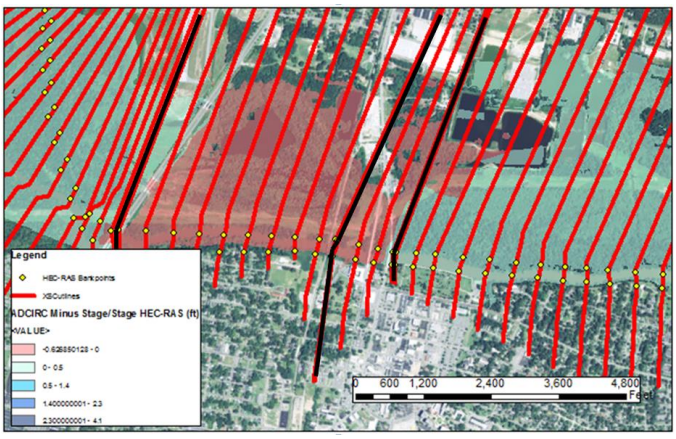

Figure 7-23 Spatial Location of Bridge Sections in HEC-RAS Model Shown in Black

AREA 5 – GREENVILLE BOULEVARD NE CROSSING

The next region of positive HEC-RAS bias occurs above a bridge section, shown in Figure 7-24. There is a very small region of positive bias upstream of the bridge itself, followed by a region following the most common divergence behavior (ADCIRC above HEC-RAS). The upstream area of positive HEC-RAS bias appears very small and may be due to one or two single ADCIRC nodes with low values.

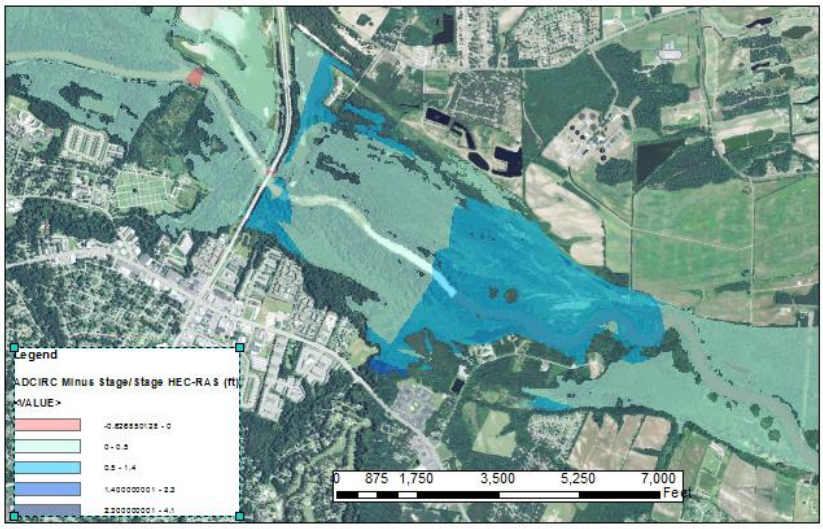

Figure 7-24 Inundation differences between ADCIRC and HEC-RAS near Greenville Blvd NE Crossing

AREA 6 – DOWNSTREAM OF GREENVILLE

The last section of the shared model domain that goes against the overall trend (HEC-RAS results being less than ADCIRC results) is roughly ½ mile downstream of the region just discussed, and is shown in Figure 7-25.

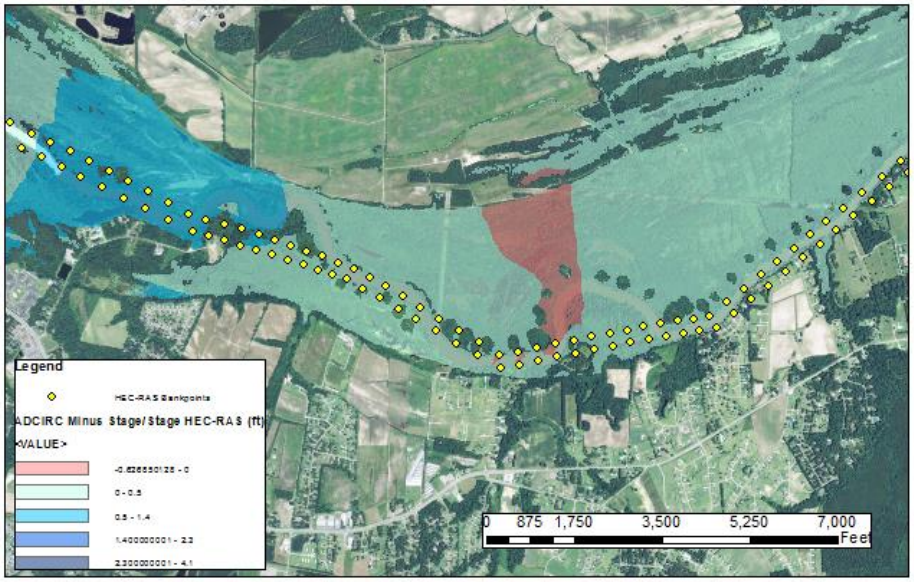

Figure 7-25 Inundation differences well downstream of Greenville Boulevard NE Crossing

On comparing results to satellite imagery, comparative model behavior in this region runs counter to the observed behavior in the above sinuous sections, where the HEC-RAS results inside of an unrepresented meander tended to be higher than ADCIRC predicts. However, if one examines Figure 7-26, the region is also "inside" a meander (river channel visible as the darkest region) located just west of the area indicated by the red oval in that figure – from this perspective, behavior here matches model comparative behavior in Area 2. This belies a difficulty in interpreting these results with respect to meanders – many regions may be considered both "inside" and "outside" meanders due to the complicated nature of river sinuosity.

The nearest bridge crossings are roughly 3 miles upstream and 7 miles downstream, and though satellite imagery shows a roadway nearby, as Figure 7-26 shows, an unprocessed LiDAR-derived digital elevation map (DEM) of the area (specifically, the 33-foot National Elevation Dataset, or NED) reveals that this roadway is not elevated compared to the surrounding terrain.

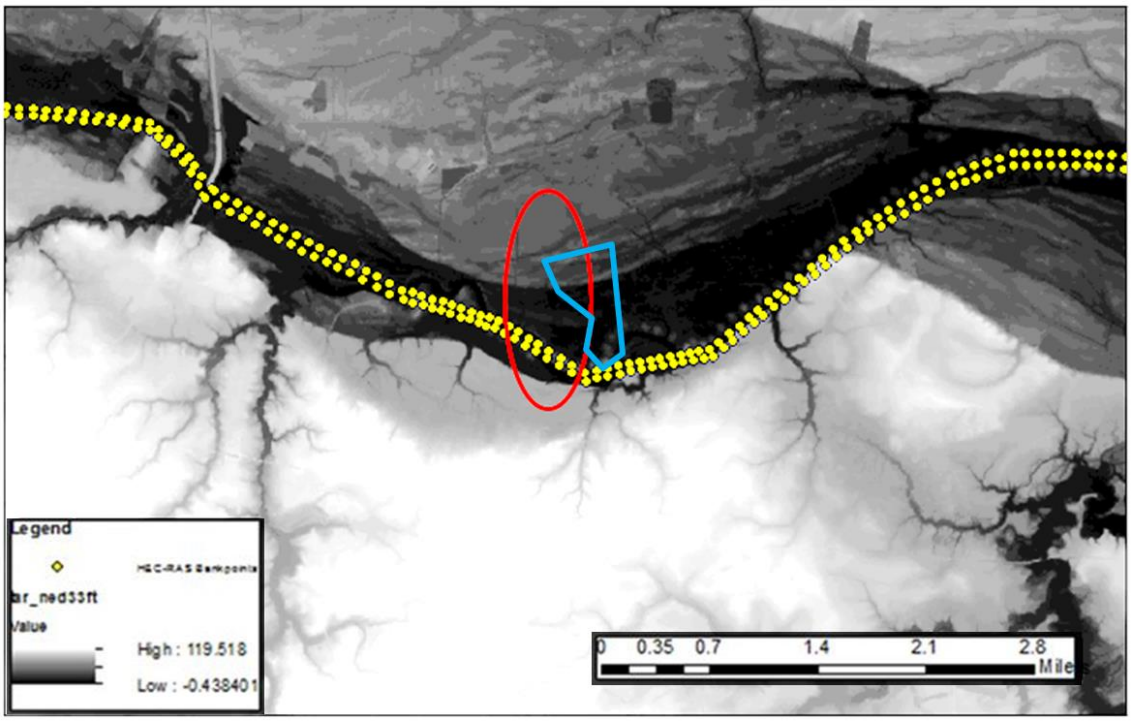

Figure 7-26 Unprocessed NED DEM downstream of Greenville Boulevard NE crossing. Red oval indicates approximate region of nearby roadway. Blue polygon indicates approximate extent of unexpected model results. Yellow dots indicate HEC-RAS Bank Points.

Summary of HEC-RAS and ADCIRC Inundation Differences

ADCIRC shows higher results than HEC-RAS for Hurricane Irene, even when HEC-RAS uses ADCIRC stages at the downstream and the upstream boundary conditions.

It is theorized that model differences can arise from three sources: boundary conditions, parameters, and underlying physics (since both models can be described as solutions to

simplifications of the Navier-Stokes equations, differences in "physics" can be more rigorously described as differences in excluded terms, e.g. vertical momentum).

This analysis in this section attempted to isolate for one of those causes (boundary conditions) but differences remain. This suggests driving factors of model disagreement can be found in parameterizations (bathymetry data, Manning's n, bridges) and in the significance of omitted terms in the underlying physics, and a full understanding of the differences between both models would require systematic study of all of these factors. For this thesis, it must suffice to say that (for this storm) HEC-RAS tends towards lower peaks than ADCIRC for reasons that are not fully understood, and that differences in model behavior may arise from numerous different sources, perhaps including but not solely limited to the 1D or 2D nature of each model, e.g. each model's spatial resolution.

Comparison of Inundation Depths – HEC-RAS Forced with ADCIRC

As discussed in Study 1, HEC-RAS forced with the riverless ADCIRC solution at the downstream boundary produces a lower peak stage result than HEC-RAS forced at the downstream boundary by an ADCIRC model which includes rivers. Note that this difference in peak stages occurs during the storm surge peak, and not during the river flow peak. Figure 7-27 shows the spatial extent and magnitude of the differences between HEC-RAS solutions based on whether they used ADCIRC with or without rivers, using HL-RDHM flows at the upstream boundary condition.

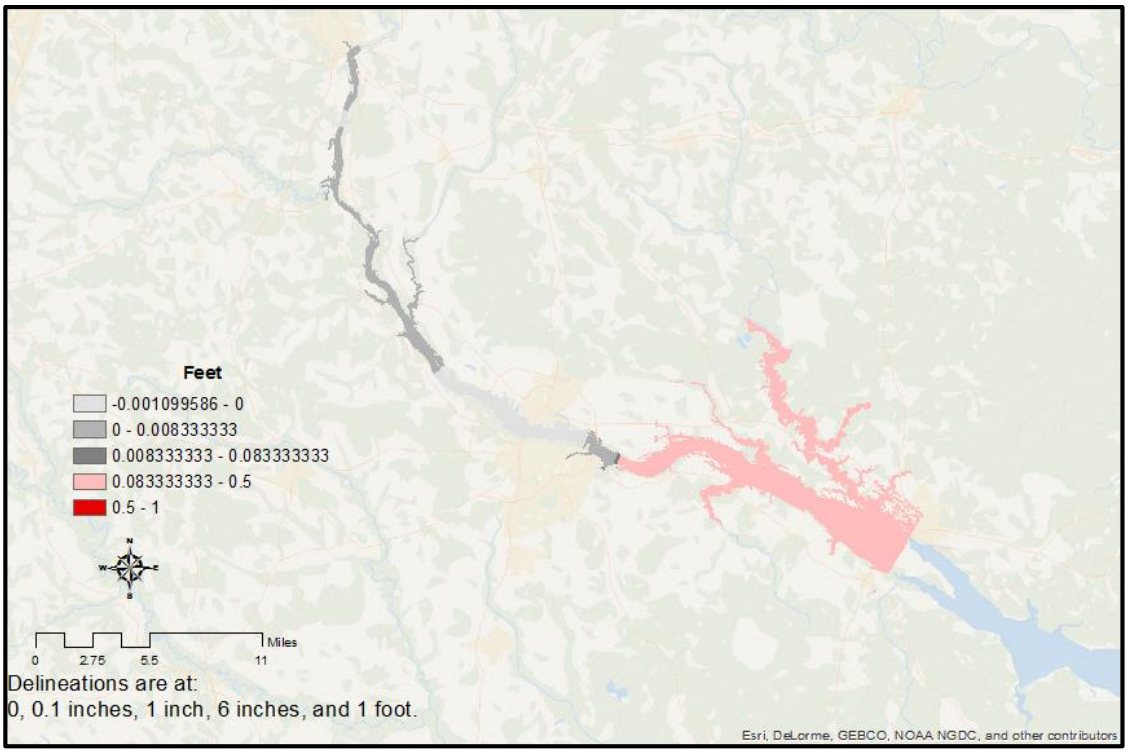

Figure 7-27 Error in HEC-RAS Solution Induced by Riverless BC – Hurricane Irene

Overall inundation depth differences between the riverless and river-forced downstream boundary conditions do not exceed 6 inches in magnitude, and are less than one inch at Greenville and upstream.

Summary of River vs. Riverless BCs

This analysis shows that using a riverless version of ADCIRC to provide a downstream boundary condition for a HEC-RAS model of Hurricane Irene would result in a flood stage estimate reduction of not more than 6 inches.

Summary of Model Comparisons for Irene

HEC-RAS is capable of modeling baseflows, but not when forced with ADCIRC data from above the HEC-RAS handoff point. ADCIRC's baseflow errors appear to range from high (at Tarboro to Greenville) to acceptable (at Grimesland and Washington) as tidal influence becomes more significant. This is consistent with the model's

development, as the ADCIRC representation of the rivers was intended solely for peak prediction. Baseflow errors are not present in the HL-RDHM solution at Tarboro, suggesting that these errors arise between ADCIRC's two handoff points and Tarboro. ADCIRC generally predicted higher stages except for a few regions that do not share any obvious characteristics and that are not limited to areas upstream of bridges. A coupled RDHM/HEC-RAS/ADCIRC model of this storm would be sensitive to the inclusion or exclusion of rivers in the ADCIRC model.

8. HURRICANE FLOYD

Hurricane Floyd serves as the second test case.

STORM DESCRIPTION

Model behavior and skill depends on many factors, therefore the specific characteristics of the hindcast event are highly relevant. The pre-storm conditions and hurricane track & wind speeds are discussed below.

PRE-STORM CONDITIONS

Hurricane Dennis impacted North Carolina less than a month prior to Hurricane Floyd, delivering high rainfall to the area. Figure 8-1 shows rainfall totals for Dennis – note that the area at and upstream of Pamlico sound experienced rainfall totals in excess of 10 inches.

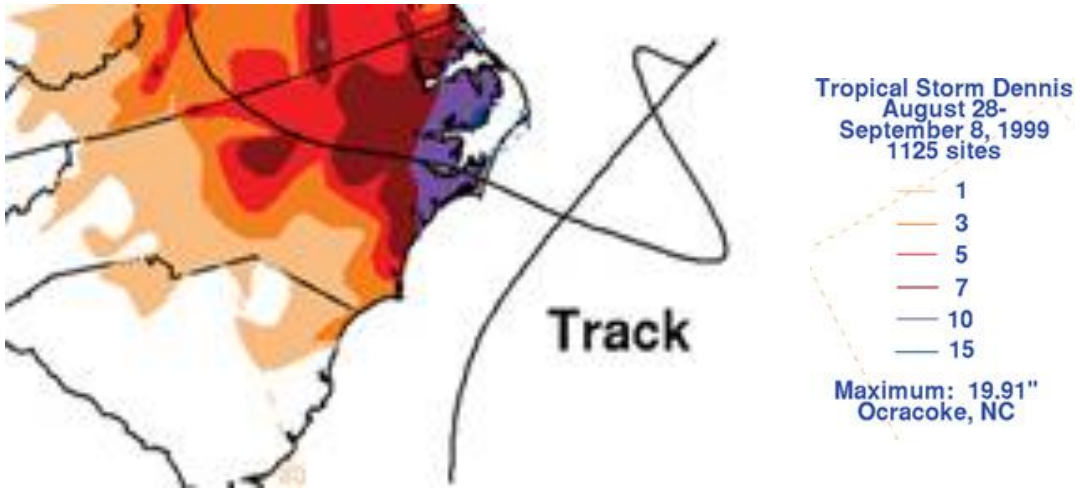

Figure 8-1 Hurricane Dennis Rainfall Totals (Newport/Morehead, NC Weather Forecast Office, NWS, n.d.)

Damage from Dennis was only moderate, but high rainfall totals increased soil moisture, leading to higher rainfall runoff quantities during Hurricane Floyd and afterwards.

HURRICANE TRACK & WINDS

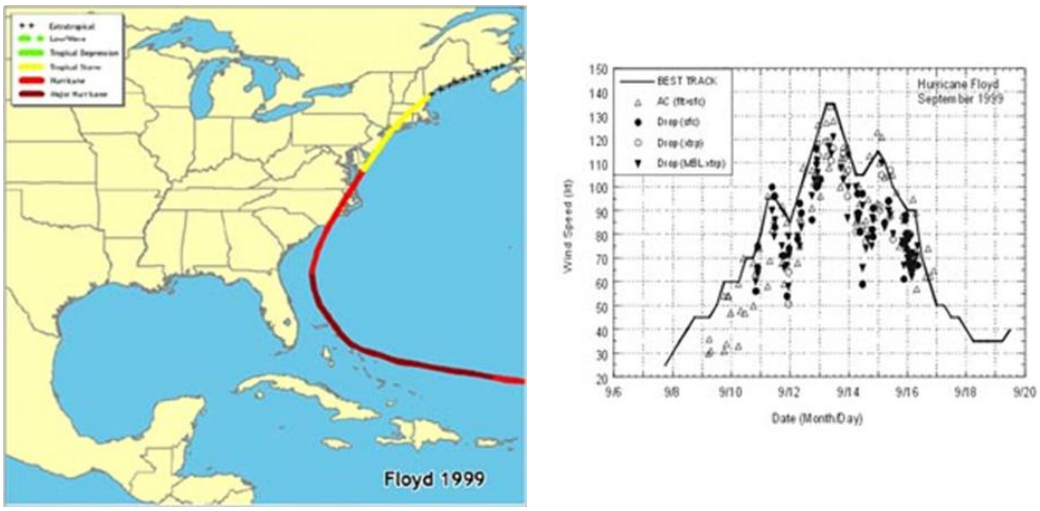

Figure 8-2 Hurricane Floyd Storm Track & Wind Speeds (Newport/Morehead, NC Weather Forecast Office, NWS, n.d.)

FORCING AND VALIDATION STRATEGY

Datasets used to force and validate each model are listed in Table 8-1 below:

Table 8-1 - Hurricane Floyd Forcing and Validation Datasets

Model	Forcing Datasets	Source(s)	Validation Datasets	Source(s)
Hydrologic Model (HL-RDHM)	NASA Tropical Rainfall Measuring Mission (TRRM) QPE	(George J. Huffman, 2016)	USGS Gauge 02083500 Tar at Tarboro Observed Flow	(USGS, 2015)
Ocean model (ADCIRC)	ARA Winds; Tidal Database	(Vickery, et al., 2000); (Mukai, et al., 2002)	Realtime wind speed & direction from NOAA NOS Buoys; coastal tidal gauges	(NOAA, 2015); (NOAA, 2013)
River Models (ADCIRC, HEC-RAS)	Hydrologic and ocean model results		Real time flow and stage measurements (3 sites)	(USGS, 2015)

Validation of the hydrologic model is discussed in Appendix B. Validation of the ocean model is discussed in Appendix C. The validation of the two river models under

comparison is of prime interest in addressing the questions posed by this research, and is discussed in detail in the following sections.

Boundary Conditions

To achieve an objective comparison of each modelling method, the error types and magnitudes present at boundary conditions should be examined and compared to the model error types and magnitudes within the shared river model domain. To quantify these errors, model results are compared to observed flow and stage timeseries collected at USGS 02083500 Tar River at Tarboro and USGS 02084472 Pamlico Sound at Washington, respectively.

Upstream Boundary Condition – Tar River at Tarboro, NC

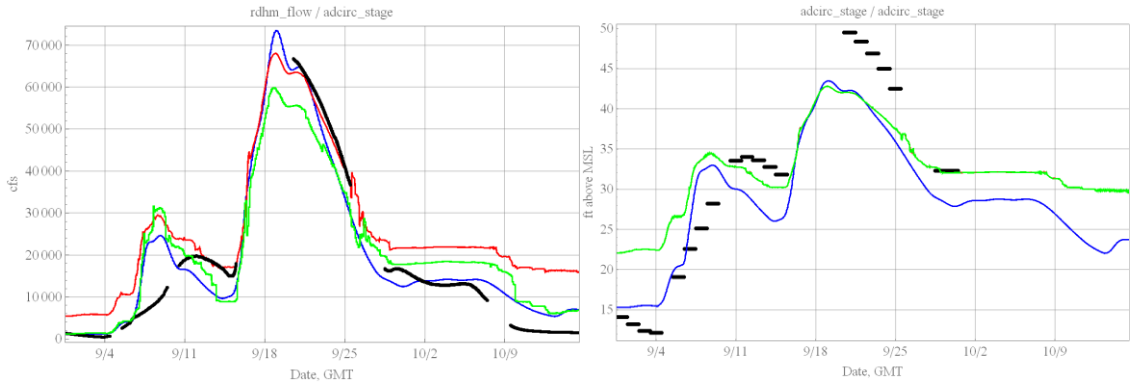

Figure 8-3 Tar River at Tarboro, NC. ADCIRC results in Green, ADCIRC results interpreted by HEC-RAS in red, HL-RDHM flows in blue, observations in black. Flow in left panel, stage in right panel

At the upstream boundary, RDHM predicts overall higher flowrates than ADCIRC. Given that ADCIRC is ultimately forced by RDHM results farther upstream of this location, this suggests that there is some mass balance error in the ADCIRC model between the RDHM/ADCIRC handoff and the ADCIRC/HEC-RAS handoff. Peak flows predicted by HL-RDHM are 72,000 cfs, while ADCIRC shows flows of 60,000 cfs, for a relative percent error of 17.5%. This runs counter to the results found in Irene, where results

suggested mass creation between those two handoffs. Possible error sources are actual mass creation due to wetting and drying, or sampling errors related to the interpolation schemes used to calculate flows from ADCIRC results.

Downstream Boundary Condition – Pamlico Sound at Washington, NC

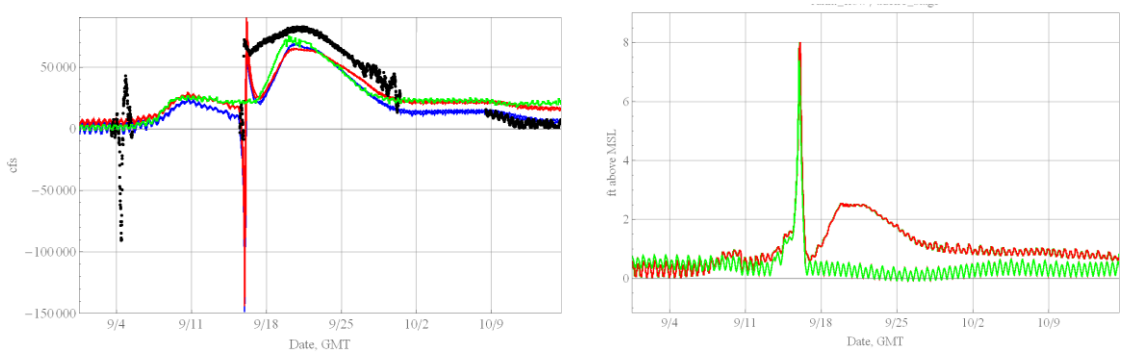

Figure 8-4 Pamlico Sound at Washington. ADCIRC results in Green, ADCIRC results interpreted by HEC-RAS in red, HL-RDHM flows in blue, observations in black. Riverless ADCIRC flows were not well resolved and are not shown. Stage observations are not available at this gauge and time period. Flow in left panel, stage in right panel

At the downstream boundary, the difference between river- and riverless-ADCIRC results is stark, visible as the difference between the green- and red lines in the right-hand figure.

River Domain Results

Each model's overall performance in the river domain was evaluated using observations at USGS gauge stations and inundation mapping.

Gauge Station Results

Figure 8-5 shows model results at the single USGS station operating during the hurricane period – USGS 02084000, Tar River at Greenville.

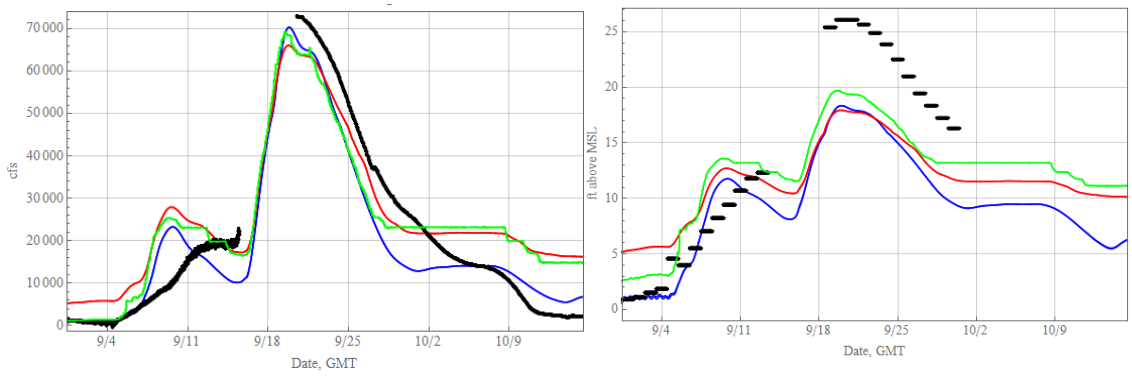

Figure 8-5 Tar River at Greenville, NC. ADCIRC results in Green, ADCIRC results interpreted by HEC-RAS in red, stage solved from HL-RDHM Flows in Blue, observations in black. Left panel flow, right panel stage. Flow in left panel, stage in right panel

Based on comparisons with gauge data, model results at the upstream boundary significantly underestimate peak stage, with a less significant underestimation of peak flow. Note that each graph shows results using ADCIRC with and without rivers (as two lines of the same color). The differences in predictions are not apparent.

Gauge Peak Accuracy by Model

The accuracy of each HEC-RAS simulation with regards to peak timing and stage was calculated. Figure 8-6 shows peak timing errors versus river station and Figure 8-7 and Figure 8-8 shows peak flow and stage errors versus river station. River station for each gauge is measured in feet upstream of the model boundary. For gauge results at Pamlico at Washington, the surge peak does not appear to be completely represented by gauge data, and is omitted – only errors in the rainfall runoff peak are represented in the following graphs.

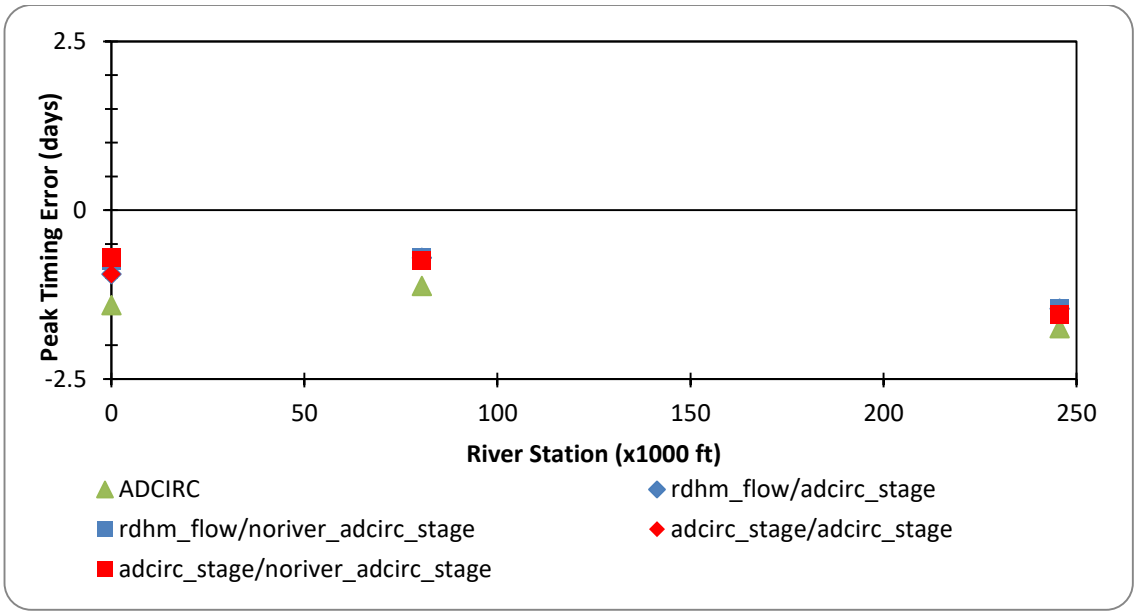

Figure 8-6 Peak Timing Error by Distance Upstream. ADCIRC results in Green, ADCIRC results interpreted by HEC-RAS in red, stage solved from HL-RDHM Flows in Blue, observations in black

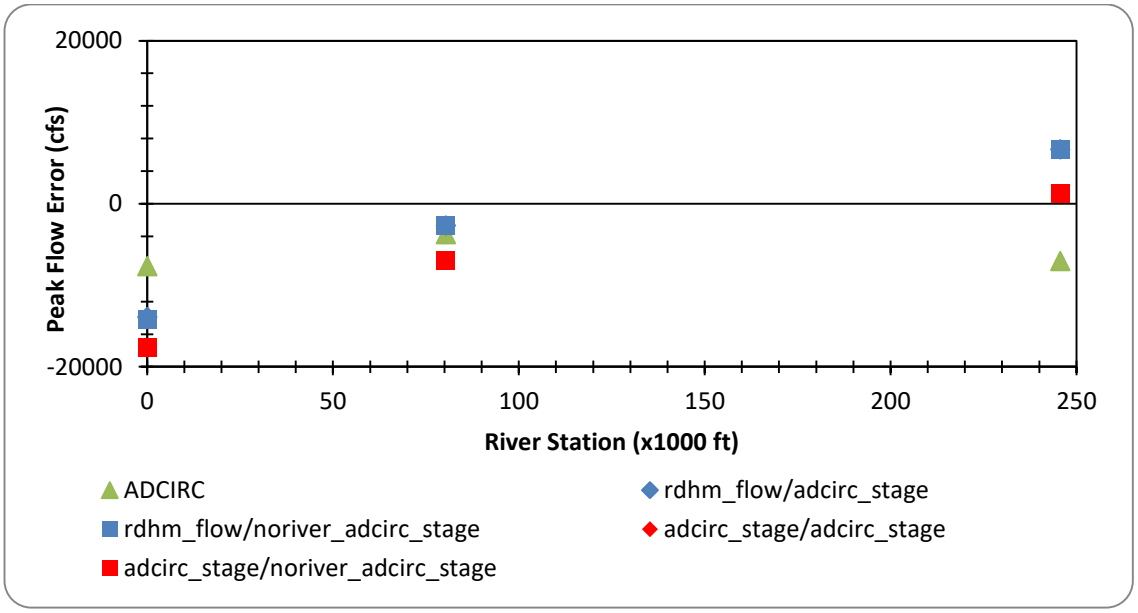

Figure 8-7 Peak Flow Error by Distance Upstream. ADCIRC results in Green, ADCIRC results interpreted by HEC-RAS in red, stage solved from HL-RDHM Flows in Blue, observations in black

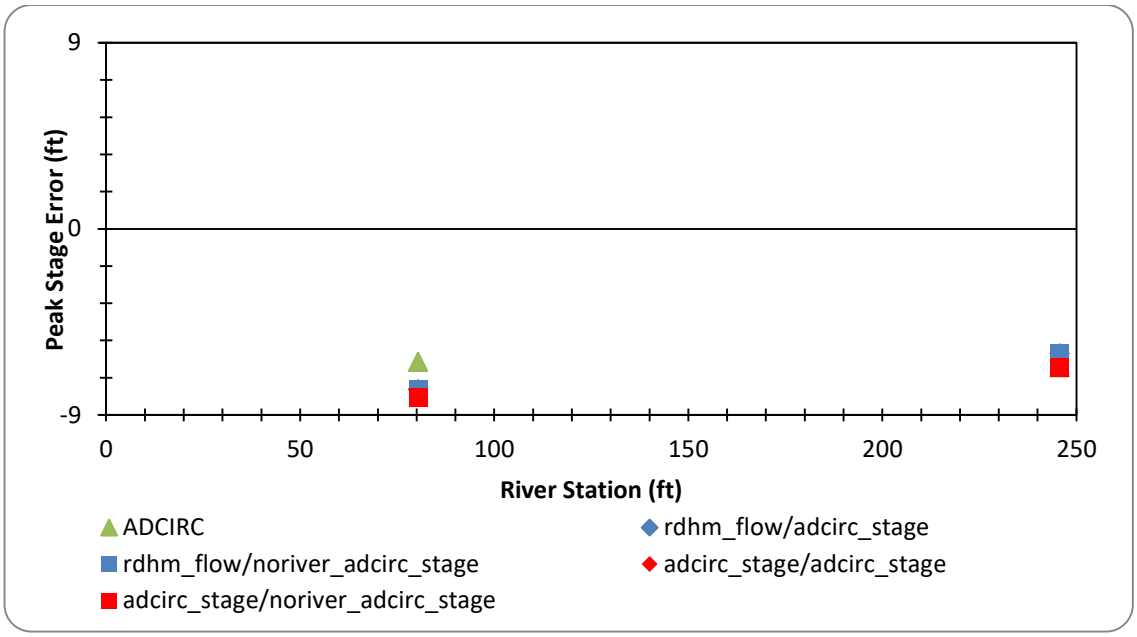

Figure 8-8 Peak Stage Error by Distance Upstream. ADCIRC results in Green, ADCIRC results interpreted by HEC-RAS in red, stage solved from HL-RDHM Flows in Blue, observations in black

Peak predictions are earlier than observed at all gauges for all model configurations. The ADCIRC model predicts peaks occurring prior to all iterations of the HEC-RAS model, including HEC-RAS forced only with ADCIRC results – this indicates something related to the ADCIRC model which leads to a different routing of flows within the channel than the HEC-RAS model.

Lateral inflows are significant (Abshire, 2012) and therefore flow errors are expected to tend towards underestimation towards the downstream boundary (River station 0). HEC-RAS model results exhibit this behavior. However, flow errors from ADCIRC results do not. ADCIRC flows are overall underestimated, with largest error magnitude at either end of the model domain.

Peak stages are highly underestimated at all gauges where stage observations are available. Given that flow results include some overestimates at Tarboro, this indicates

that, at least at that handoff, there may be errors in the stage/discharge relationship in the HEC-RAS model for this event.

Inundated Area

As a second and final method of comparison, model results were used to generate peak inundation maps, which in turn are compared qualitatively and quantitatively, below. Figure 8-9, Figure 8-10, Figure 8-11, Figure 8-12, and Figure 8-13 plot comparative flood inundation coverage by model. Note that layers in each figure are ordered formally, so that all three colors are visible, even if only by a few pixels.

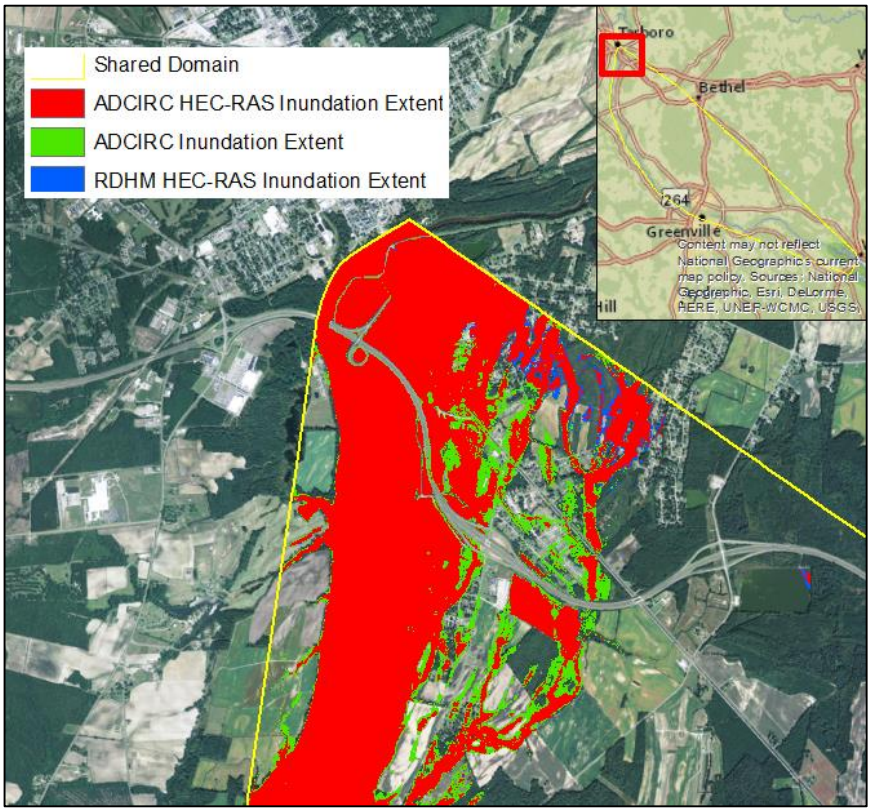

Figure 8-9 Hurricane Floyd Inundation at Tarboro

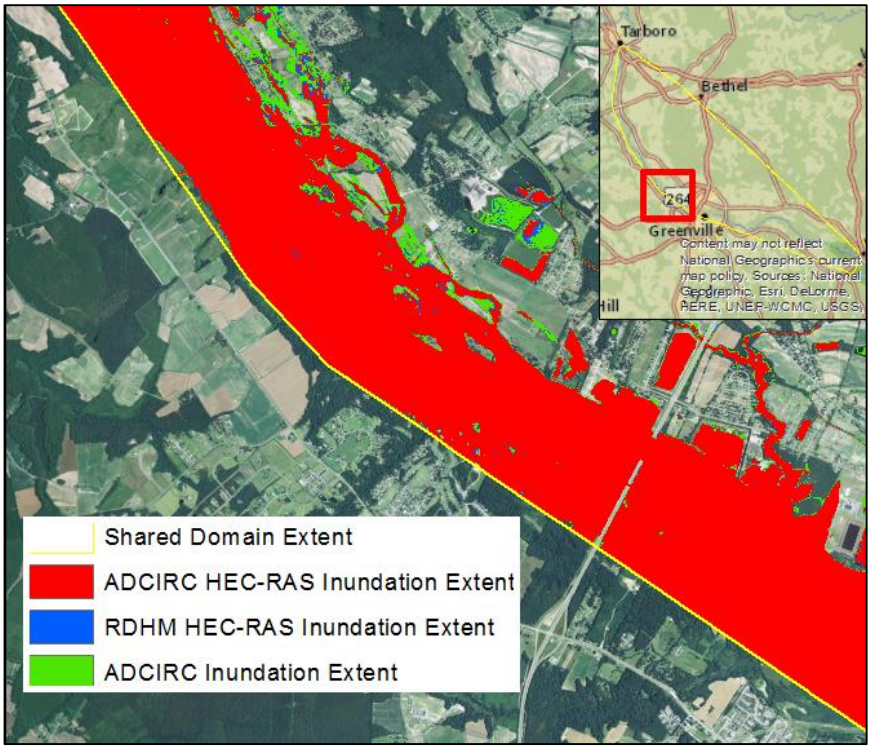

Figure 8-10 Hurricane Floyd Inundation at Rock Spring

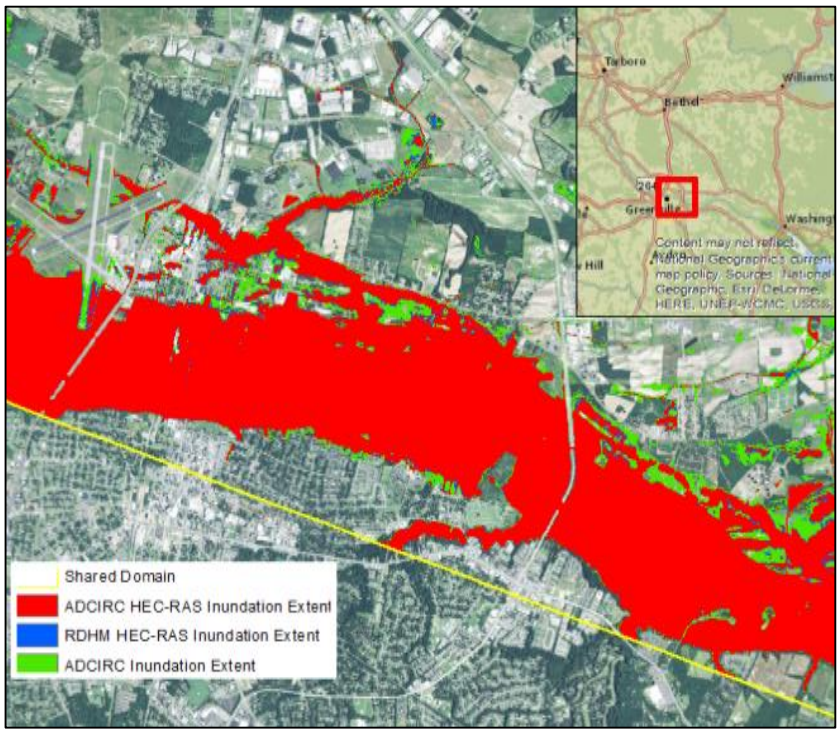

Figure 8-11 Hurricane Floyd Inundation at Greenville

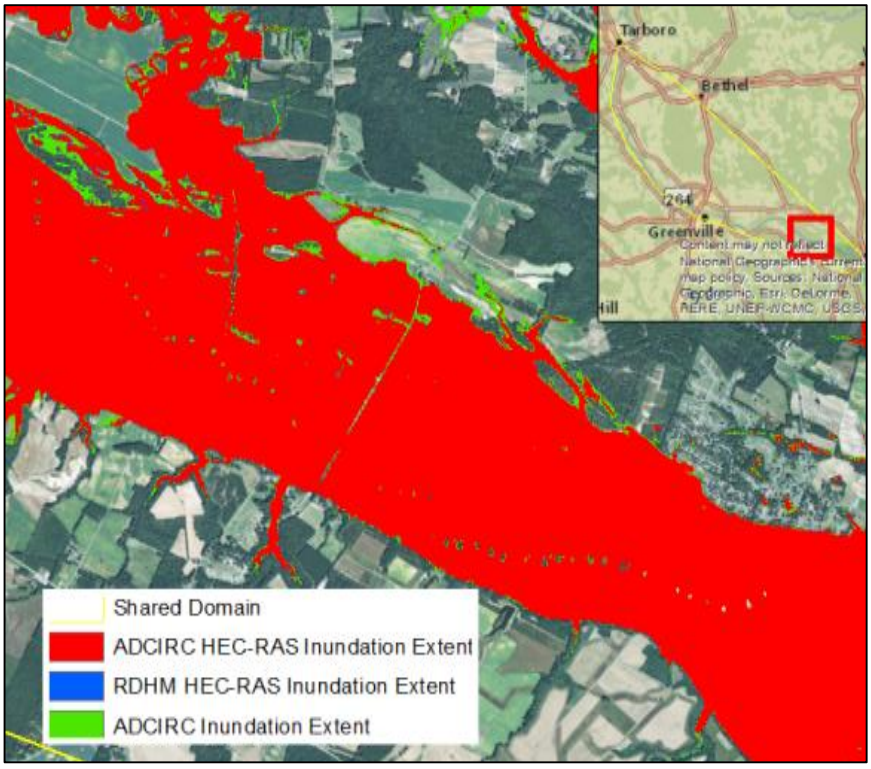

Figure 8-12 Hurricane Floyd Inundation at Grimesland

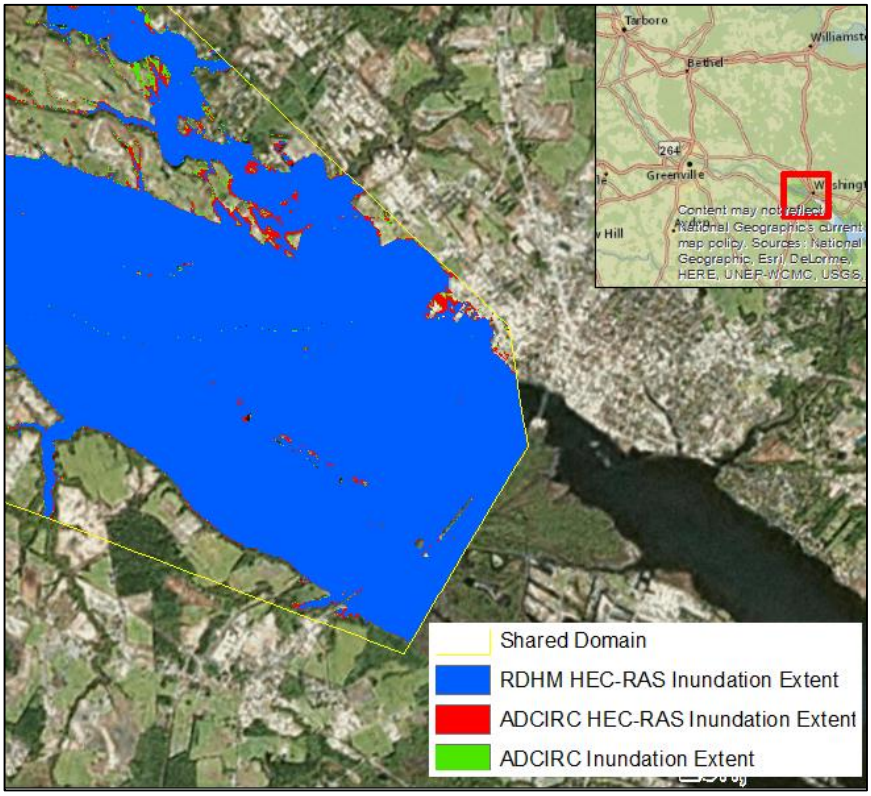

Figure 8-13 Hurricane Floyd Inundation at Washington, NC

Overall inundation extent across models is largely similar. ADCIRC predicts deeper inundation than either HEC-RAS model at each location except for a small region near Tarboro, and the impact this has on resulting inundation is most apparent at the upstream sites (Tarboro, Rock Springs, and Greenville).

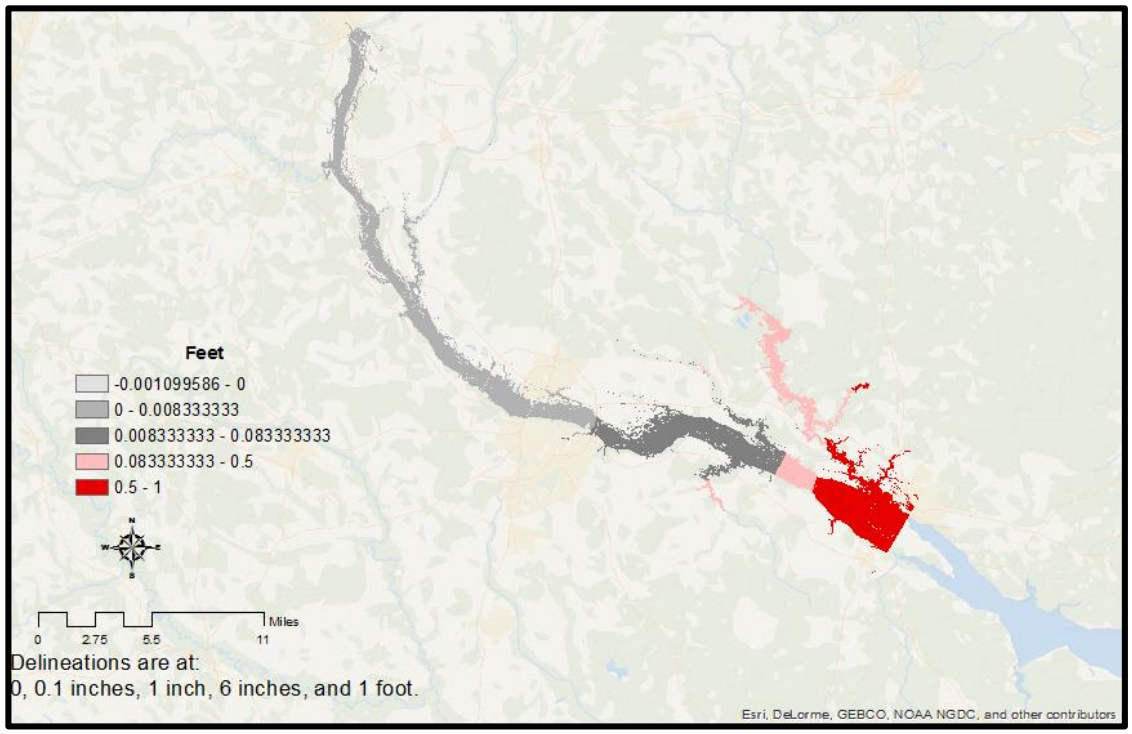

Figure 8-14 Error in HEC-RAS Solution Induced by Riverless BC – Hurricane Floyd

Using inundation mapping, the extent of errors induced by the use of a riverless boundary condition becomes visible. Errors in the Pamlico Sound area are up to 1' in magnitude. At Greenville and upstream, errors in inundation depths induced by a riverless boundary condition are less than 0.1 inches.

Summary of Model Comparisons for Floyd

Flow predictions using HEC-RAS as middleware did not vary significantly when using river (fine mesh) vs noriver (coarse mesh) ADCIRC results. Errors in flow estimates using RDHM predictions and ADCIRC stage results follow expected patterns due to lateral inflows (overestimate upstream, underestimate downstream) however flow results derived directly from ADCIRC did not. ADCIRC predicted slightly higher inundation than HEC-RAS at all locations except for the upstream handoff point (Tarboro). Errors due to riverless boundary conditions were less than one inch in regions above Pamlico Sound, but are up to one foot within the Sound itself.

9. APRIL 2003 RAINFALL EVENT

An unnamed, high-volume rainfall event serves as the final test case. This test case was selected due to a combination of high observed runoff and little to no winds (i.e. limited surge).

STORM DESCRIPTION

Model behavior and skill depends on many factors, therefore the specific characteristics of the hindcast event are highly relevant. The weather characteristics in the Tar River Basin during April, 2003 included low wind speeds and high rainfall.

EVENT CONDITIONS

Wind speeds for the entire month of April in seas off the coast of North Carolina were below 20 MPH at every measured time period. Wind speed recordings for the month of April were retrieved from the NDBC at buoy site 41025. The location of and recordings at NBDC 41025 are shown in Figure 9-1. Tropical Storm (TS) Ana occurred in April of 2003, forming in the region near Bermuda and heading generally eastward, as shown in Figure 9-2. However Ana did not make landfall, so the influence of the storm on wind and pressure behavior (and thus surge height) in the Tar River Basin is expected to have been minimal.

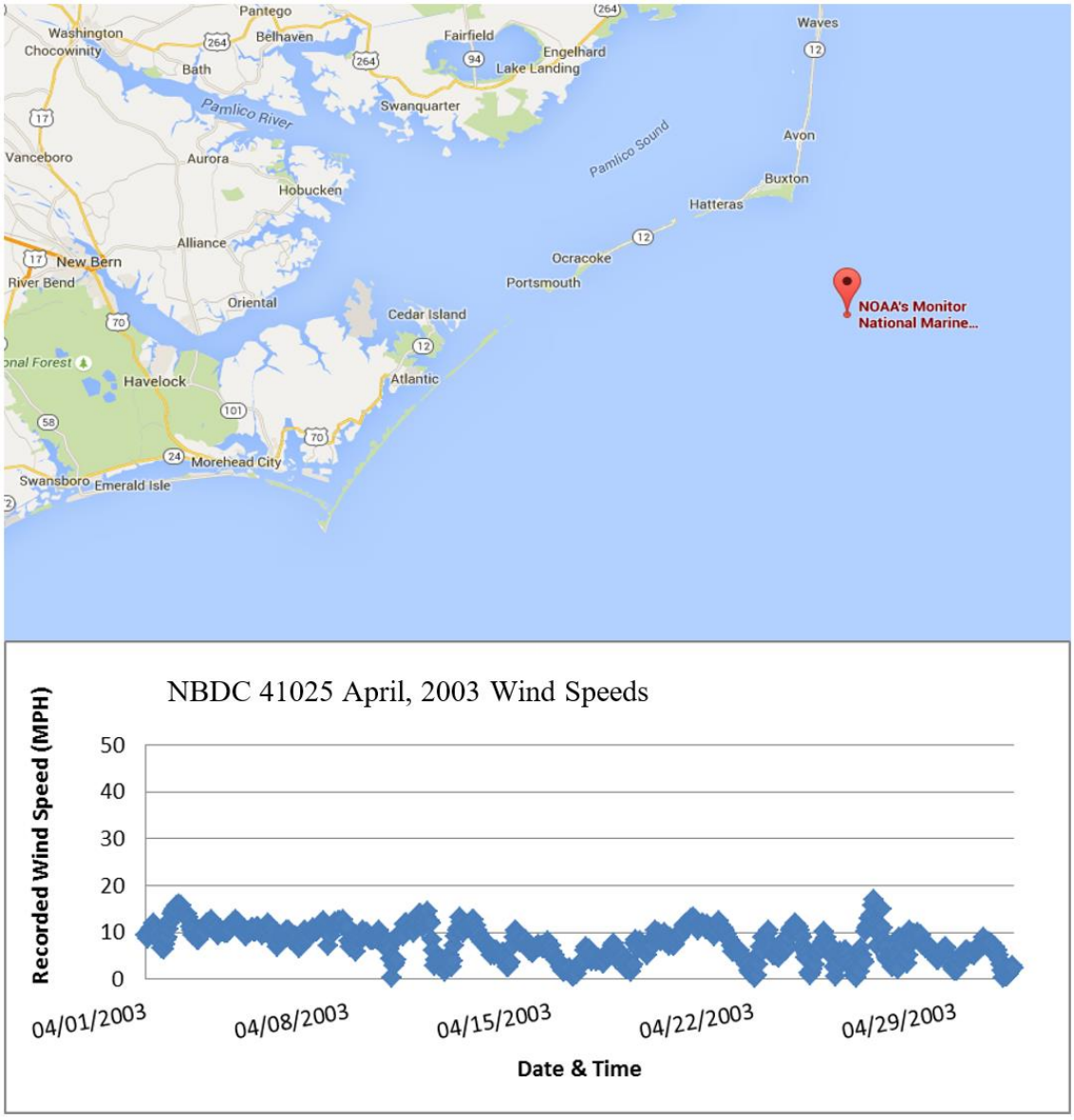

Figure 9-1 Location and Wind Speed Results at NBDC 41025

Given observed wind speeds and track of the nearest tropical storm, April 2003 is considered a period representative of high rainfall without high influence of storm surge or wind effects.

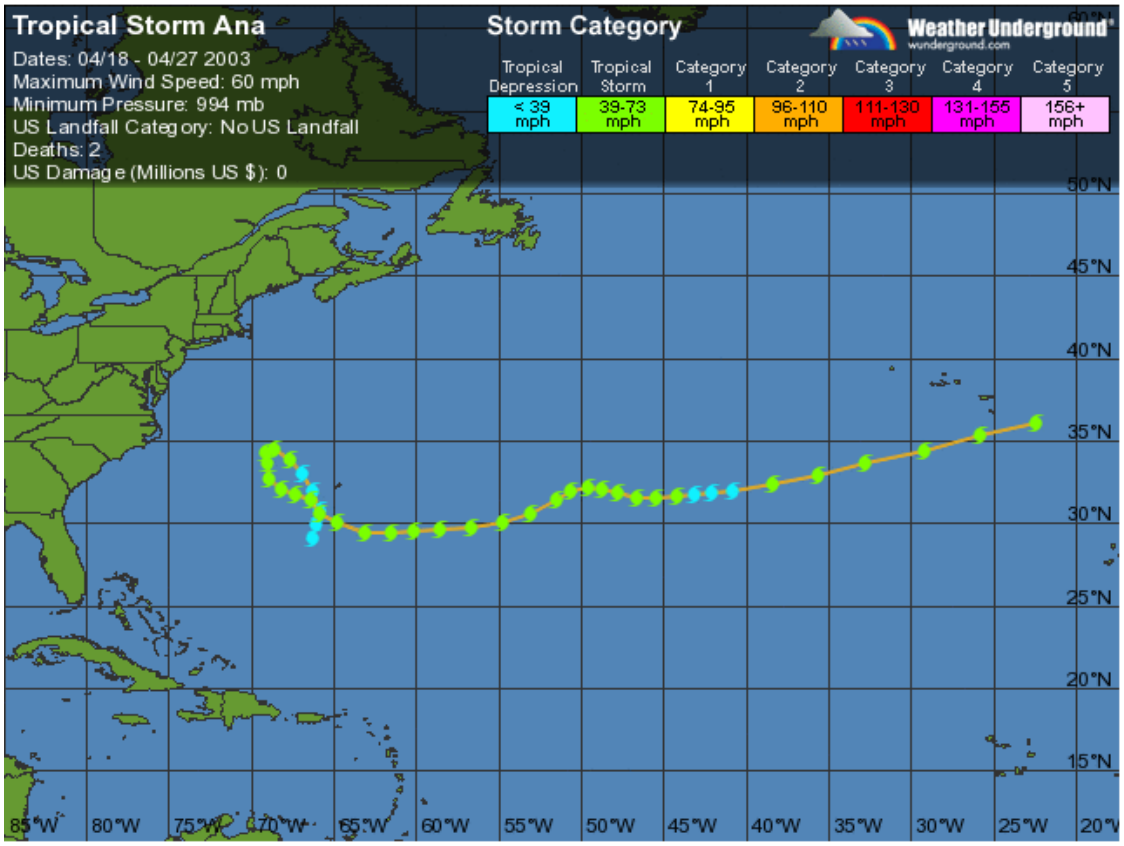

Figure 9-2 TS Ana Track, (The Weather Company, 2017)

FORCING AND VALIDATION STRATEGY

Datasets used to force and validate each model are listed in Table 9-1. Validation of the hydrologic model is discussed in Appendix B. Validation of the ocean model is discussed in Appendix C. The validation of the two river models under comparison is of prime interest in addressing the questions posed by this research, and is discussed in detail in the following sections.

Table 9-1 - Forcing and Validation Datasets - April, 2003

Model	Forcing Datasets	Source(s)	Validation Datasets	Source(s)
Hydrologic Model (HL-RDHM)	Stage IV Multisensor QPE	(NWS NCEP, 2011)	USGS Gauge 02083500 Tar at Tarboro Observed Flow	(USGS, 2015)
Ocean model (ADCIRC)	No winds; Tidal Database	N/A; (Mukai, et al., 2002)	Realtime wind speed & direction from NOAA NOS Buoys; coastal tidal gauges	(NOAA, 2015); (NOAA, 2013)
River Models (ADCIRC, HEC-RAS)	Hydrologic and ocean model results		Real time flow and stage measurements (3 sites)	(USGS, 2015)

Boundary Conditions

To achieve an objective comparison of each modelling method, the error types and magnitudes present at boundary conditions should be examined and compared to the model error types and magnitudes within the shared river model domain. To quantify these errors, model results are compared to observed flow and stage timeseries collected at USGS 02083500 Tar River at Tarboro and USGS 02084472 Pamlico Sound at Washington, respectively.

UPSTREAM BOUNDARY CONDITION – TAR RIVER AT TARBORO, NC

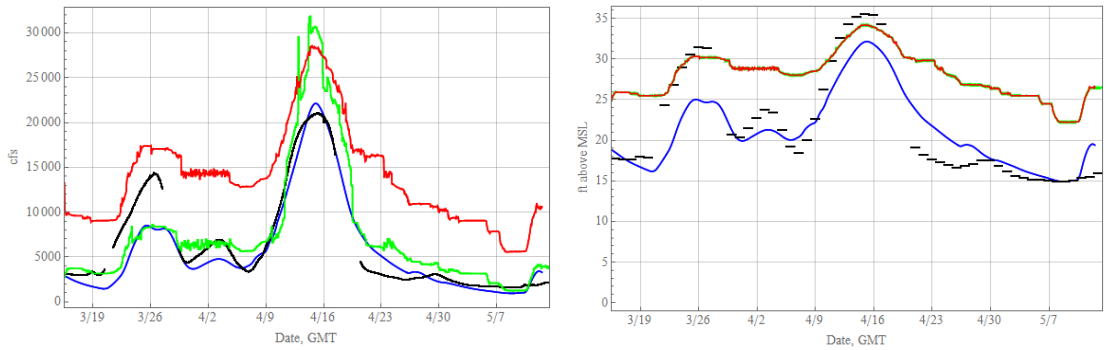

Figure 9-3 Tar River at Tarboro, NC. ADCIRC results in Green, ADCIRC results interpreted by HEC-RAS in red, HL-RDHM flows in blue, observations in black. Flow in left panel, stage in right panel

At Tarboro, flows were overestimated by ADCIRC and by ADCIRC-forced HEC-RAS, including multiple examples of "square-edged" hydrograph shapes (seen also in falling limbs of other storms). RDHM-forced HEC-RAS accurately predicted both peak and baseflows. ADCIRC and ADCIRC-forced HEC-RAS more accurately predicted peak stages (while still failing to resolve baseflows accurately). RDHM-forced HEC-RAS underpredicted peak stage.

DOWNSTREAM BOUNDARY CONDITION – PAMLICO SOUND AT WASHINGTON, NC

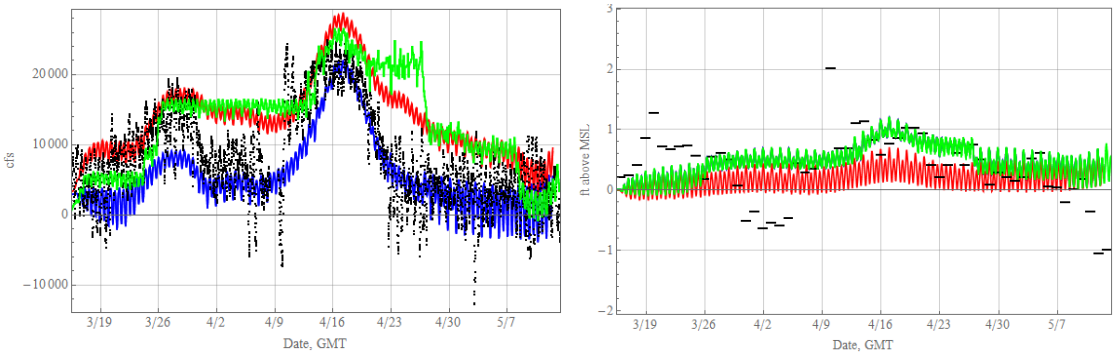

Figure 9-4 Pamlico Sound at Washington - ADCIRC results in Green, ADCIRC results interpreted by HEC-RAS in red, HL-RDHM flows in blue, observations in black. Flow in left panel, stage in right panel

Unlike in the two other hindcast storm events, April 2003's downstream boundary results largely mimic the error types of the upstream boundary results – ADCIRC and ADCIRC-forced HEC-RAS come closer to predicting the largest peak stages, while HEC-RAS forced with river flows directly from the hydrologic model show superior agreement to the largest peak flows.

Note that in the image of stages at the Pamlico gauge, all models utilizing the same downstream boundary conditions overlay each other, and so (barring numerical or data interpretation errors) the two lines visible (in this case, red and green) will simply be the results of ADCIRC with (green) and without (red) rivers. The total net difference between river- and riverless ADCIRC at this boundary is on the order of one foot – this explains the relatively small differences between models forced with ADCIRC with or without rivers – in most figures, the separation between each pair of same-colored lines is not visible.

River Domain Results

Each model's overall performance in the river domain was evaluated using observations at a USGS gauge station and compared using inundation mapping.

Gauge Station Results

Figure 9-5 shows model results at the USGS station operating during the model period – USGS 02084000, Tar River at Greenville.

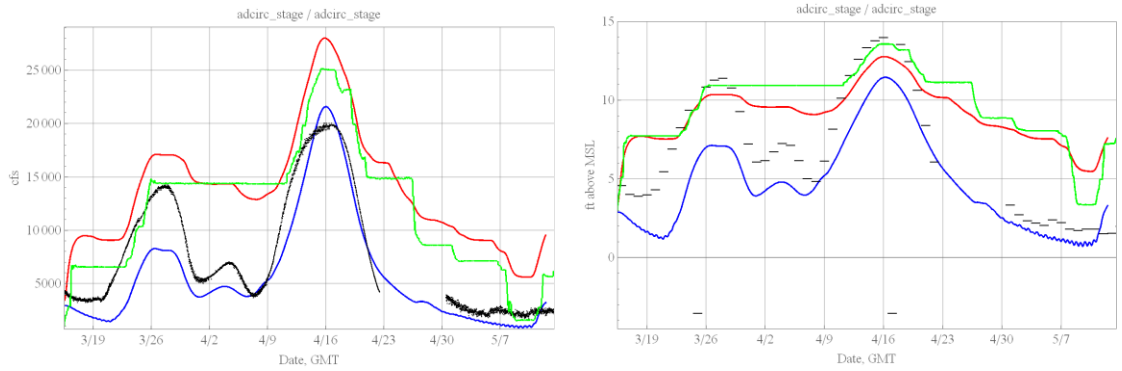

Figure 9-5 Tar River at Greenville, NC. ADCIRC results in Green, ADCIRC results interpreted by HEC-RAS in red, stage solved from HL-RDHM Flows in Blue, observations in black. Left panel flow, right panel stage. Flow in left panel, stage in right panel

Given that error morphologies remain relatively consistent at both boundaries, it comes as no surprise that these patterns repeat within the river model domain as well. ADCIRC captures peak stages, HEC-RAS forced with HL-RDHM flows captures main peak flows. Unlike at other gauges, results here show significant square-edged hydrograph shapes, i.e. significant artifacts.

Gauge Peak Accuracy by Model

The accuracy of each HEC-RAS simulation with regards to peak timing and stage was calculated. Figure 9-6 shows peak timing errors versus river station and Figure 9-7 and Figure 9-8 shows peak flow and stage errors versus river station. River station for each gauge is measured in feet upstream of the model boundary.

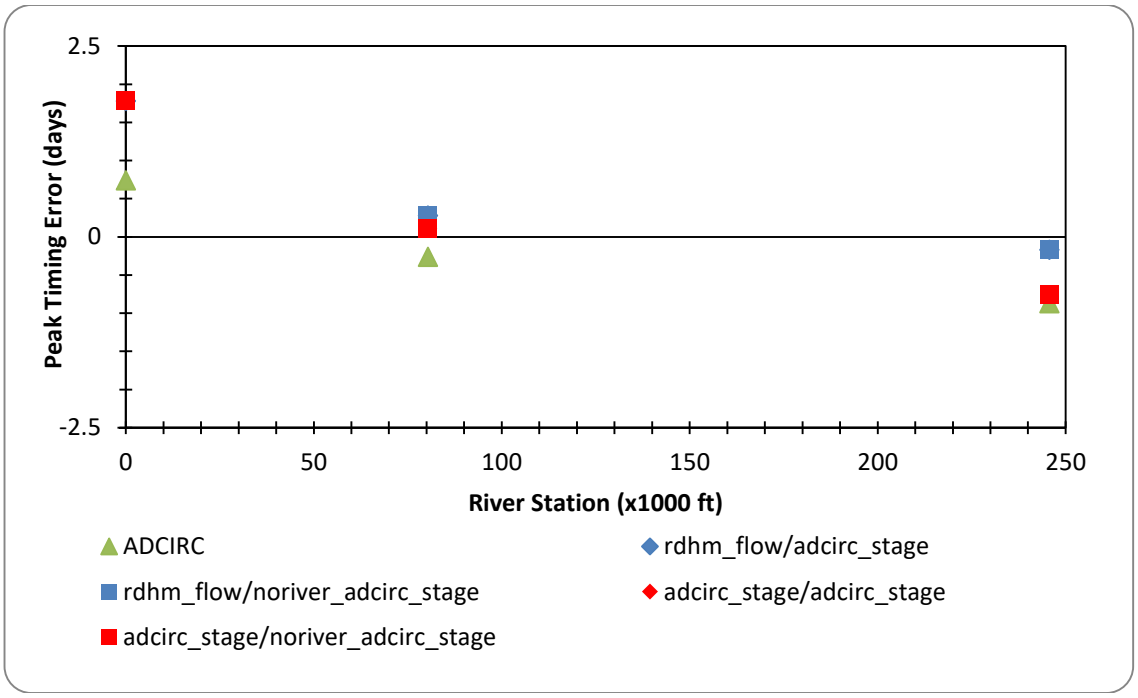

Figure 9-6 Peak Timing Error by Distance Upstream. ADCIRC results in Green, ADCIRC results interpreted by HEC-RAS in red, stage solved from HL-RDHM Flows in Blue, observations in black

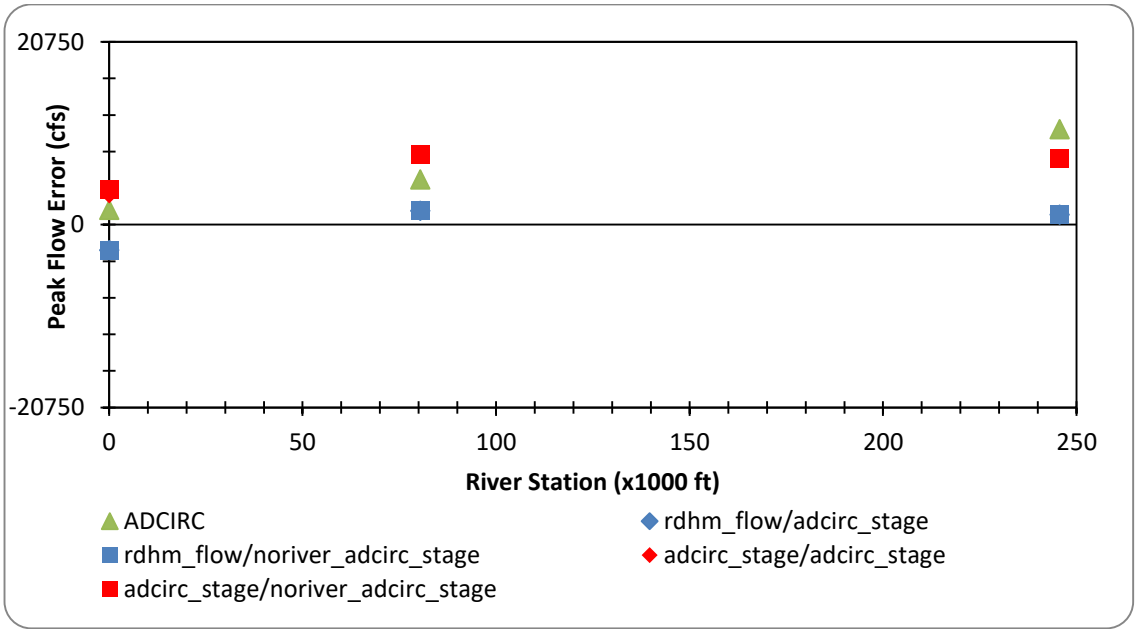

Figure 9-7 Peak Flow Error by Distance Upstream. ADCIRC results in Green, ADCIRC results interpreted by HEC-RAS in red, stage solved from HL-RDHM Flows in Blue, observations in black

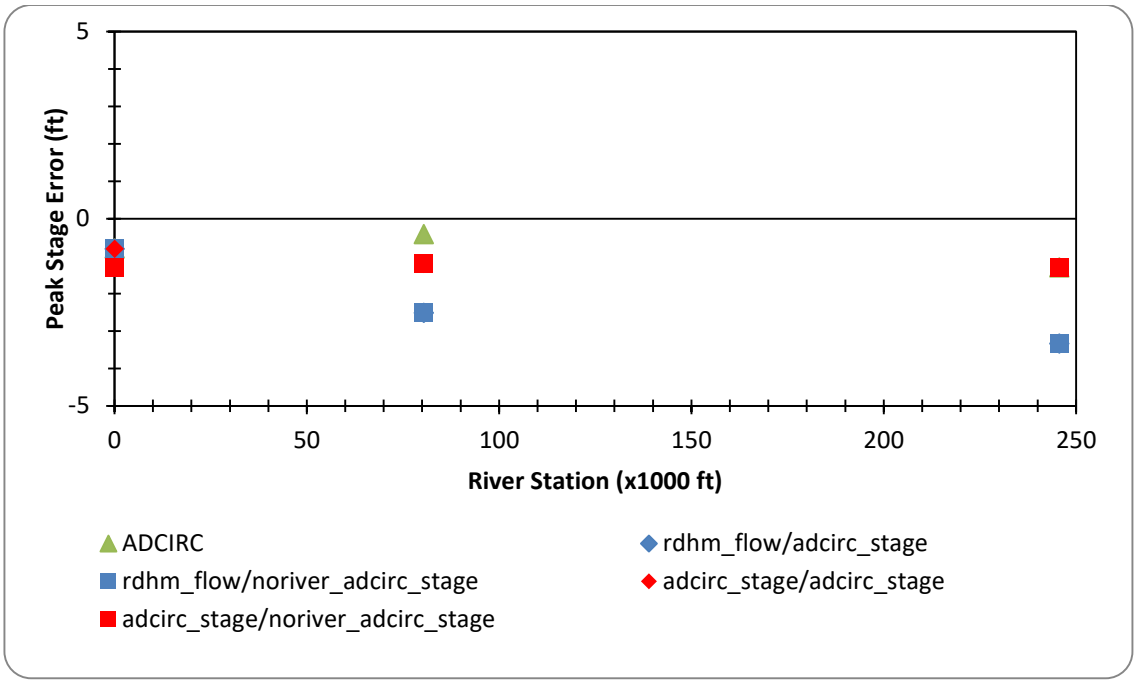

Figure 9-8 Peak Stage Error by Distance Upstream. ADCIRC results in Green, ADCIRC results interpreted by HEC-RAS in red, stage solved from HL-RDHM Flows in Blue, observations in black

Peak prediction goes from being early at the upstream boundary to late at the downstream boundary. Peak flows at the upstream boundary are overpredicted, and approach observed values towards the downstream boundary. Peak Stages are consistently underpredicted.

INUNDATED AREA

As a second and final method of comparison, model results were used to generate peak inundation maps, which are shown below.

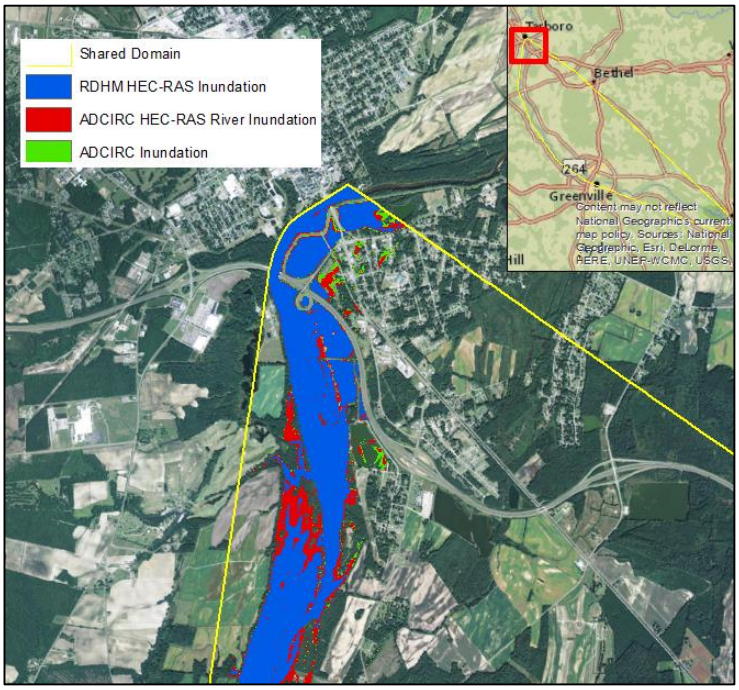

Figure 9-9 April 2003 Rainfall Event Inundation at Tarboro

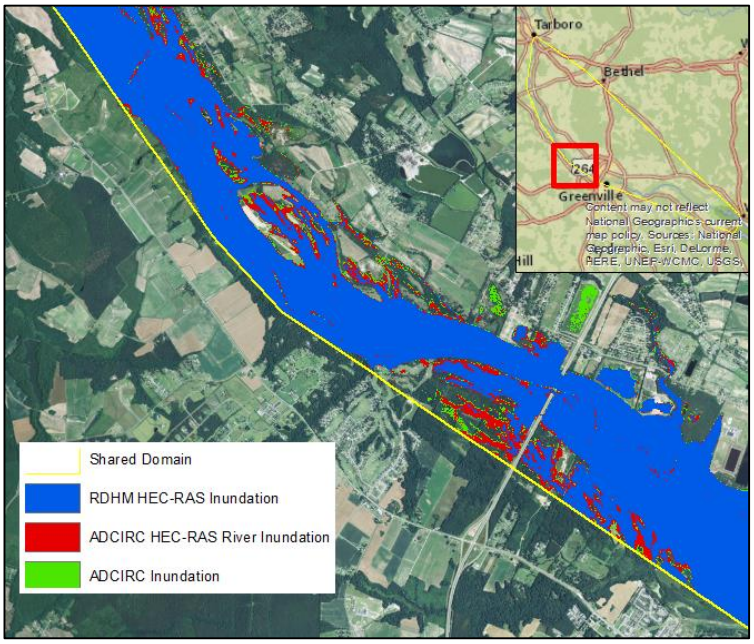

Figure 9-10 April 2003 Rainfall Event Inundation at Rock Spring

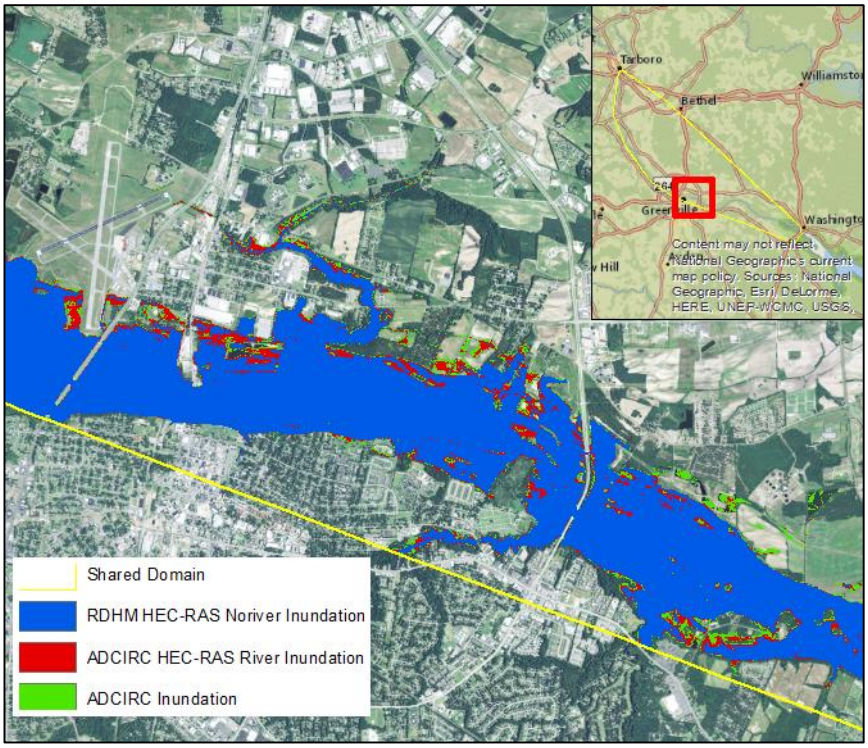

Figure 9-11 April 2003 Rainfall Event Inundation at Greenville

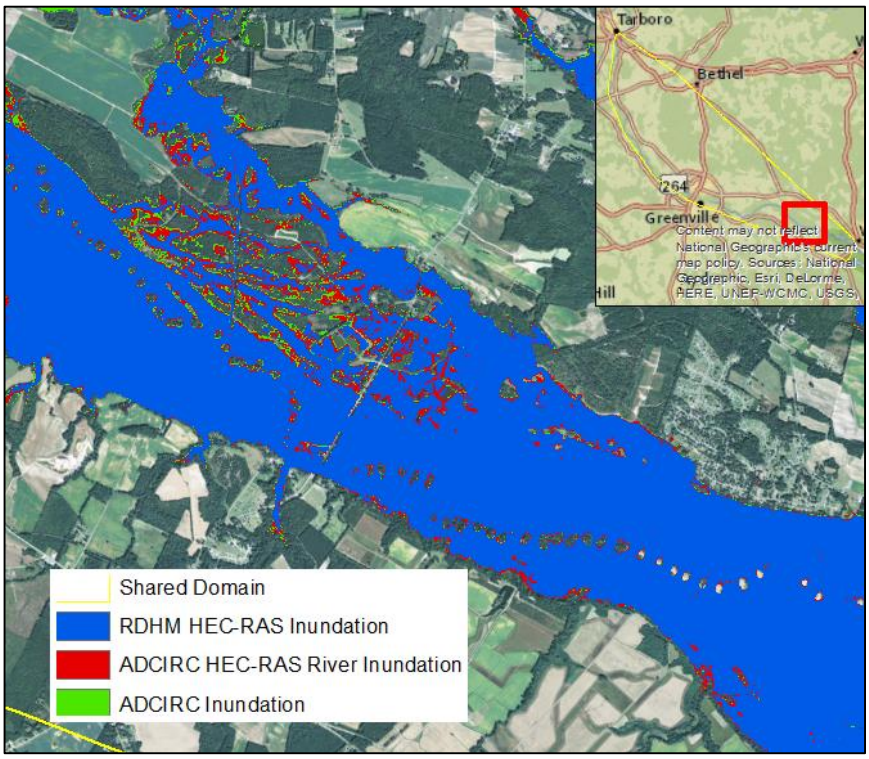

Figure 9-12 April 2003 Rainfall Event Inundation at Grimesland

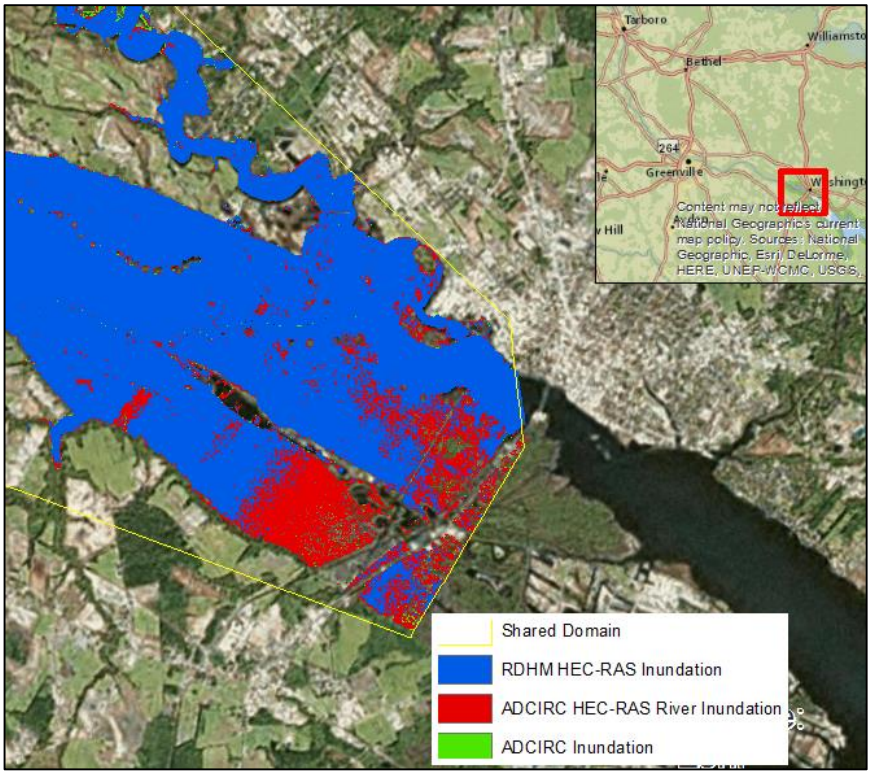

Figure 9-13 April 2003 Rainfall Event Inundation at Washington, NC

Figure 9-9, Figure 9-10, Figure 9-11, Figure 9-12, and Figure 9-13 show hindcast inundation at Tarboro, Rock Spring, Greenville, Grimesland, and Washington, respectively. Inundation results follow the trends seen in gauge hydrographs –RDHM HEC-RAS results show the least inundation extent and ADCIRC inundation extent is the most extreme, but overall results are fairly similar.

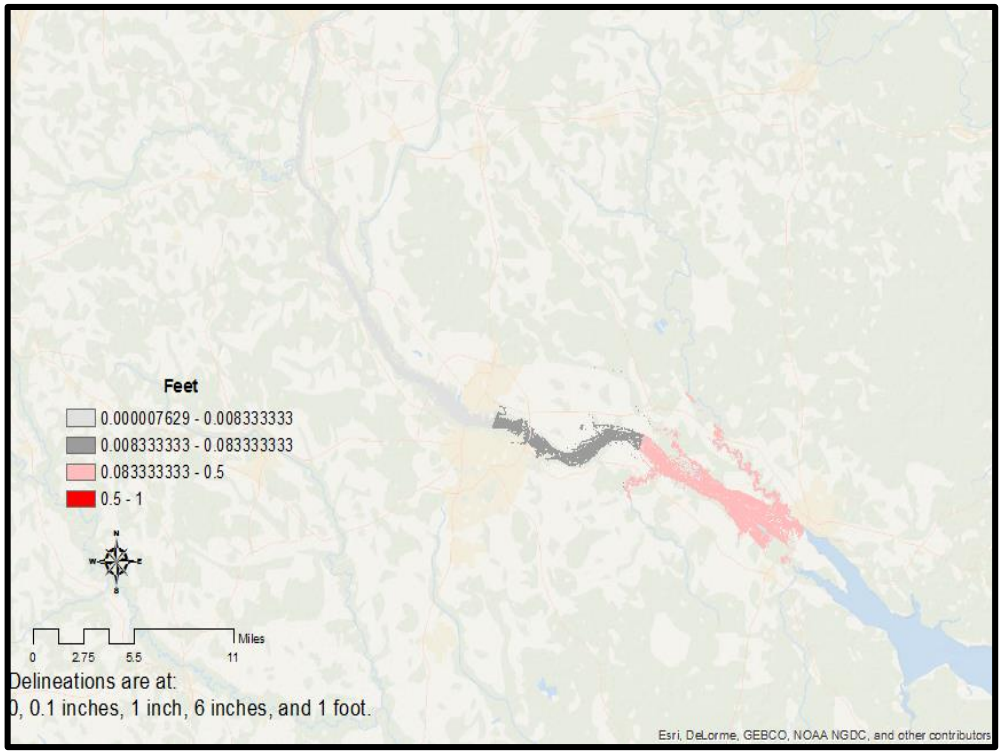

Figure 9-14 Error in HEC-RAS Solution Induced by Riverless BC – April, 2003

As expected, errors associated with a riverless boundary condition at the HEC-RAS model's downstream boundary are localized near the estuary. Interestingly, the spatial extent of errors in excess of one inch (0.083 feet) is larger than the extent of the same error magnitude during Floyd, but smaller than the same region during Irene.

SUMMARY OF MODEL COMPARISONS FOR APRIL, 2003

Predictions using HEC-RAS as middleware did not vary significantly when using river (fine mesh) vs noriver (coarse mesh) ADCIRC results. HEC-RAS forced with RDHM flows show more accurate flowrates than results from ADCIRC or from HEC-RAS forced with ADCIRC flows. ADCIRC predicted slightly higher inundation than HEC-RAS at all locations except for the upstream handoff point (Tarboro). Errors due to riverless boundary conditions were less than six inches in regions above Pamlico Sound.

10. TIMING ADVANTAGES OF RIVERLESS VS. RIVER ADCIRC

INTRODUCTION

In order to establish the benefits of modelling a river in HEC-RAS rather than in ADCIRC, the cost of simulating or not simulating that river in ADCIRC should be found. To do this, simulations of Hurricane Irene (as described in Chapter 7) were recreated, with the timestep adjusted until the model failed to converge. This "maximum stable timestep" was recorded, and is used to provide a rough, system- and hardware-independent measure of the time cost of simulating different configurations.

METHODS

MESHES USED

Runs were performed using three grids: "coarse", "rivers off," and "rivers on." The coarse grid was developed by removing the river from the mesh and interpolating nodal attributes onto this coarsened grid. The "rivers off" mesh is the full-resolution ADCIRC mesh with no river boundary condition applied. The "rivers on" mesh is the full-resolution ADCIRC mesh as used in prior sections.

COARSE MESH DESCRIPTION

Maps of the coarse mesh are included in Appendix A. The coarse mesh is typified by grid scales larger than the scale of the river itself, and a lack of upstream river boundary condition.

FINE MESH DESCRIPTION

Maps of the fine mesh are included in Appendix A. The fine mesh includes a one-element wide resolution of the river channel. The formulation of this grid and the implications of

this coarse resolution on simulation results are discussed in detail in the work by Tromble (2011).

Determination of Stable Timestep

The maximum stable timestep was determined by performing model runs according to a binary search algorithm. This algorithm is diagrammed in Figure 10-1. After five iterations, the range of possible values for the maximum stable timestep was reduced from 8s to 0.25s. At this point the process was ceased. In this way, a range of 0.25s was determined, where the maximum stable timestep is known to fall within.

By inverting the minimum of this range, a rough estimate of time-cost can be determined, which represents the number of timesteps which must be calculated to simulate a given period.

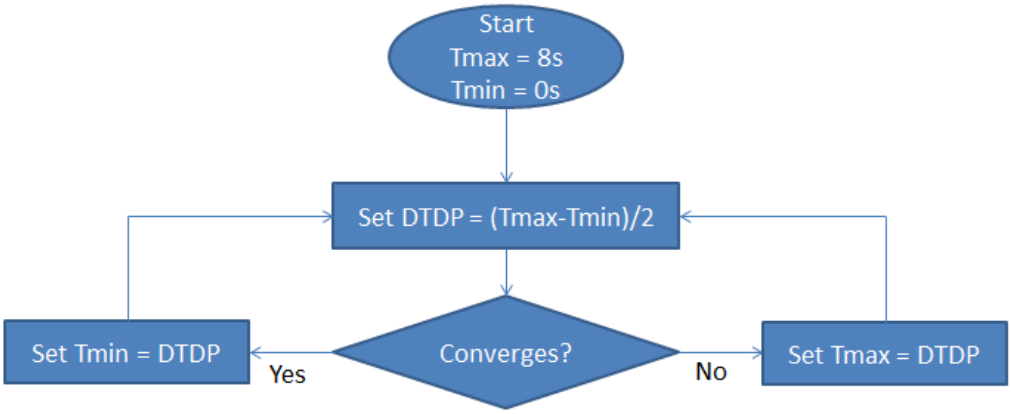

Figure 10-1 Binary Search Algorithm

Results & Conclusions

The ranges of maximum stable timestep and the corresponding cost factors for each grid are shown in Table 10-1. As expected, costs for resolving rivers in the ADCIRC grid are significant, ranging from 150% to more than 450%.

One result that is somewhat surprising is the difference between the stable timestep associated with an identical grid, with rivers on or off. It is not known whether the reduction in stability with rivers on is due to the presence of small, wetted elements near the river boundary condition, or if the instability is occurring due to the boundary condition itself. If the result is the former, then it should be noted that resolving rivers in ADCIRC meshes without including a river boundary condition may lead to unexpected instability during events of unprecedented severity – as storm surge propagates into a resolved but previously dry river domain, smaller elements would become wetted, potentially rendering a previously-stable simulation unstable.

These results are compared to the changes in model accuracy in Chapters 7, 8, and 9 of this thesis.

Table 10-1 - Maximum Stable Timesteps by Grid

Grid	**Coarse**	**Rivers Off**	**Rivers On**
Range Of Maximum Stable Timestep	3.5-3.75 seconds	2.25-2.5 seconds	0.75-1 seconds
Time-cost Factor	0.286	0.444	1.333
% of Time Cost vs. “Coarse”	100%	155%	466%

11. Discussions and Future Work

Discussion of Hypotheses

The implications of results from this research on each hypothesis are discussed below. Each is discussed in terms of qualitative results (hydrograph shapes) and quantitative results (peak stage errors in feet, peak timing errors in hours).

Hypothesis 1 - Is HEC-RAS more accurate than ADCIRC in the Tar River?

Prior to this research, it was believed that the use of HEC-RAS to model riverine systems, forced with ADCIRC at the downstream boundary, would produce forecasts with reduced simulation time and without reduced accuracy compared to the use of ADCIRC to model the same riverine areas, given the same boundary condition information. The independent variable in this study was the model configuration, with model performance (accuracy) as the measured, dependent variable.

Qualitatively, this hypothesis will be confirmed if, in the standard comparison hydrographs, model results using the same boundary conditions show improved agreement with gauges within the model domain (Grimesland, Greenville, Rock Springs). Specifically, this will be confirmed if results show HEC-RAS results (Red) as being in greater agreement with observations (Black) than ADCIRC results forced with the same information (Green). Irene results do not consistently confirm or deny this conclusion – instead, they indicate that HEC-RAS results are consistently lower than ADCIRC results. Floyd results similarly do not confirm nor deny this conclusion, as again, results at Greenville can be qualitatively be described as similar, where HEC-RAS has a slight reduction in stages and flows. In the April, 2003 event, there is an apparent reduction in square-edging in the HEC-RAS results, and a small peak prior to the largest peak shows

more realistic recession behavior than the ADCIRC results at that time. Taken as a whole, these results qualitatively show that the HEC-RAS model shows increased realism and skill at producing hydrographs at low flows (April, 2003) but during more severe events (Floyd, Irene) model skill at producing peak stages or flows appears similar.

Results were quantified by comparing predicted and observed maxima in each hydrograph. Peak stage and timing errors were calculated using Equation 6. Results shown are expressed as a percentage representing the ratio of errors between two models, calculated using Equation 7.

Equation 7 – Model Error Factor

$$Error\ Factor\ (\%) = \frac{|Model\ 1|}{|Model\ 2|} x100$$

To evaluate Hypothesis 1, error factors were calculated using HEC-RAS as "Model 1" and ADCIRC as "Model 2," with the specific models used being the two models with the same upstream and downstream boundary conditions.

Table 11-1 - Peak Prediction Error Factors, HEC-RAS/ADCIRC

Event	Floyd			Irene			April, 2003		
Parameter	Stage	Flow	Timing	Stage	Flow	Timing	Stage	Flow	Timing
Grimesland	n/a	n/a	n/a	45%	n/a	178%	n/a	n/a	n/a
Greenville	127%	187%	67%	8674%	122%	500%	295%	156%	42%
Rock Springs	n/a	n/a	n/a	389%	n/a	214%	n/a	n/a	n/a

Hypothesis 1 would confirmed by results in the table that are <100%, indicating that the HEC-RAS error is smaller in magnitude than the ADCIRC error. Results overall tend to reject this hypothesis as neither stage, nor flow, nor timing results are consistently more accurate than ADCIRC results.

Note that the error factor formula described in Equation 7 results in abnormal results when the error in one model is particularly low. While in most scenarios the errors at gauges are similar in magnitude, in the single example of stage results at Greenville during Hurricane Irene, ADCIRC errors were very, very low – nearing to zero – resulting in a very high error factor.

By considering both qualitative and quantitative results, it can be seen that the original Hypothesis 1 (that HEC-RAS model results are more accurate than ADCIRC results when supplied with the same boundary conditions) has been partially rejected by this research – HEC-RAS shows notable improvements in producing “realistic-looking” hydrographs, but does not consistently show increased skill in predicting peak severity (stage, flow) or timing.

Hypothesis 2 – What are the costs/benefits associated with incorporating rivers in an ADCIRC model?

Second, it was believed that using a more coarsely resolved ADCIRC mesh to develop a downstream boundary condition for a HEC-RAS model would:

A. not result in a loss of accuracy in the HEC-RAS model
B. result in a reduction in the computation time required to achieve a stable ADCIRC solution

The independent variable for this model was the mesh resolution in riverine areas, with model performance (accuracy) and CPU time (cost) as the measured, dependent variables. Each of this hypothesis's two component statements are discussed separately.

Hypothesis 2A

This hypothesis's validity can be seen qualitatively by comparing results for models both with and without riverine ADCIRC (i.e. separation within each of the blue and red bifurcated lines on standard results hydrographs) within the shared model domain (Grimesland, Greenville, Rock Springs). This separation is only visible at Greenville and Grimesland, and then only in the low flow/baseflow portions of those sites' hydrographs. In the general case of predicting peak flood conditions, a river-forced solution at the downstream edge offers essentially no benefit at least as far downstream as Rock Springs. Results were quantified by comparing predicted and observed maxima in each hydrograph. Peak stage and timing errors were calculated using Equation 6.

. Results shown are expressed as a percentage representing the error in HEC-RAS with and without a resolved river downstream boundary condition, calculated using Equation

7. In that equation, HEC-RAS forced with riverine ADCIRC is taken as Model 1, and HEC-RAS forced with riverless ADCIRC is taken as Model 2.

Table 11-2 - Peak Prediction Error Factors, HEC-RAS (RDHM Upstream), Rivers/No Rivers

Event	Floyd			Irene			April, 2003		
Parameter	Stage	Flow	Timing	Stage	Flow	Timing	Stage	Flow	Timing
Grimesland	n/a	n/a	n/a	137%	n/a	84%	n/a	n/a	n/a
Greenville	100%	100%	100%	100%	100%	100%	100%	100%	100%
Rock Springs	n/a	n/a	n/a	100%	n/a	100%	n/a	n/a	n/a

Table 11-3 - Peak Prediction Error Factors, HEC-RAS (ADCIRC Upstream), Rivers/No Rivers

Event	Floyd			Irene			April, 2003		
Parameter	Stage	Flow	Timing	Stage	Flow	Timing	Stage	Flow	Timing
Grimesland	n/a	n/a	n/a	143%	n/a	84%	n/a	n/a	n/a
Greenville	100%	100%	100%	100%	100%	100%	100%	100%	100%
Rock Springs	n/a	n/a	n/a	100%	n/a	100%	n/a	n/a	n/a

Hypothesis 2A would be confirmed if HEC-RAS riverless results show equal or lesser errors than HEC-RAS river results. In the tables above, that is indicated by error factors that are greater than 100%.

By considering both qualitative and quantitative results for all three events, it can be seen that the validity of the original Hypothesis 2A is spatially dependent – incorporation of a coarsely resolved ADCIRC mesh would result in a reduction in predicted peaks of up to 1 foot in depth, as far upstream as Rock Springs, but farther upstream results show essentially no reduction in accuracy. Whether this hypothesis can be considered confirmed or rejected depends on the location of interest and the required prediction accuracy.

HYPOTHESIS 2B

Qualitative model results are not relevant for this hypothesis. Based on timing test results, the computational cost associated with the incorporation of rivers into the ADCIRC model are on the order of 50% or higher. Hypothesis 2B (that using a more coarsely resolved ADCIRC mesh to develop a downstream boundary condition for a HEC-RAS model would result in a reduction in the computation time required to achieve a stable ADCIRC solution) has been strongly confirmed.

HYPOTHESIS 2 – COMBINED

Taken as a whole, the reduction in model accuracy associated with removing the resolution from the Tar River domain is spatially variable, and the time savings of doing so are significant. If results are desired at Greenville or farther upstream, errors are minimal. However, errors accrue nearer the downstream boundary.

HYPOTHESIS 3

As a conclusion of the first two original hypotheses, it was believed that simply coupling the existing HEC-RAS model to the coarsely resolved ADCIRC model used in this research would immediately enable river simulations at significant reduction of cost with either improvements or insignificant reductions in model accuracy. This hypothesis was examined qualitatively and quantitatively by implementing a model coupling that would be immediately feasible for adoption.

Qualitatively, the skill of this potential coupling (shown in Blue on the standard hydrographs) can be compared to the skill of the current model (shown in Green on the standard hydrographs) and their skill can be evaluated based on hydrograph shape. In Irene, the ADCIRC river model showed higher skill in capturing peak stages at Greenville

and Grimesland, with HEC-RAS results more accurately representing results at Rock Springs. In Floyd, peak flows are captured best by HEC-RAS. Neither model captures peak stages well, but ADCIRC showed slightly better skill. In April, 2003, the HEC-RAS model captured flows comparatively well, while ADCIRC captured peak stages.

Results were quantified by comparing predicted and observed maxima in each hydrograph. Peak stage and timing errors were calculated using Equation 6. Results shown are expressed as a percentage representing the error in HEC-RAS as a fraction of the ADCIRC error, calculated using Equation 7, with the proposed new coupling as "Model 1" and with the base ADCIRC results as "Model 2".

Table 11-4 - Peak Prediction Error Factors, HEC-RAS/ADCIRC

Event	Floyd			Irene			April, 2003		
Parameter	Stage	Flow	Timing	Stage	Flow	Timing	Stage	Flow	Timing
Grimesland	n/a	n/a	n/a	35%	n/a	213%	n/a	n/a	n/a
Greenville	71%	63%	121%	5953%	25%	3450%	31%	108%	615%
Rock Springs	n/a	n/a	n/a	275%	n/a	1289%	n/a	n/a	n/a

Error factors greater than 100% in the table above reject hypothesis 3, i.e. they indicate that the adoption of the currently-feasible model coupling would result in reductions in model accuracy.

By comparing qualitative and quantitative results between the proposed new coupling and the currently-operational model, it can be seen that peak prediction skill would suffer substantially during Irene, but would have been improved during Hurricane Floyd. Hypothesis 3 is considered rejected due to multiple instances of substantially increased error.

RECOMMENDATIONS

Recommendations for future work are divided into a summary of the implications of this work for model users, and a discussion of potential directions for future studies.

OPERATIONAL IMPLICATIONS

Based on this research, while costs of the current model coupling scheme are high (Hypothesis 2B), and while HEC-RAS shows potential as middleware when forced with identical boundary conditions to ADCIRC (Hypothesis 1, 2A), currently there is significant error during certain events due to the presently available upstream boundary conditions from HL-RDHM (Hypothesis 3, Hurricane Irene).

POSSIBLE FUTURE STUDIES

This research indicates possible future studies in at least four areas: determination of the radius of impact of downstream boundary condition errors, development of more accurate boundary conditions, quantification of timing advantages of proposed couplings, and the impact of improved resolution in the river representation in the hydrodynamic model.

RADIUS OF IMPACT OF DOWNSTREAM BC ERRORS

The Tar River (as with all rivers with shallow bed slopes) is impacted by both upstream and downstream conditions in varying ways. From the maps of inundation error associated with a riverless downstream boundary condition (Figure 7-27, Figure 8-14, and Figure 9-14), the spatial map of differences in a total water level river stage prediction due to changes in boundary condition vary widely with changing event conditions. It remains to be seen if, with sufficient parameterization, a functional guidance could be developed to estimate a storm surge prediction's impact on stage predictions in terms of distance upstream. If this "radius of impact" associated with resolved rivers in a 2D model

could be established for all expected storm conditions, the implementation of this sort of middleware coupling would be rendered more predictable in terms of error behaviors.

Boundary Condition Development

Boundary conditions at the upstream edge of the riverine domain dominate the differences between HEC-RAS models. Additional attention to this boundary condition may reduce or eliminate the errors associated with the proposed scheme in the regions outside of the "radius of impact" of the downstream boundary.

Cost-Benefit Quantification

This research used a rough "rule-of-thumb" factor to determine computational costs. A rigorous timing trial on operational-scale architectures may reveal more precisely the time costs associated with resolving rivers. If the quality of a proposed new coupling can be improved, then a more formal cost/benefit analysis can be produced which statistically accounts for the reduction in expected error associated with additional ensemble modelling members. In addition, this comparison did not formally examine the additional cost of developing the HEC-RAS model (as this work was performed by Abshire (2012)) nor did it examine the cost or workload of operating a third model as middleware, as the coupling implementation used here (of single-event, non-dynamic coupling, with manually-passed data) would appear very different in a real-time operational scheme, ideally featuring automated data passing, perhaps with a dynamic coupling scheme.

Improved River Resolution

This research did not attempt to modify the resolution of the operational riverine mesh, as it was considered cost-prohibitive. However, given that there is always a tradeoff between simulation time and model accuracy, the development of a more finely-resolved

river model may justify the increased simulation cost if it produces a very high degree of predictive skill. For example, if costs per member double, but the resulting error envelope of an ensemble simulation with ½ the member size was reduced, then increased resolution in the rivers will have justified the increased cost.

WORKS CITED

1. Abshire, K. E., 2012. *Impacts of Hydrologic and Hydraulic Model Connection Schemes on Flood Simulation,* s.l.: Duke University.

2. Astite, S. W. et al., 2015. Cartography of flood hazard by overflowing rivers using hydraulic modeling and geographic information system: Oued El Harrach case (North of Algeria). *REVISTA DE TELEDETECCIÓN,* pp. 67-79.

3. Baugh, J. & Altuntas, A., 2016. *Modeling a discrete wet-dry algorithm for hurricane storm surge in Alloy.* s.l., Springer international Publishing, pp. 256-261.

4. Baugh, J., Altuntas, A., Dyer, T. & Simon, J., 2015. An exact reanalysis technique for storm surge and tides in a geographic region of interest. *Coastal Engineering,* pp. 60-77.

5. Blain, C. A. & Massey, T. C., 2007. *Coastal Ocean Models as Planning Tools: A Case Study from Hurricane Katrina Storm Surge.* [Online] Available at: http://www.dtic.mil/docs/citations/ADA488127

6. Blanton, B. et al., 2012. Urgent computing of storm surge for North Carolina's coast. *Procedia Computer Science,* pp. 1677-1686.

7. Blanton, B. O. & Luettich, R. A., 2008. *North Carolina,* Chapel Hill, NC: Renaissance Computing Institute.

8. Bleichrodt, F., Bisseling, R. H. & Djikstra, H. A., 2012. Accelerating a barotropic ocean model using a GPU. *Ocean Modeling,* pp. 16-21.

9. Brunner, G. W., 2010. *Software.* [Online] Available at: http://www.hec.usace.army.mil/software/hec-ras/documentation/HEC-RAS_4.1_Reference_Manual.pdf [Accessed 23 February 2017].

10. Cardone, V. J. & Cox, A. T., 2009. Tropical cyclone wind field forcing for surge models: critical issues and sensitivities. *Natural Hazards,* 51(1), pp. 29-47.

11. CBOFS, 2013. *The Chesapeake Bay Operational Forecast System (CBOFS).* [Online]
Available at: https://tidesandcurrents.noaa.gov/ofs/cbofs/cbofs_info.html
[Accessed 26 10 2017].

12. Cho, K.-H.et al., 2012. A modeling study on the response of Chesapeake Bay to hurricane events of Floyd and Isabel. *Ocean Modeling,* pp. 22-46.

13. Christian, J. et al., 2013. Uncertainty in floodplain delineation: expression of flood hazard and risk in a Gulf Coast watershed. *Hydrological Processes,* pp. 2774-2784.

14. CREOFS, 2013. *Columbia River Estuary Operational Forecast System (CREOFS).* [Online]
Available at:
https://tidesandcurrents.noaa.gov/ofs/creofs/creofs_info.html
[Accessed 26 10 2017].

15. Crowell, M. et al., 2010. An Estimate of the U.S. Population Living in 100-Year Coastal Flood Hazard Areas. *Journal of Coastal Research,* pp. 201-211.

16. Dawson, C. et al., 2011. Discontinuous Galerkin methods for modeling Hurricane Storm Surge. *Advances in Water Resources,* pp. 1165-1176.

17. Dietrich, J. C., 2005. *Implementation and assessment of ADCIRC's wetting and drying algorithm,* Norman, OK: University of Oklahoma.

18. Dietrich, J. et al., 2012. Performance of the Unstructured-Mesh, SWAN+ADCIRC Model in Computing Hurricane Waves and Surge. *Journal of Scientific Computing,* pp. 468-497.

19. Dietrich, J. et al., 2012. Surface Trajectories of Oil Transport along the Northern Coastline of the Gulf of Mexico. *Continental Shelf Research,* pp. 17-47.

20. Dresback, K. M. et al., 2013. Skill assessment of a real-time forecast system utilizing a coupled hydrologic and coastal hydrodynamic model during Hurricane Irene (2011). *Continental Shelf Research,* pp. 78-94.

21. DuChene, M. et al., 2011. A framework for running the ADCIRC discontinuous galerkin storm surge model on a GPU. *Procedia Computer Science,* pp. 2017-2026.

22. Dyer, T. & Baugh, J., 2016. An interface for localized storm surge modeling. *Advances in Engineering Software,* pp. 27-39.

23. Fink, P., Bodi, G. & Haider, S., 2006. Abschatzung des Vertrauensbereichs von berechneten Hochwasser-Spiegellagen. *Osterreichische Wasser- und Abfallwirtschaft,* pp. a15-a18.

24. Fleming, J. G. et al., 2008. A Real Time Storm Surge Forecasting System using ADCIRC. *Estuarine and Coastal Modeling,* pp. 893-912.

25. Fleming, J. et al., 2016. *Real-Time Guidance for Combined Flooding Hazards and Active Flood Control Structures using the ADCIRC Surge Guidance System.* Kingston, RI, 14th Estuarine and Coastal Modeling Conference (ECM14).

26. George J. Huffman, D. T. B., 2016. *Real-Time TRMM Multi-Satellite Precipitation Analysis Data Set Documentation.* [Online]
Available at:
https://pmm.nasa.gov/sites/default/files/document_files/3B4XRT_doc_V7.pdf
[Accessed 19 December 2016].

27. Gupta, H. V. & Kling, H., 2011. On typical range, sensitivity, and normalization of Mean Squared Error and Nash-Sutcliffe Efficiency type metrics. *Water Resources Research,* 47(W10601).

28. Horritt, M. S. & Bates, P. D., 2002. Evaluation of 1D and 2D numerical models for predicting river flood inundation. *Journal of Hydrology,* pp. 87-99.

29. Hydrology Laboratory, 2008. *The HL Research Distributed Hydrologic Model (HL-RDHM) Developer's Manual.* 2.0 ed. s.l.:s.n.

30. Kinnmark, I., 1986. *The Shallow Water Wave Equations: Formulation, Analysis and Application. Lecture Notes in Engineering Vol. 15.* Berlin: Springer.

31. Kitzmiller, D. et al., 2011. Evolving multisensor precipitation estimation methods: Their impacts on flow prediction using a distributed hydrologic model. *Journal of Hydrometeorology,* pp. 1414-1431.

32. Kolar, R. L., Gray, W. G., Westerink, J. J. & Leuttich, Jr., R. A., 1994. Shallow water modeling in spherical coordinates: equation formulation, numerical implementation, and application. *Journal of Hydraulic Research,* pp. 32(1):3-24.

33. Kolar, R. L. et al., 2009. Process-oriented tests for validation of baroclinic shallow water models: The lock-exchange problem. *Ocean Modelling,* pp. 137-152.

34. Koren, V. et al., 2003. Hydrology laboratory research modeling system (HL-RMS) of the US national weather service. *Journal of Hydrology,* pp. 297-318.

35. Lanerolle, L. W. J., Patchen, R. C. & Aikman III, F., 2011. *Technical Report NOS CS 29 - The Second Generation Chesapeake Bay Operational Forecast System (CBOFS2): Model Development and Skill Assessment,* s.l.: NOAA.

36. Leuttich, R. & Westerink, J., 2004. *Theory Report and Formulation.* [Online] Available at: http://www.unc.edu/ims/adcirc/adcirc_theory_2004_12_08.pdf [Accessed 23 February 2017].

37. Liang, Q., Xia, X. & Hou, J., 2016. Catchment-scale High-resolution flash flood simulation using the GPU-based technology. *Procedia Engineering,* pp. 975-981.

38. Lian, J., Xu, K. & Ma, C., 2013. Joint impact of rainfall and tidal level on flood risk in a coastal city with a complex river network: a case study of Fuzhou City, China. *Hydrology and Earth System Sciences,* pp. 679-689.

39. Martinez, M., Wheeler, M. F. & Dawson, C. N., 1998. *A priori error estimates of finite element models of systems of shallow water equations,* Houston, TX: ProQuest Dissertations Publishing.

40. Mashriqui, H. S., Halgren, J. S. & Reed, S. M., 2014. 1D River Hydraulic Model for Operational Flood Forecasting in the Tidal Potomac: Evaluation for Freshwater, Tidal, and Wind-Driven Events. *Journal of Hydraulic Engineering,* pp. 04014005 1-14.

41. Mattocks, C. & Forbes, C., 2008. A real-time, event-triggered storm surge forecasting system for the state of North Carolina. *Ocean Modeling,* pp. 95-119.

42. McKay, P. & Blain, C. A., 2010. *Toward Developing a Hydrodynamic Flow and Inundation Model of the Lower Pearl River,* Stennis Space Center, MS: Naval Research Laboratory.

43. Mejia, A. & Reed, S., 2011. Evaluating the effects of parameterized cross sections with a coupled distributed hydrologic and hydraulic model. *Journal of Hydrology,* Volume 409, pp. 512-524.

44. Melillo, J. M., Richmond, T. (. & Yohe, G. W., 2014. *Climate Change Impacts in the United States: The Third National Climate Assessment. ,* s.l.: U.S. Global Change Research Program.

45. MHX Case Study Team, 2012. *Hurricane Irene, August 26-27, 2011.* [Online] Available at: http://www.erh.noaa.gov/mhx/EventReviews/20110827/20110827.php [Accessed 16 11 2015].

46. Mukai, A. Y., Westerink, J. J. & Leuttich, R. A., 2002. *Guidelines for Using Eastcoast 2001 Database of Tidal Constituents within Western North Atlantic Ocean, Gulf of Mexico and Caribbean Sea,* s.l.: US Army Corps of Engineers.

47. Nash, J. E. & Sutcliffe, J. V., 1970. River Flow Forecasting Through Conceptual Models Part I - A Discussion of Principles. *Journal of Hydrology,* pp. 282-290.

48. Newport/Morehead, NC Weather Forecast Office, NWS, n.d. *Event Overview: Hurricane Floyd Storm Summary.* [Online] Available at: http://www.weather.gov/mhx/Sep161999EventReview [Accessed 8 April 2016].

49. Newport/Morehead, NC Weather Forecast Office, n.d. *Hurricane Floyd Storm Summary.* [Online] Available at: http://www.weather.gov/mhx/Sep161999EventReview [Accessed 19 December 2016].

50. NOAA/NOS/CO-OPS, 2013. *ODIN MAP.* [Online] Available at: http://tidesandcurrents.noaa.gov/map/index.shtml?lat=35.07946034047981&lng=-76.41265869140625&zoom=8&type=active [Accessed 14 November 2017].

51. NOAA, 2012. *Service Assessment: Hurricane Irene, August 21-30, 2011.* Silver Springs, Maryland: s.n.

52. NOAA, 2013. *Historic Water Levels - Station Selection.* [Online]
Available at:
https://tidesandcurrents.noaa.gov/stations.html?type=Historic+Water+Levels
[Accessed 2 December 2015].

53. NOAA, 2015. *Home Page.* [Online]
Available at: http://www.ndbc.noaa.gov/
[Accessed 2 December 2015].

54. North Carolina Department of Environmental Quality (DEQ) Division of Water Resources (DWR), 2014. *2014 Tar-Pamlico River Basin Water Resources Plan,* Raleigh, NC: NC DEQ.

55. NWS AHPS, 2015. *QPE: Quantitative Precipitation Estimates.* [Online]
Available at: http://water.weather.gov/precip/
[Accessed 16 11 2015].

56. NWS NCEP, 2011. *National Stage IV QPE Product.* [Online]
Available at: http://www.emc.ncep.noaa.gov/mmb/ylin/pcpanl/stage4/
[Accessed 16 November 2011].

57. NWS, 2015. *River Gauge Hydrographs.* [Online]
Available at:
http://water.weather.gov/ahps2/hydrograph.php?wfo=RAH&gage=TARN7
[Accessed 16 11 2015].

58. Oceanweather Inc., 2001. *About.* [Online]
Available at: www.oceanweather.com/about/
[Accessed 21 11 2017].

59. Pappenberger, F., Beven, K., Horritt, M. & Blazkova, S., 2005. Uncertainty in the calibration of effective roughness parameters in HEC-RAS using inundation and downstream level observations. *Journal of Hydrology,* pp. 46-69.

60. Ramakrishnan, L. et al., 2006. *Real-time storm surge ensemble modeling in a grid environment.* s.l., s.n.

61. Ray, T., Stepinski, E., Sebastian, A. & Bedient, P. B., 2011. Dynamic Modeling of Storm Surge and Inland Flooding in a Texas Coastal Floodplain. *Journal of Hydraulic Engineering,* pp. 1103-1110.

62. Schmalz, R. A., 2011. *Technical Memorandum NOS CS 24 - Skill Assessment of the Delaware River and Bay Operational Forecast System (DBOFS),* s.l.: NOAA.

63. Szpilka, C. et al., 2016. Improvements for the Western North Atlantic, Caribbean and Gulf of Mexico Tidal Database (EC2015). *Journal of Marine Science and Engineering,* p. 72.

64. The Weather Company, 2017. *wunderground.com.* [Online]
Available at:
https://www.wunderground.com/hurricane/atlantic/2003/Tropical-Storm-Ana
[Accessed 30 October 2017].

65. Tromble, E. M., 2011. *Advances Using the ADCIRC Hydrodynamic Model: Parameter Estimation and Aspects of Coupled Hydrologic-Hydrodynamic Flood Inundation Mapping.* Norman, OK: UMI.

66. United States Army Corps of Engineers, 2000. *Hurricane Floyd High Water Marks and Inundation Mapping,* Charleston, SC: United States Army Corps of Engineers.

67. USGS, 2012. *Monitoring Inland Storm Tide and Flooding from Hurricane Irene along the Atlantic Coast of the United States, August 2011,* Reston, Virginia: U.S. Geological Survey.

68. USGS, 2015. *Web Interface.* [Online]
Available at: http://nwis.waterdata.usgs.gov/usa/nwis/
[Accessed 16 11 2015].

69. Van Cooten, S. et al., 2011. The CI-FLOW Project - A system for total water level prediction from the summit to the sea. *Bulletin of the American Meteorological Society,* 92(11), pp. 1427-1442.

70. Vickery, P. J., Skerlj, P. F., Steckley, A. C. & Twisdale, L. A., 2000. Hurricane Wind Field Model for Use In Hurricane Simulation. *Journal of Structural Engineering,* pp. 1203-1221.

71. Wei, E. & Zhang, A., 2011. *Technical Report NOS CS 30 - The Tampa Bay Operational Forecast System (TBOFS): Model Development and Skill Assessment,* s.l.: NOAA.

72. Westerink, J. J. et al., 2008. A Basin- to Channel-Scale Unstructured Grid Hurricane Storm Surge Model Applied to Southern Louisiana. *Monthly Weather Review,* pp. 833-864.

73. Yamagishi, T. & Matsumura, Y., 2016. GPU acceleration of a non-hydrostatic ocean model with a multigrid poisson/helmholtz solver. *Procedia Computer Science,* pp. 1658-1669.

APPENDIX A – MAPS OF NODAL ATTRIBUTES

This appendix details the two ADCIRC grids used in the associated research discussed in the main body of this thesis. Two grids were used – the first, "fine" mesh, features a highly resolved river domain and was developed by (Tromble, 2011). The second, "coarse" mesh uses nodes and bathymetry from prior work (Blanton & Luettich, 2008) but with the roughness coefficients developed by Tromble (2011) interpolated onto the mesh using a FORTRAN script.

Nodal attributes used in model runs include:

- Horizontal Eddy Viscosity
- Initial River Elevation (Not used in coarse mesh)
- Mannings n at Sea Floor
- Primitive Weighting in Continuous Flow Equation (Tau0)
- Surface Canopy Coefficient
- Surface Directional Effective Roughness Length (Not mapped)
- Other mapped parameters that are included in this appendix include:
- Mesh Spacing, representing the approximate scale of mesh elements
- Bathymetry, representing the depth below MSL of ground surface or seafloor

Graphs are presented below without commentary. Lengths are presented in meters (m).

FINE MESH PARAMETER MAPS

FINE MESH HORIZONTAL EDDY VISCOSITY

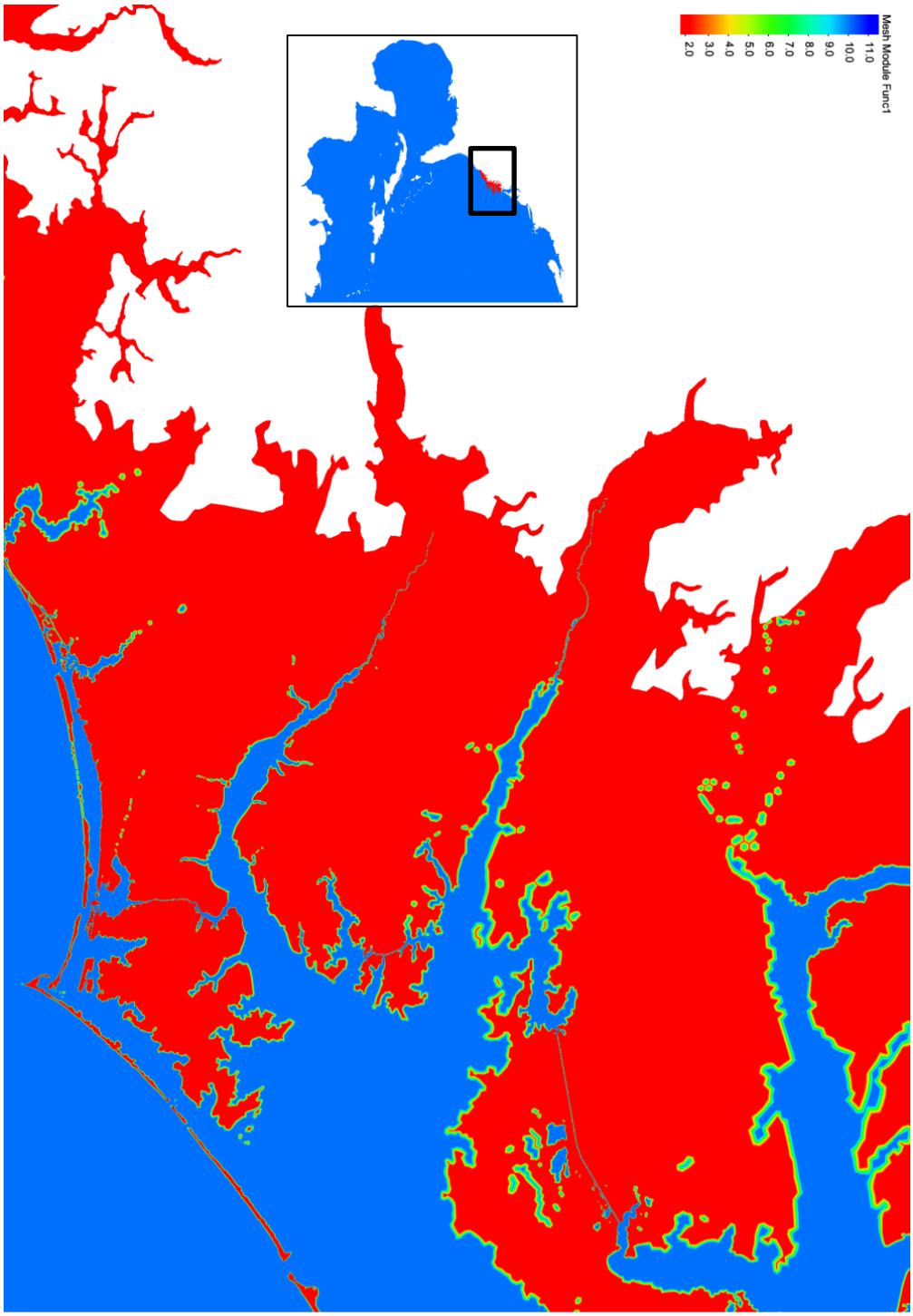

FINE MESH INITIAL RIVER ELEVATION

FINE MESH MANNING'S N AT SEA FLOOR

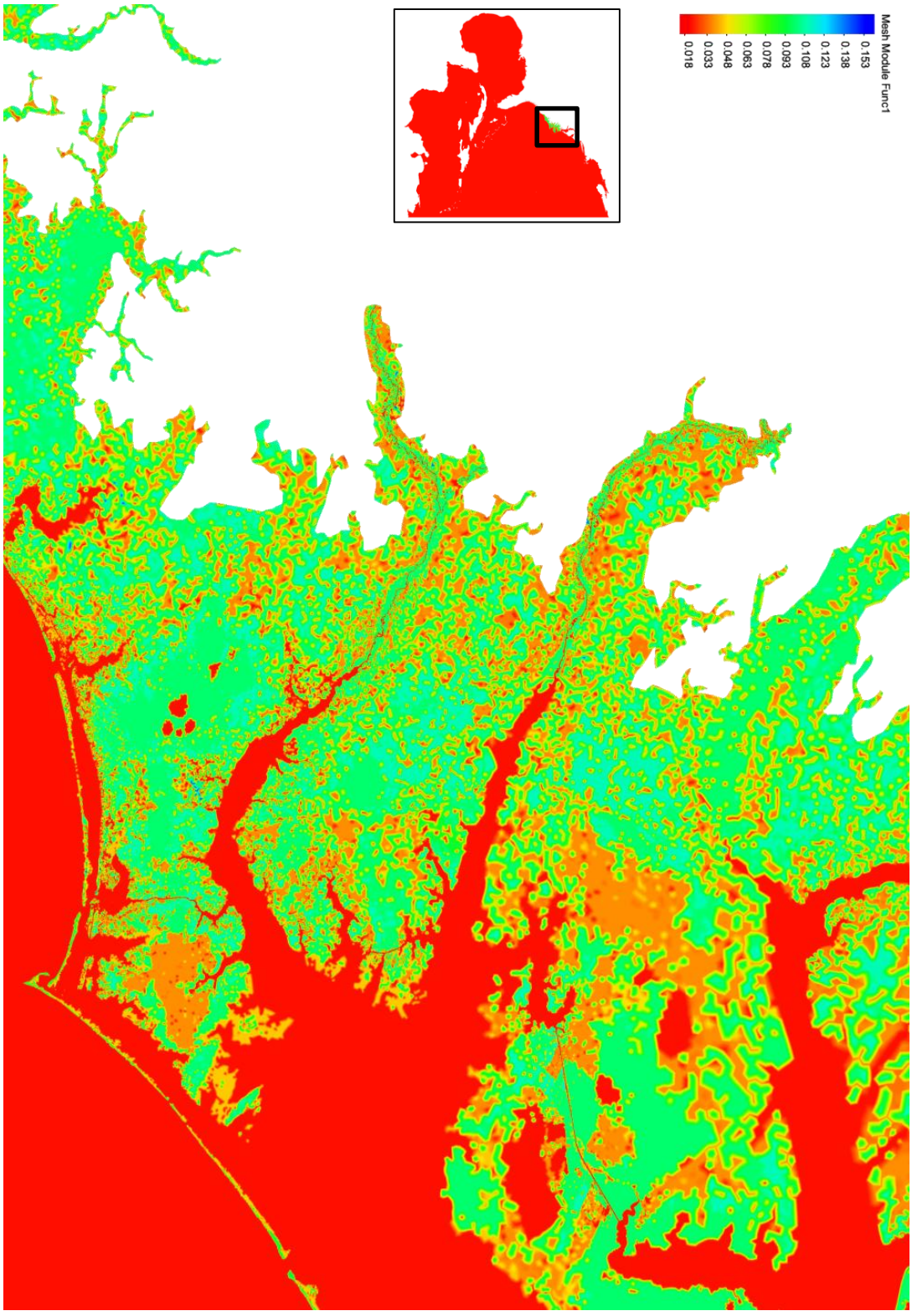

FINE MESH PRIMITIVE WEIGHTING IN CONTINUITY EQUATION (TAU0)

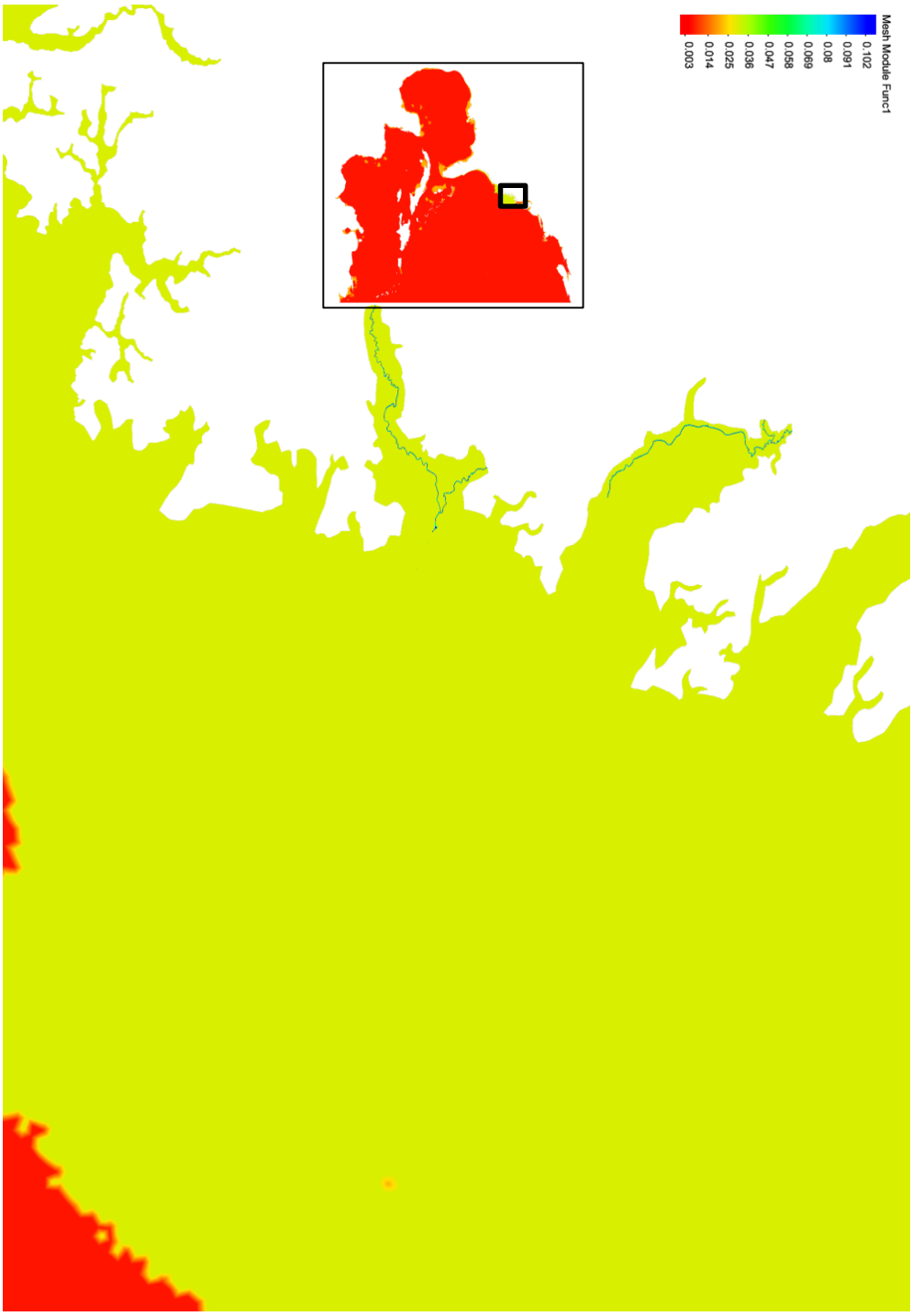

FINE MESH SURFACE CANOPY COEFFICIENT

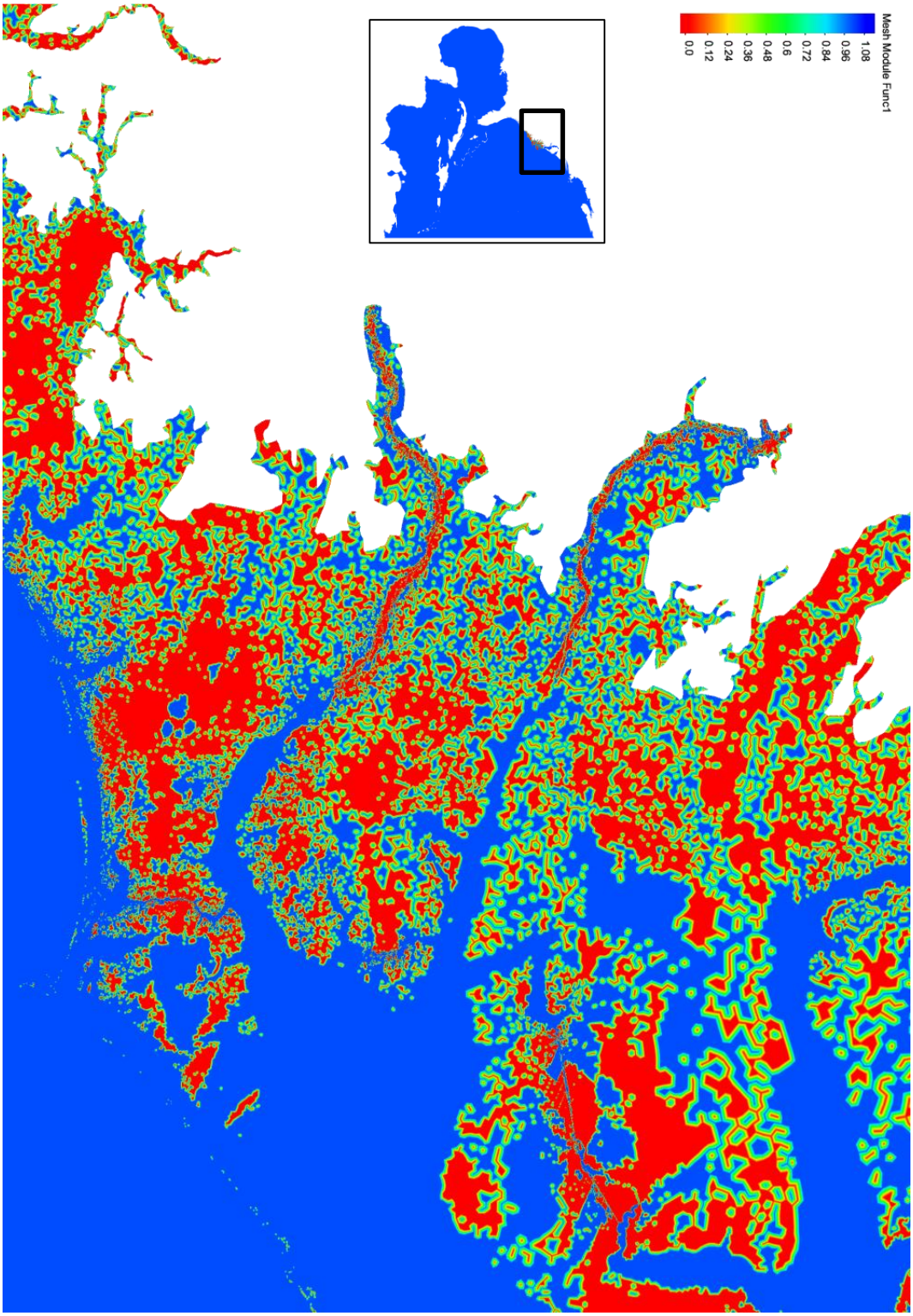

FINE MESH BATHYMETRY

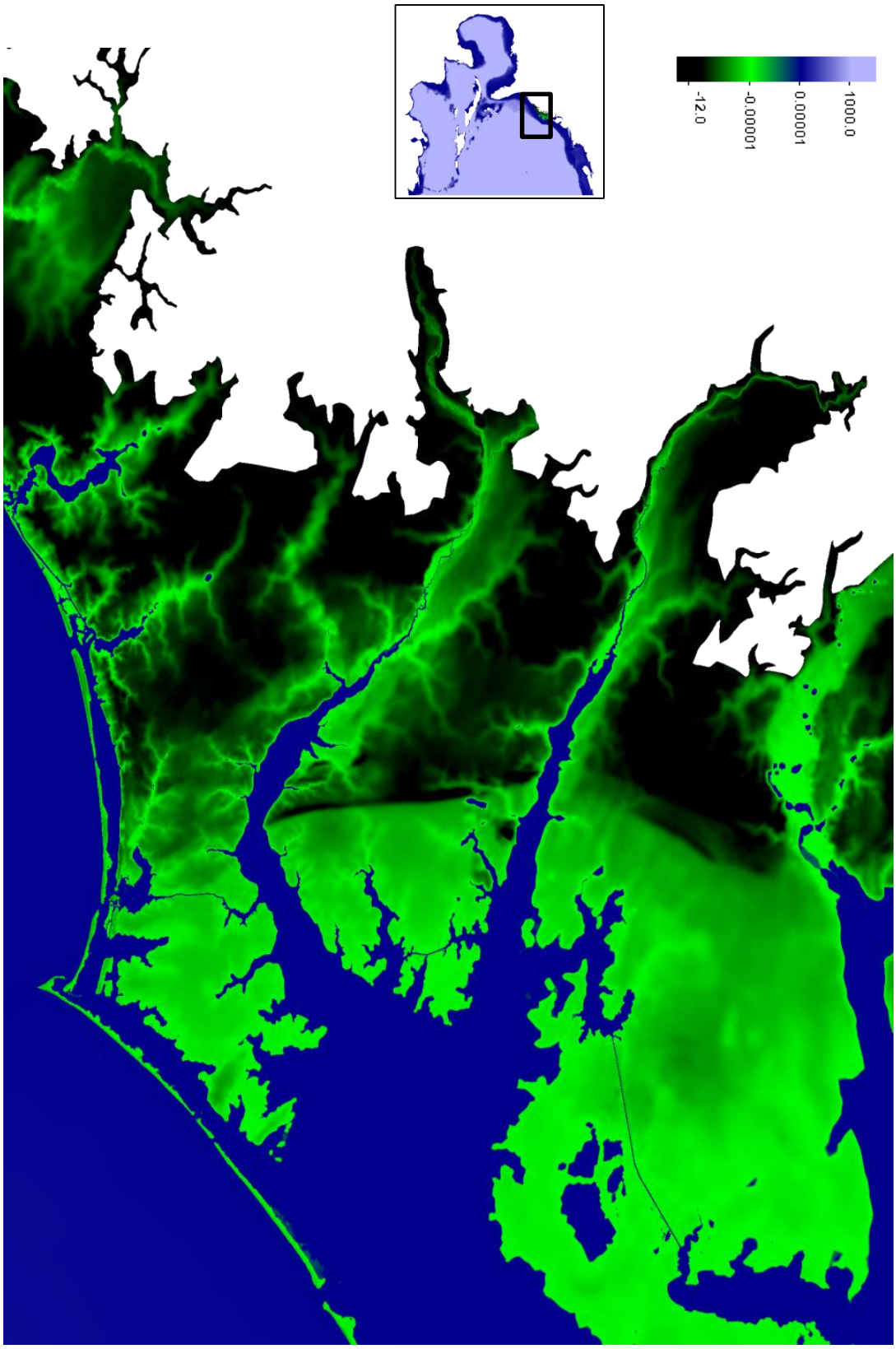

FINE MESH NODE SPACING

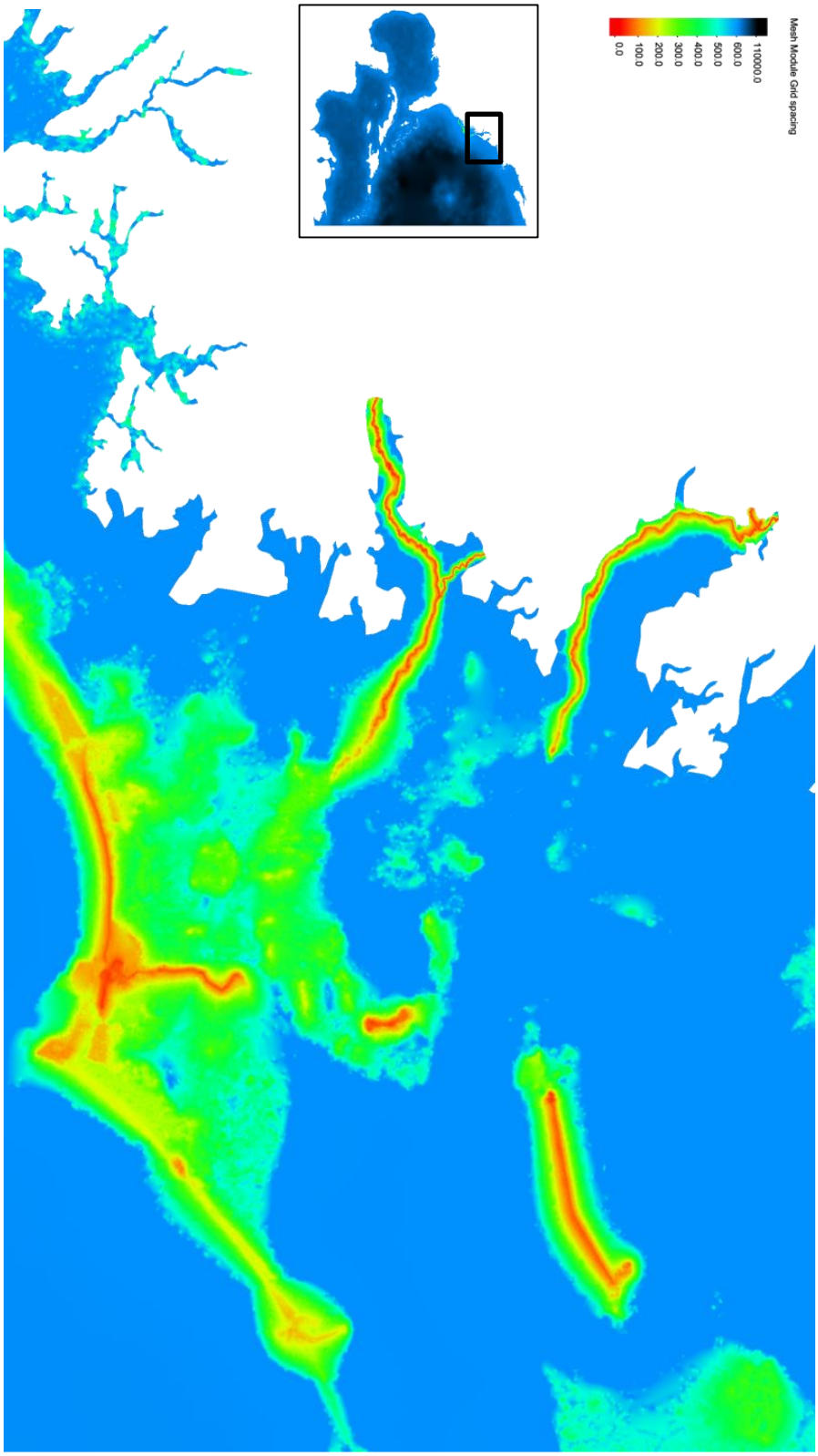

COARSE MESH PARAMETER MAPS

COARSE MESH HORIZONTAL EDDY VISCOSITY

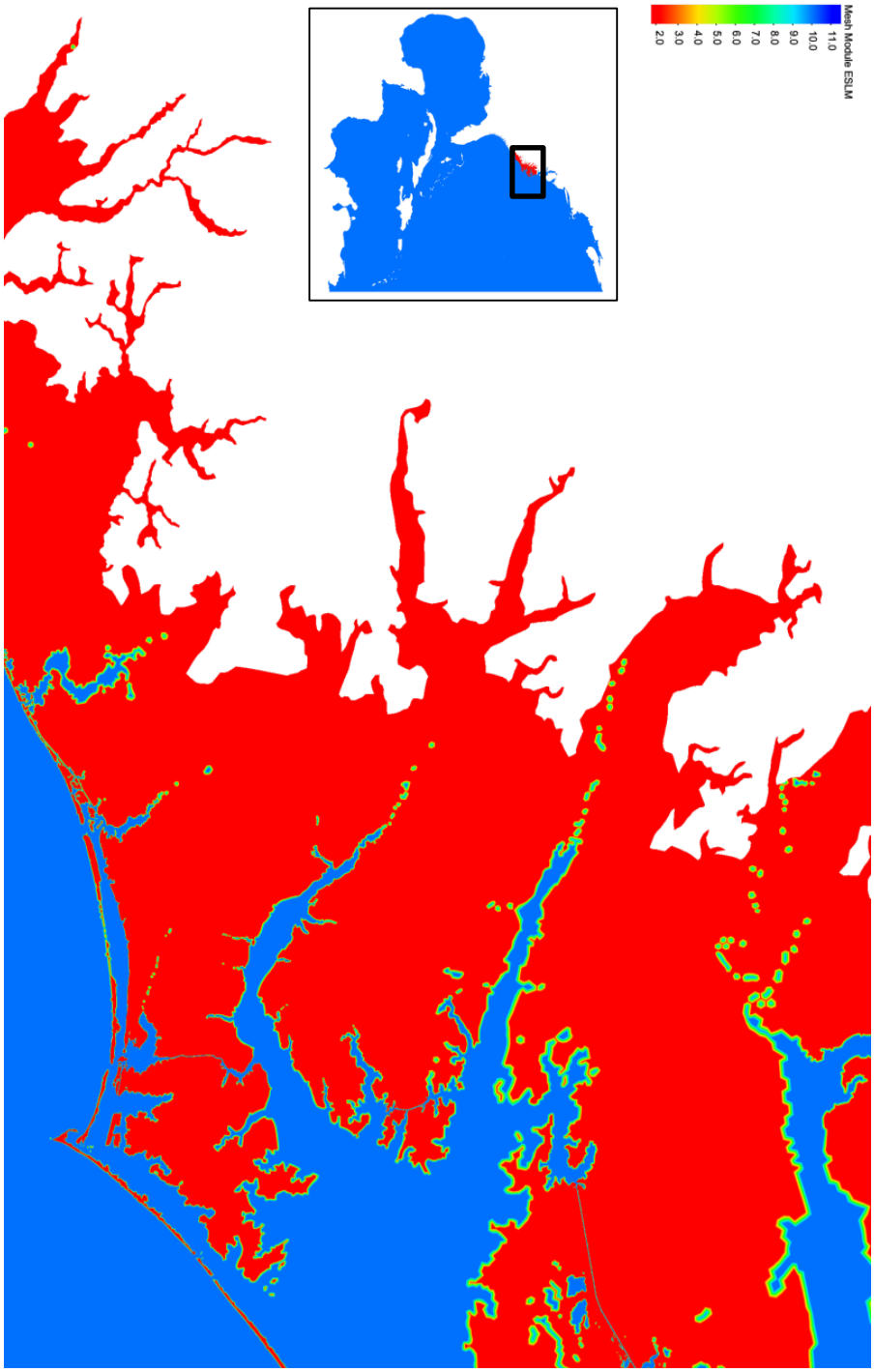

COARSE MESH MANNING'S N AT SEA FLOOR

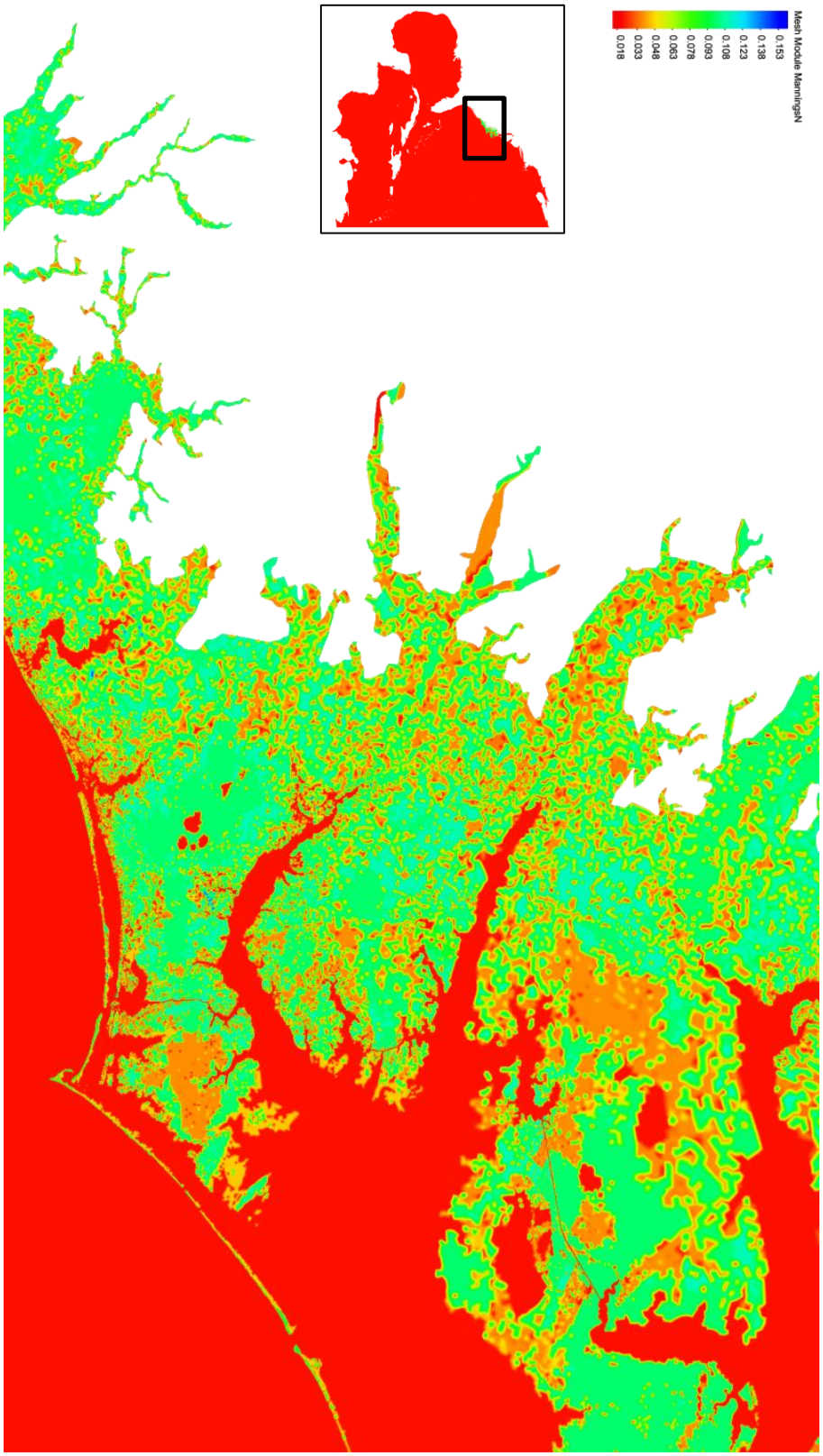

COARSE MESH PRIMITIVE WEIGHTING IN CONTINUITY EQUATION (TAU0)

COARSE MESH SURFACE CANOPY COEFFICIENT

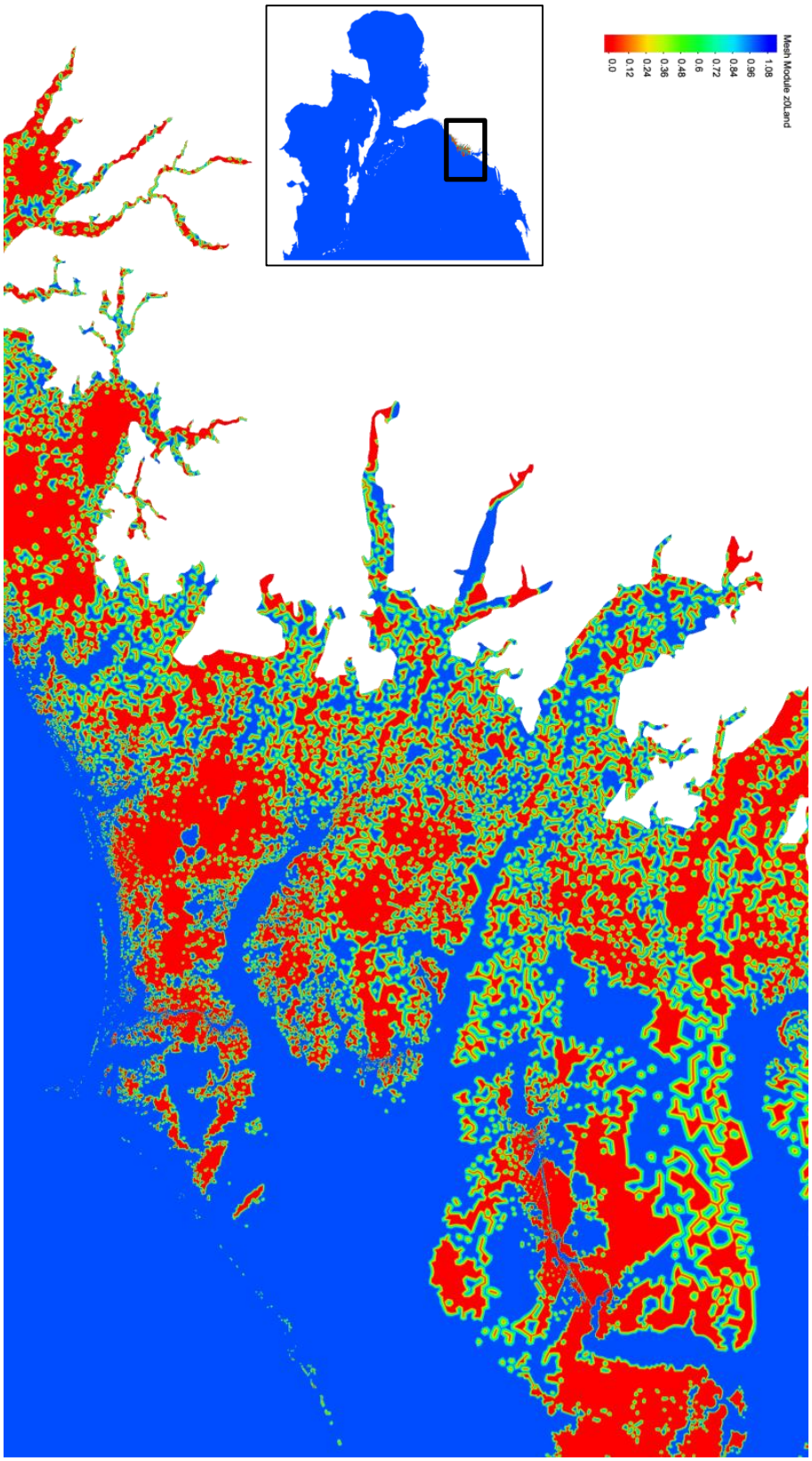

COARSE MESH BATHYMETRY

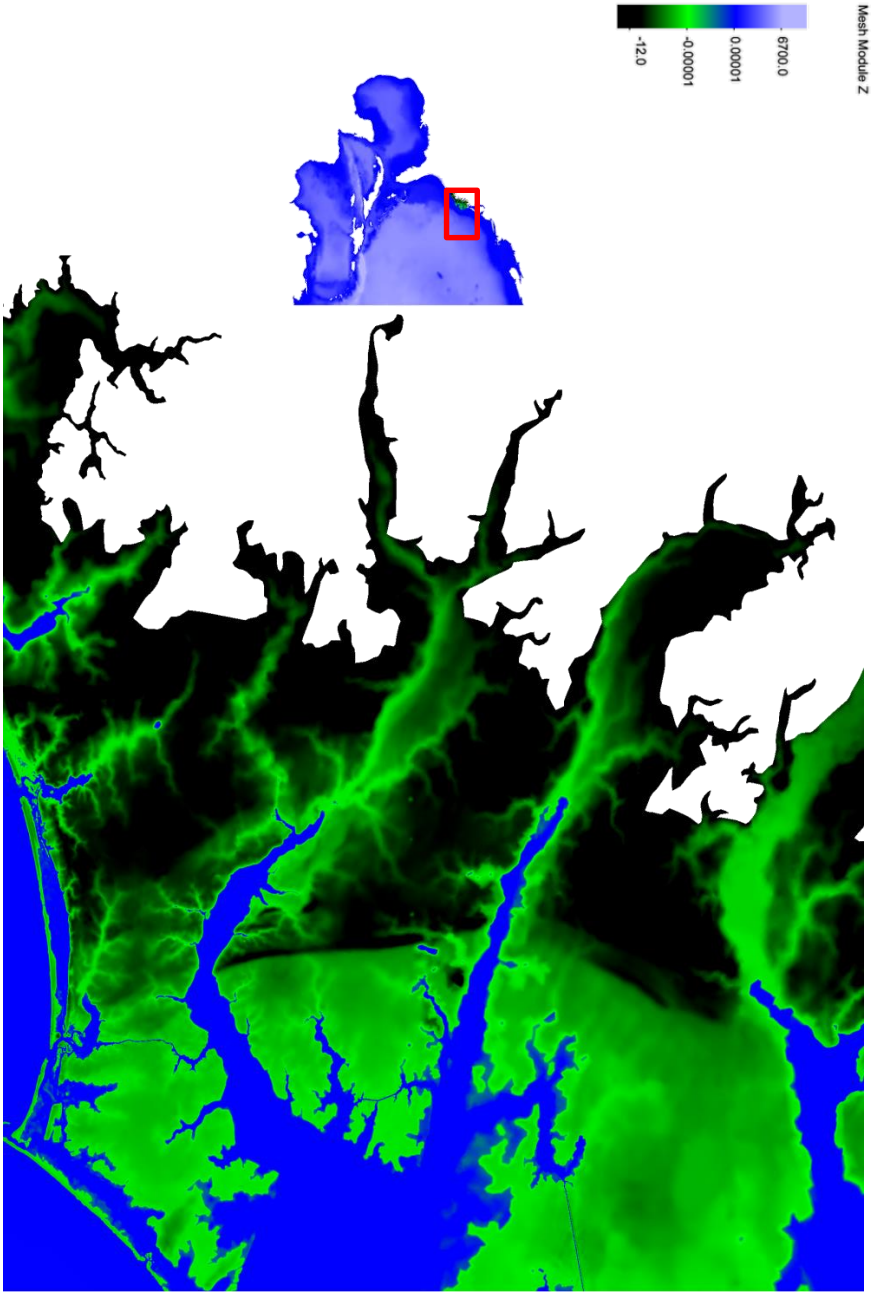

COARSE MESH NODE SPACING

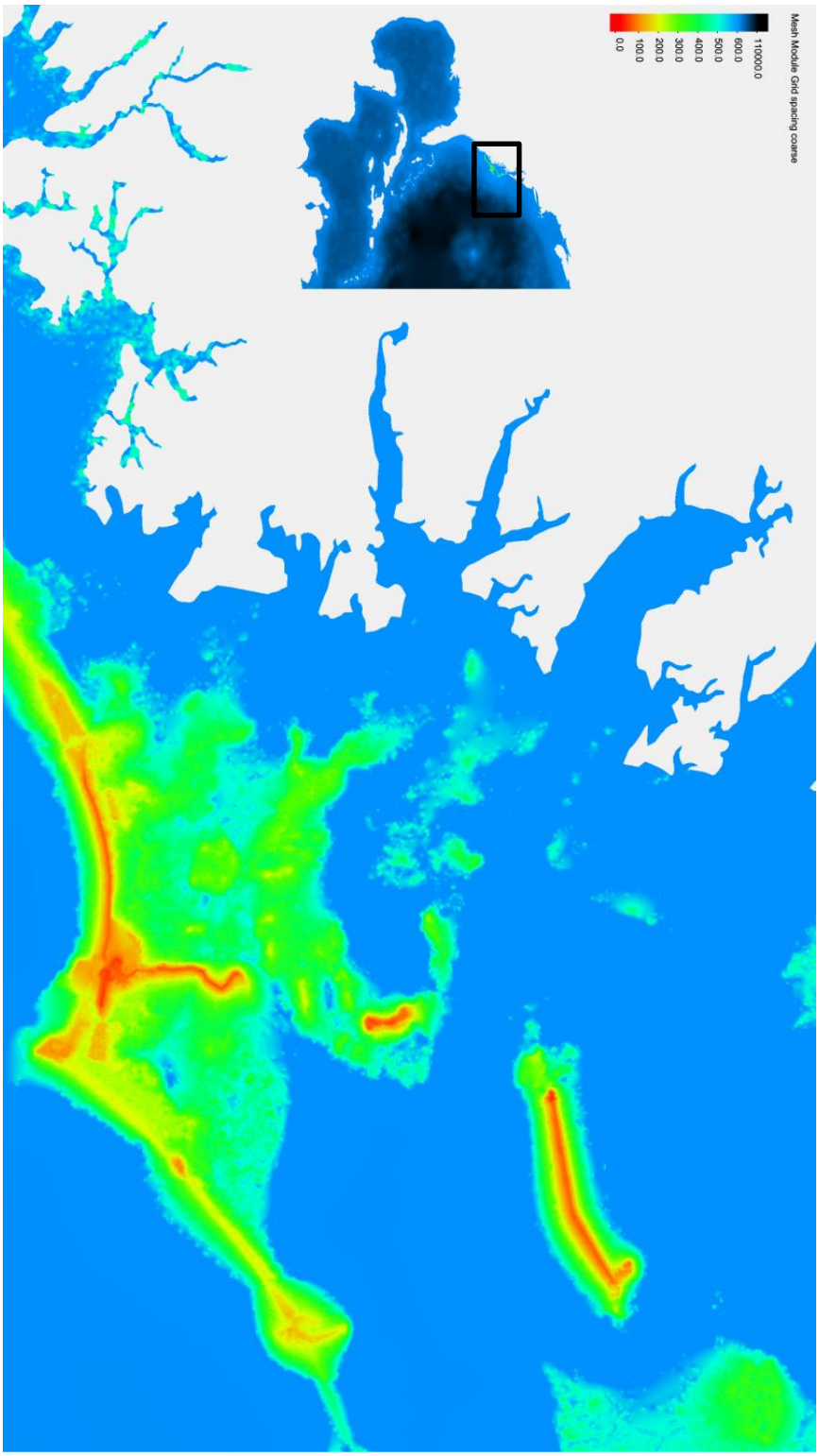

APPENDIX B – HL-RDHM MODEL VALIDATION

This appendix documents the results of HL-RDHM simulations in comparison to observations taken at USGS 02083500.

HURRICANE ISABEL

HL-RDHM simulations using the standard 128-member ensemble described in Chapter 5 were completed for the simulation period of August 1, 2010 to October 31, 2011. As ADCIRC runs began on calendar date July 06, 2011, this provided an HL-RDHM warmup period of 339 days.

The "best" member to be used was selected based on the simulation's agreement with observations taken at USGS 02083500 – Tar River at Tarboro, during the target period of July 6, 2011 to September 29, 2011. Figure B-1 shows each member of the 128-member ensemble (colored lines) in relation to observed data (black dots).

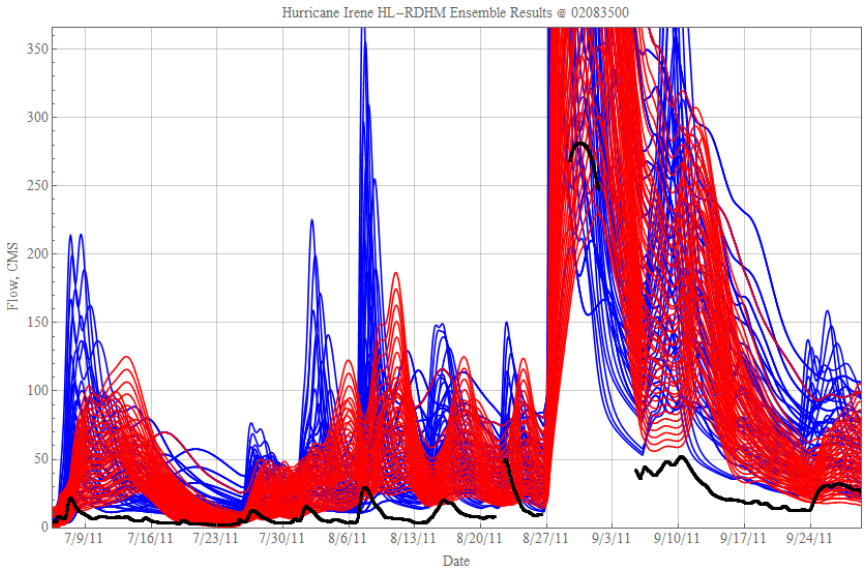

Figure B-1 - RDHM Ensemble Members at USGS 02083500. Calibrated in Red, *A Priori* in Blue, Observed in Black

For improved visibility, the calibrated and *a priori* members are displayed separately in Figure B-2 and Figure B-3, respectively.

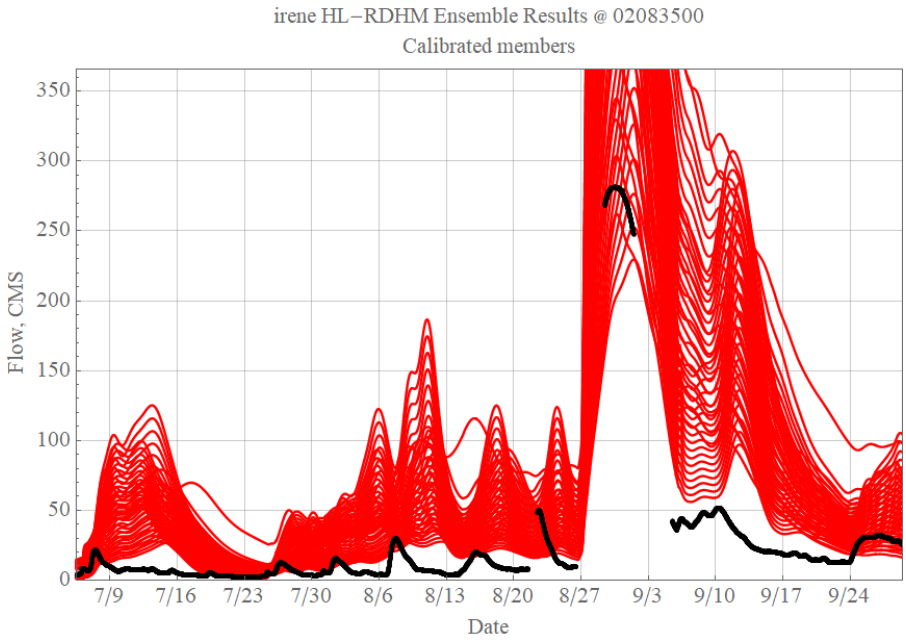

Figure B-2 - RDHM Ensemble Calibrated Members at USGS 02083500. Modelled in Red, Observed in Black

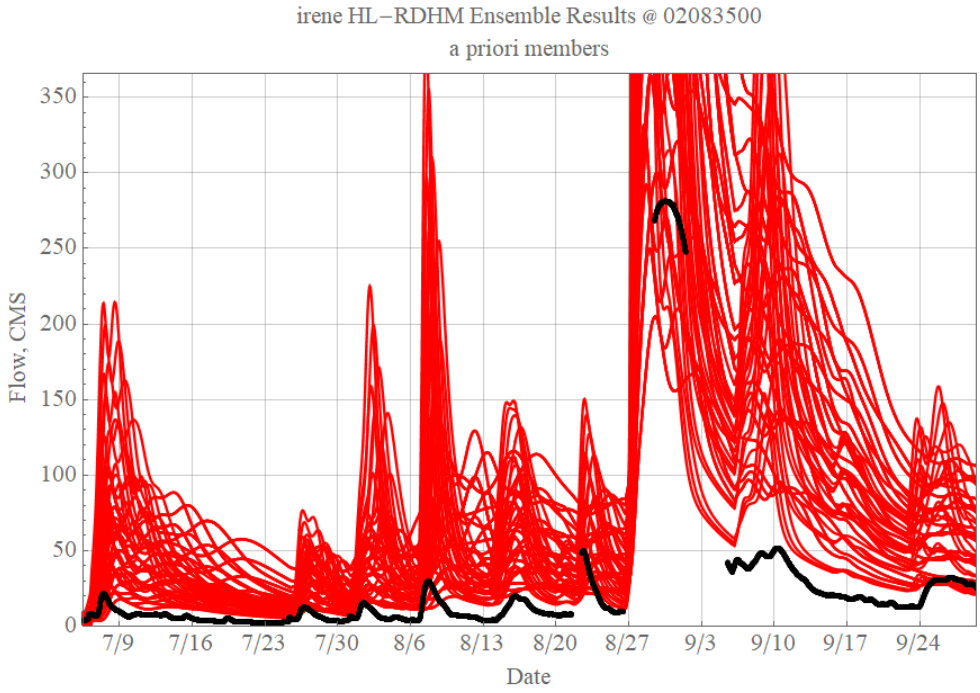

Figure B-3 - RDHM Ensemble *a priori* Members at USGS 02083500. Modelled in Red, Observed in Black

Agreement with observation was quantified using Nash-Sutcliffe Efficiency (NSE), described in Chapter 5. An NSE of 1 represents a perfect prediction, an NSE of 0

represents a prediction with the same quality of fit as the mean of observed data, and an NSE of less than zero represents a prediction worse than the mean.

The NSE values for the HL-RDHM simulations were calculated for the period of July 6, 2011 to September 29, 2011 and varied between -13.8 and 0.83, distributed as shown in Figure B-4.

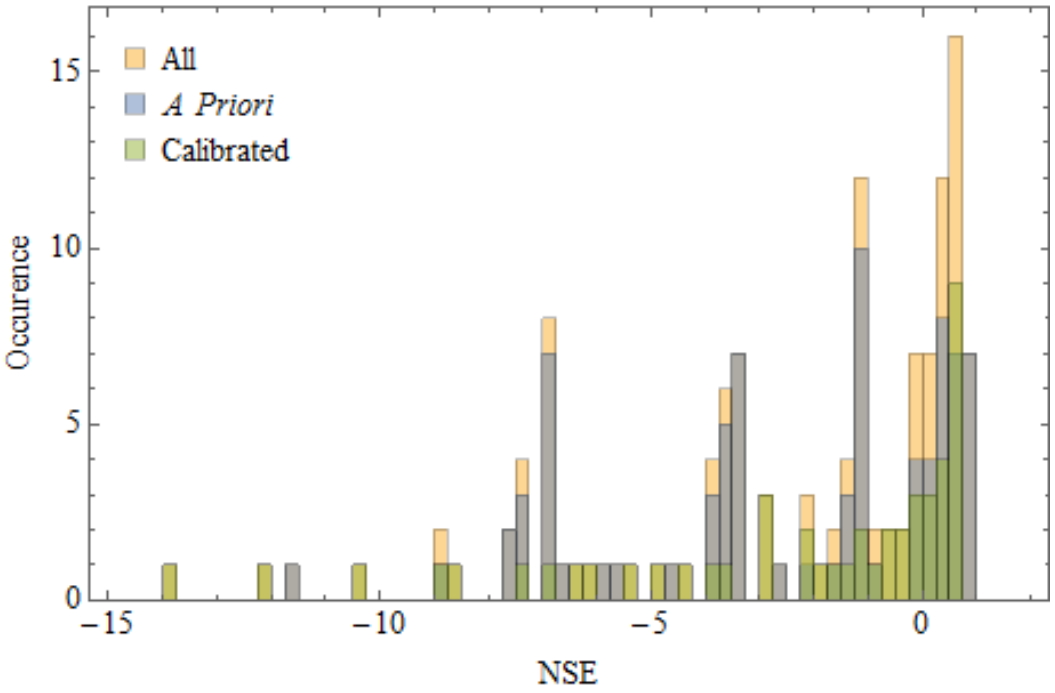

Figure B-4 - Hurricane Irene HL-RDHM Ensemble Skill Summary, Bin = 0.25

As shown, the best performing (highest NSE) members came from the perturbed *a priori* dataset. The ensemble member with the highest NSE was member number 16. A plot of that member's predicted response at 02083500 is shown as Figure B-5.

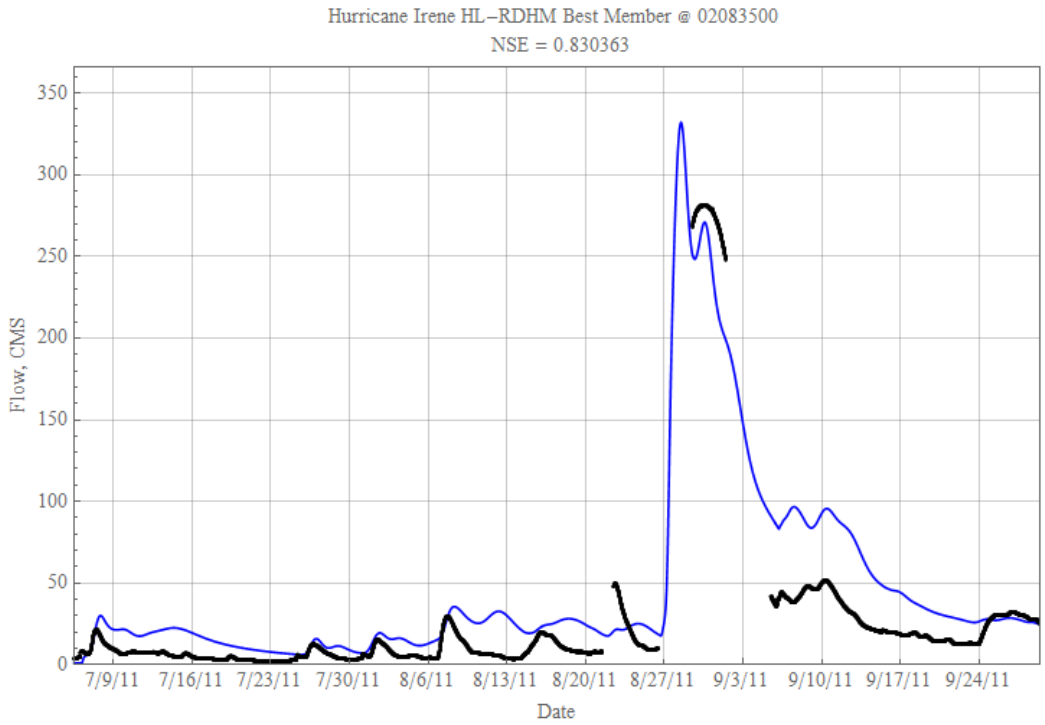

Figure B-5 - RDHM Ensemble Member 16 at USGS 02083500 during Hurricane Irene. Modelled in Blue, Observed in Black

While this member shows excellent agreement with pre-peak observations and predicts the observed peak flow, post-peak observations are overestimated. Furthermore, real observations during this period did not encompass the rising or falling limbs of the peak, presumably due to gauge washout. Therefore while this member is the best predictor of observed values, the observed values themselves are subject to some doubt and the real error in this flow estimate is unknown. The weighting factors used to perturb the *a priori* dataset are shown in Table 5.

Table B-5- Selected "Best" RDHM Member Properties

Parameter	Variable Name	Weighting Factor*
Rainfall	xmrg	0.8
Channel Routing Linear Adjustment	rutpix_Q0CHN	1.2
Channel Routing Exponential Adjustment	rutpix_QMCHN	0.3

Note: When writing input decks, weighting factors are applied as negative values

The flows predicted by this member were passed to ADCIRC. More discussion about boundary condition passing methods is included in Chapter 5 of the attached thesis.

HURRICANE FLOYD

HL-RDHM simulations using the standard 128-member ensemble described in Chapter 5 were completed for a simulation period of September 1, 1998 to October 16, 1999. As ADCIRC runs began on calendar date August 11, 1999, this provided an HL-RDHM warmup period of 344 days.

The “best” member to be used was selected based on the simulation’s agreement with observations taken at USGS 02083500 – Tar River at Tarboro, during the target period of August 12, 1999 to October 16, 1999. Figure B-6 shows each member of the 128-member ensemble (colored lines) in relation to observed data (black dots).

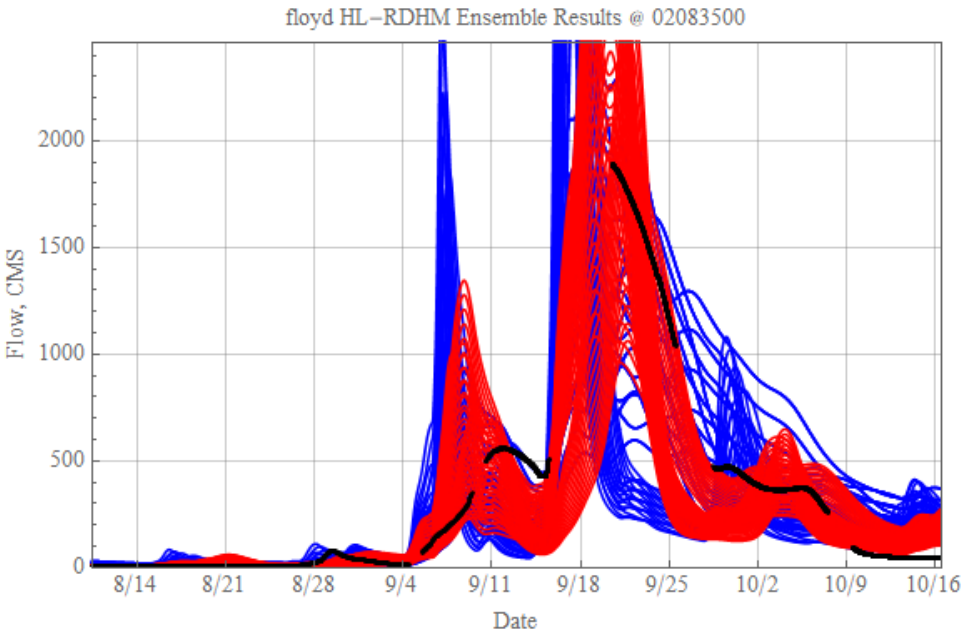

Figure B-6 - RDHM Ensemble Members at USGS 02083500. Calibrated in Red, *A Priori* in Blue, Observed in Black

For improved visibility, the calibrated and *a priori* members are displayed separately in Figure B-7 and Figure B-8, respectively.

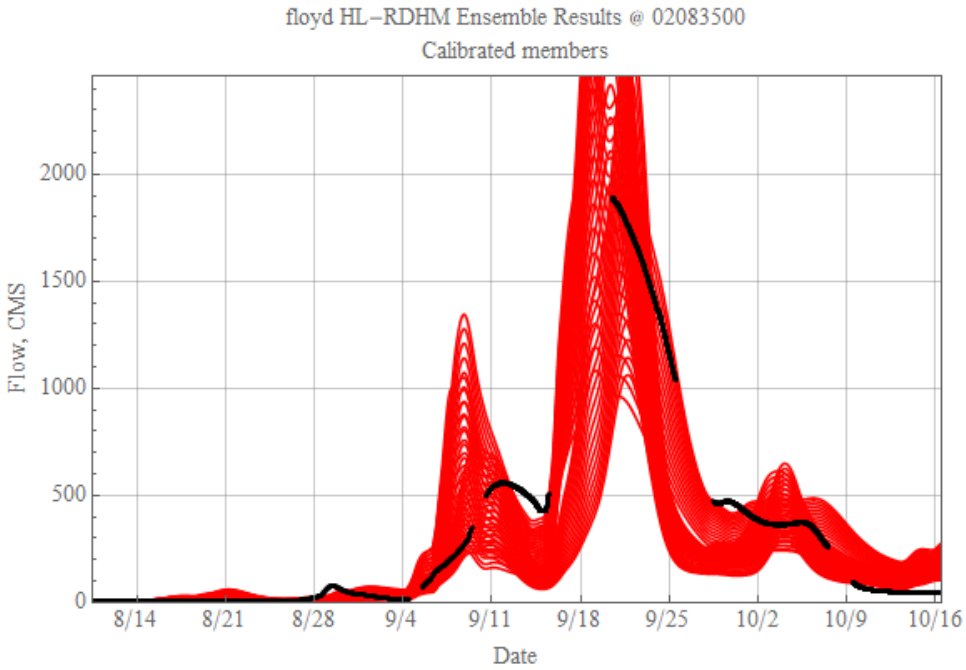

Figure B-7 - RDHM Ensemble Calibrated Members at USGS 02083500. Modelled in Red, Observed in Black

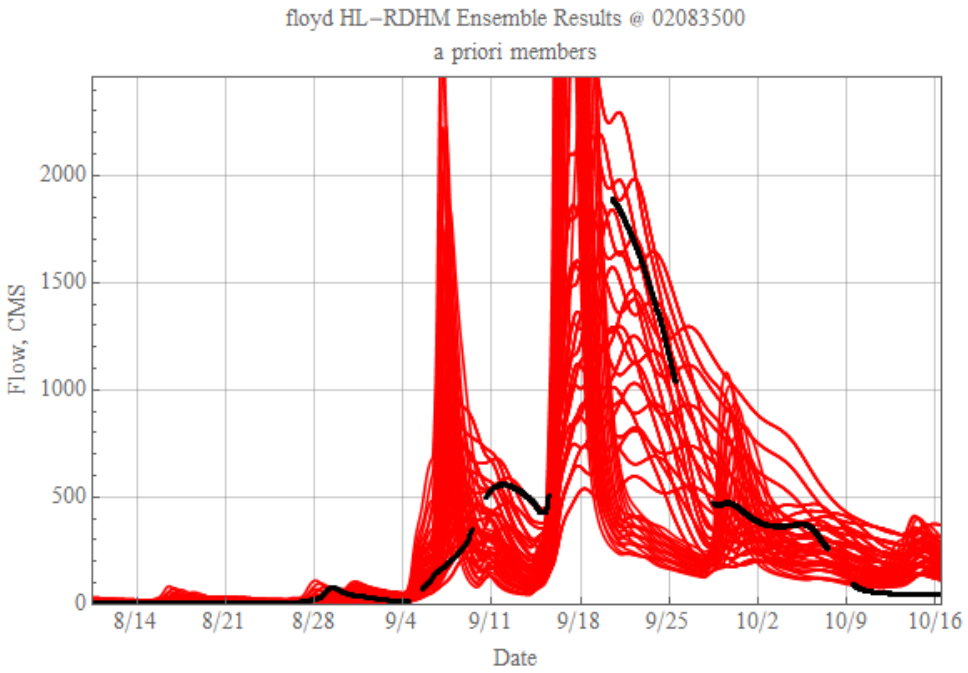

Figure B-8 - RDHM Ensemble *a priori* Members at USGS 02083500. Modelled in Red, Observed in Black

Agreement with observation was quantified using Nash-Sutcliffe Efficiency (NSE), described in Chapter 5. An NSE of 1 represents a perfect prediction, an NSE of 0 represents a prediction with the same quality of fit as the mean of observed data, and an NSE of less than zero represents a prediction worse than the mean.

The NSE values for the HL-RDHM simulations were calculated for the period of August 11, 1999 to October 16, 1999 and varied between -0.18 and 0.94, distributed as shown in Figure B-9.

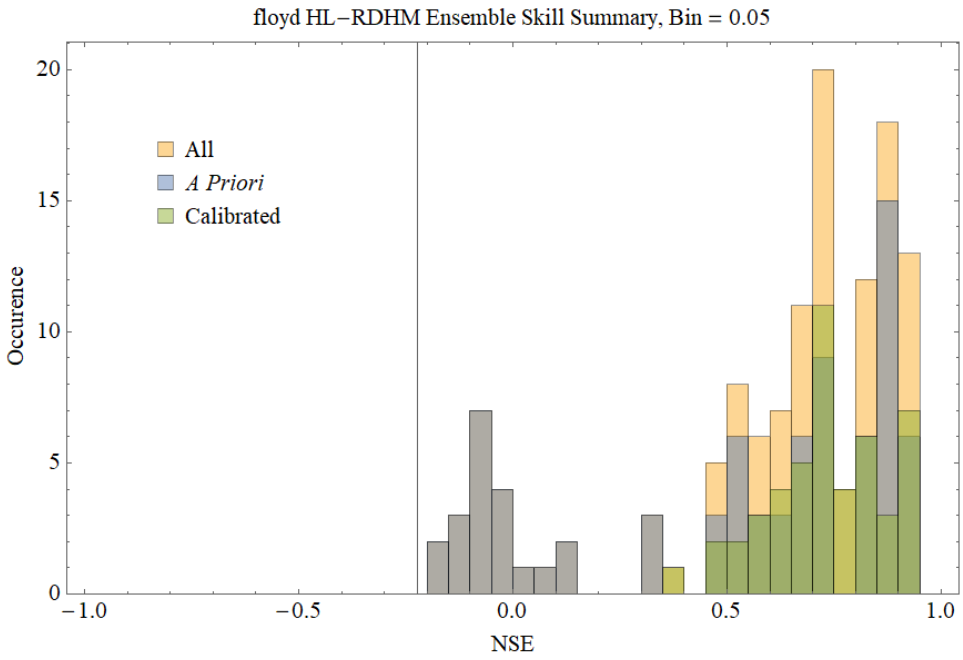

Figure B-9 - Hurricane Floyd HL-RDHM Ensemble Skill Summary, Bin = 0.05

As shown, the best performing (highest NSE) members came from both the *a priori* and calibrated datasets. The ensemble member with the highest NSE was member number 107. A plot of that member's predicted response at 02083500 is shown as Figure B-10.

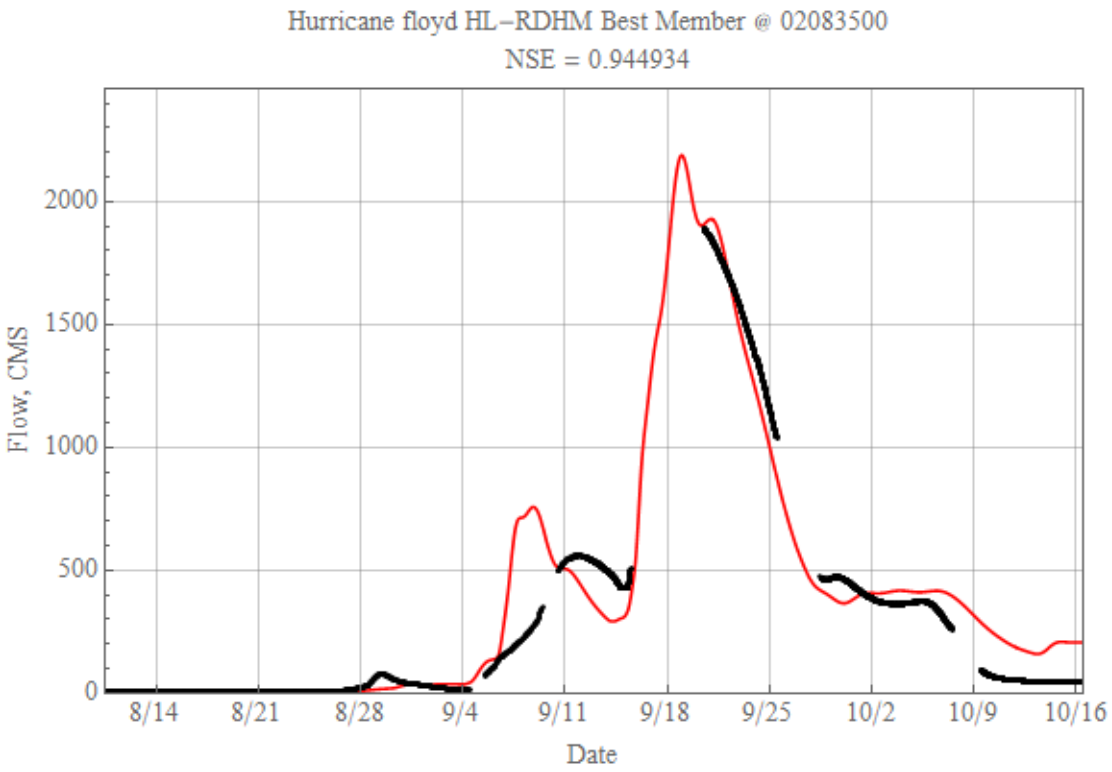

Figure B-10 - RDHM Ensemble Best Member at USGS 02083500 during Hurricane Floyd. Modelled in Red, Observed in Black

APRIL, 2003

HL-RDHM simulations using the standard 128-member ensemble described in Chapter 5 were completed for a simulation period of July 1, 2002 to September 30, 2003. As ADCIRC runs began on calendar date March 15, 2003, this provided an HL-RDHM warmup period of 257 days.

The "best" member to be used was selected based on the simulation's agreement with observations taken at USGS 02083500 – Tar River at Tarboro, during the target period of March 15, 2003 to May 15, 2003. Figure B-11 shows each member of the 128-member ensemble (colored lines) in relation to observed data (black dots).

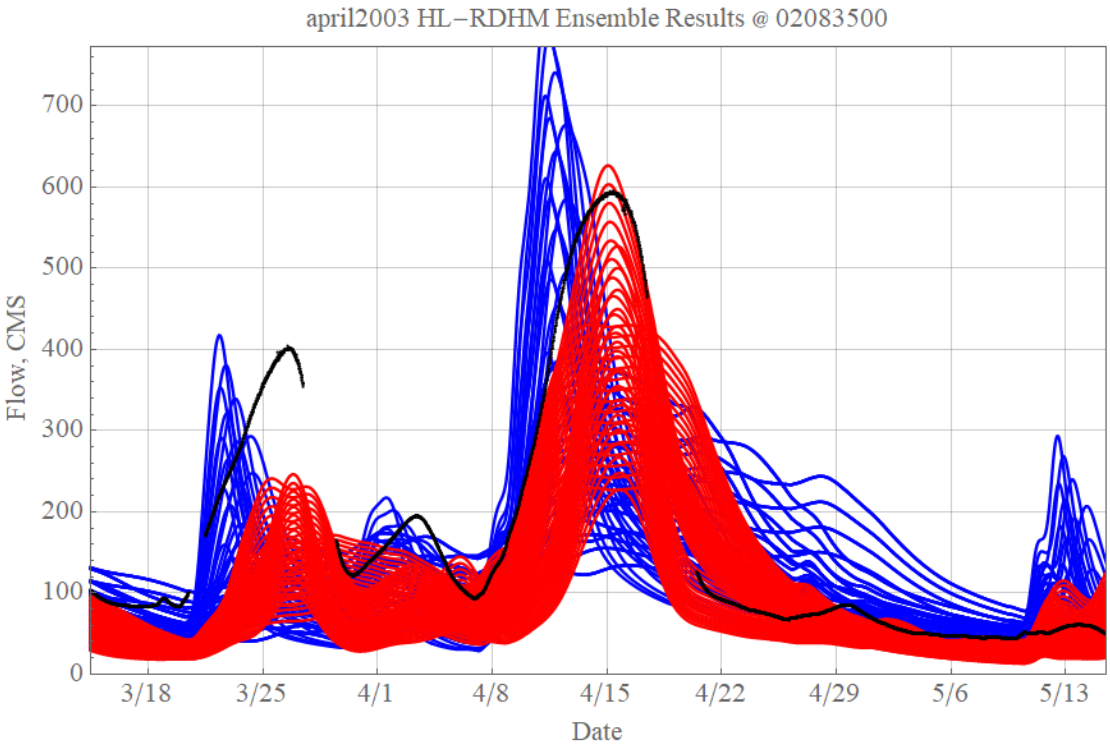

Figure B-11 - RDHM Ensemble Members at USGS 02083500. Calibrated in Red, *A Priori* in Blue, Observed in Black

For improved visibility, the calibrated and *a priori* members are displayed separately in Figure B-12 and Figure B-13, respectively.

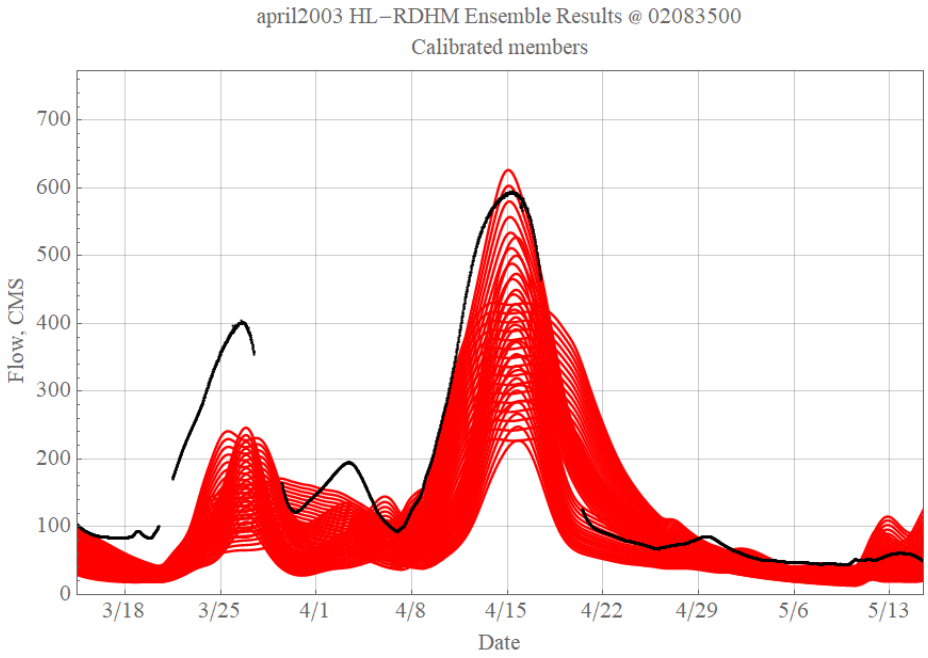

Figure B-12 - RDHM Ensemble Calibrated Members at USGS 02083500. Modelled in Red, Observed in Black

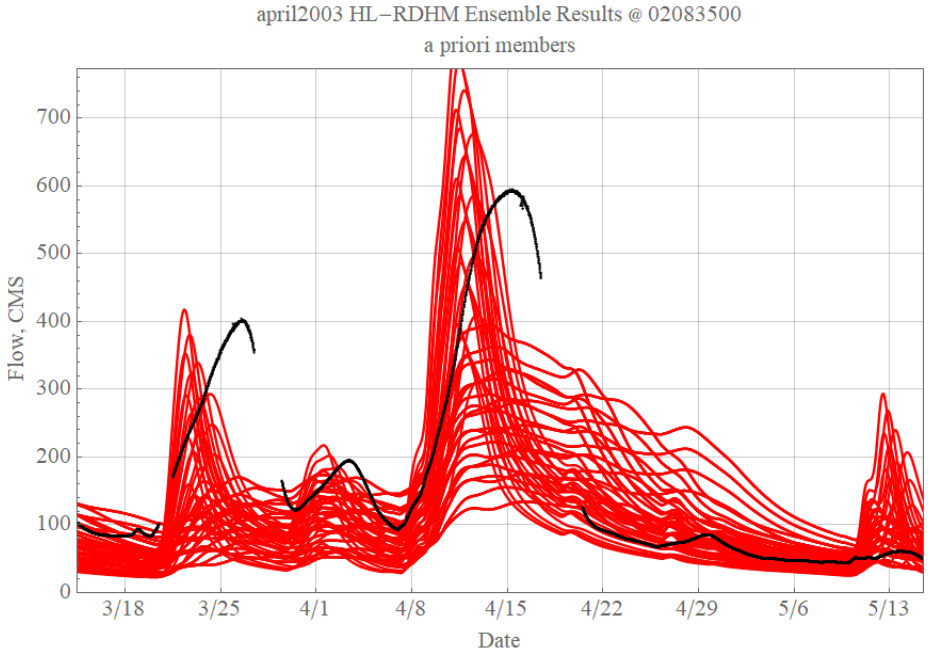

Figure B-13 - RDHM Ensemble *a priori* Members at USGS 02083500. Modelled in Red, Observed in Black

Agreement with observation was quantified using Nash-Sutcliffe Efficiency (NSE), described in Chapter 5. An NSE of 1 represents a perfect prediction, an NSE of 0

represents a prediction with the same quality of fit as the mean of observed data, and an NSE of less than zero represents a prediction worse than the mean.

The NSE values for the HL-RDHM simulations were calculated for the period of March 15, 2003 to May 15, 2003 and varied between -0.24 and 0.88, distributed as shown in Figure B-14.

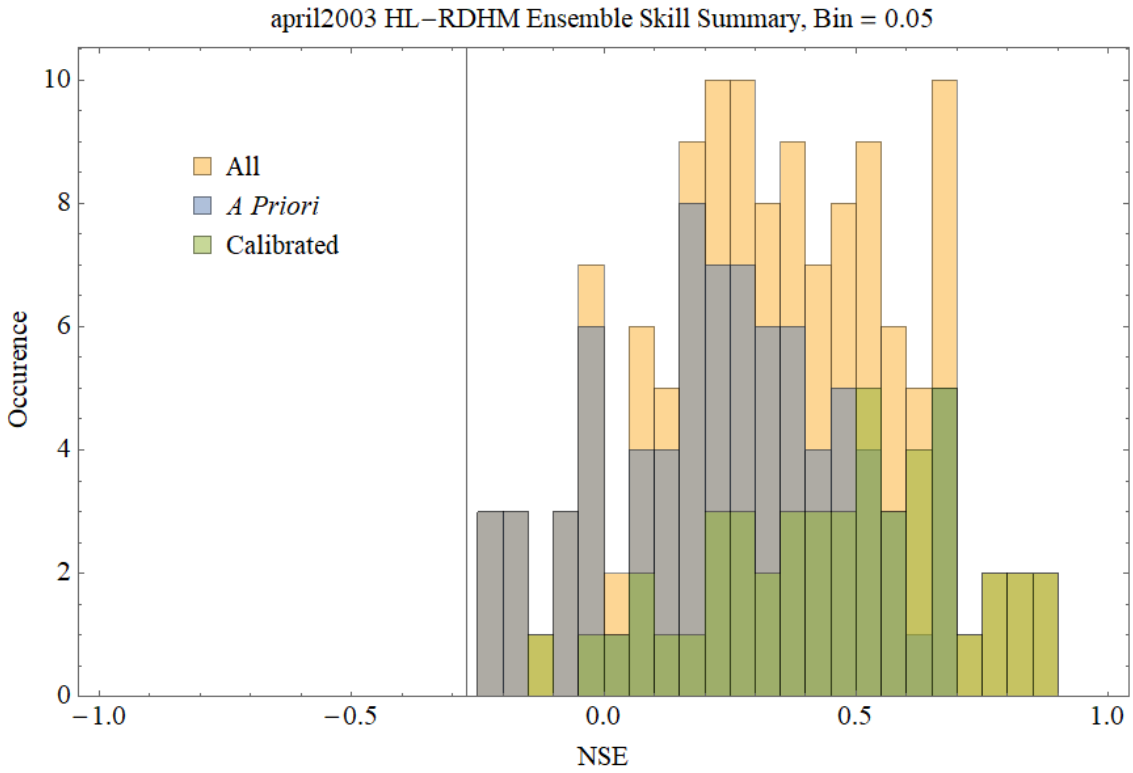

Figure B-14 - Hurricane Floyd HL-RDHM Ensemble Skill Summary, Bin = 0.05

As shown, the best performing (highest NSE) members came from the calibrated dataset. The ensemble member with the highest NSE was member number 96. A plot of that member's predicted response at 02083500 is shown as Figure B-15.

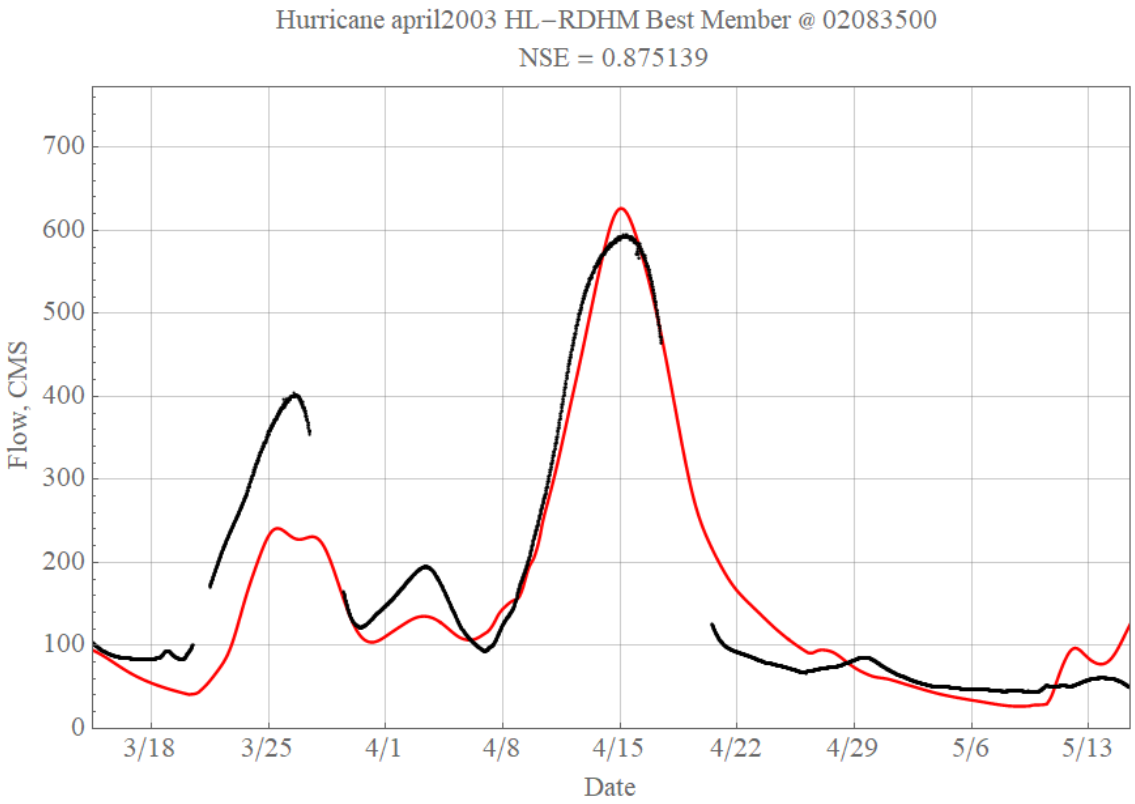

Figure B-15 - RDHM Ensemble Best Member at USGS 02083500 during April, 2003. Modelled in Red, Observed in Black

APPENDIX C – OCEANIC MODEL VALIDATION

This appendix includes graphs of water surface elevation observations at three NOS-operated gauges, at Duck Pier (8651370), Beaufort (8656483), and Oregon Inlet (8652587). The purpose of this appendix is to give the reader a qualitative impression of the skill of the oceanic model used in hindcasts. No work was performed in this research to optimize or analyze the skill of this model.

GAUGE LOCATIONS

The locations of these gauges are indicated in Figure C-1. A fourth gauge is present at Hatteras, NC, however results were not available at this gauge for Hurricane Floyd or for the April, 2003 event.

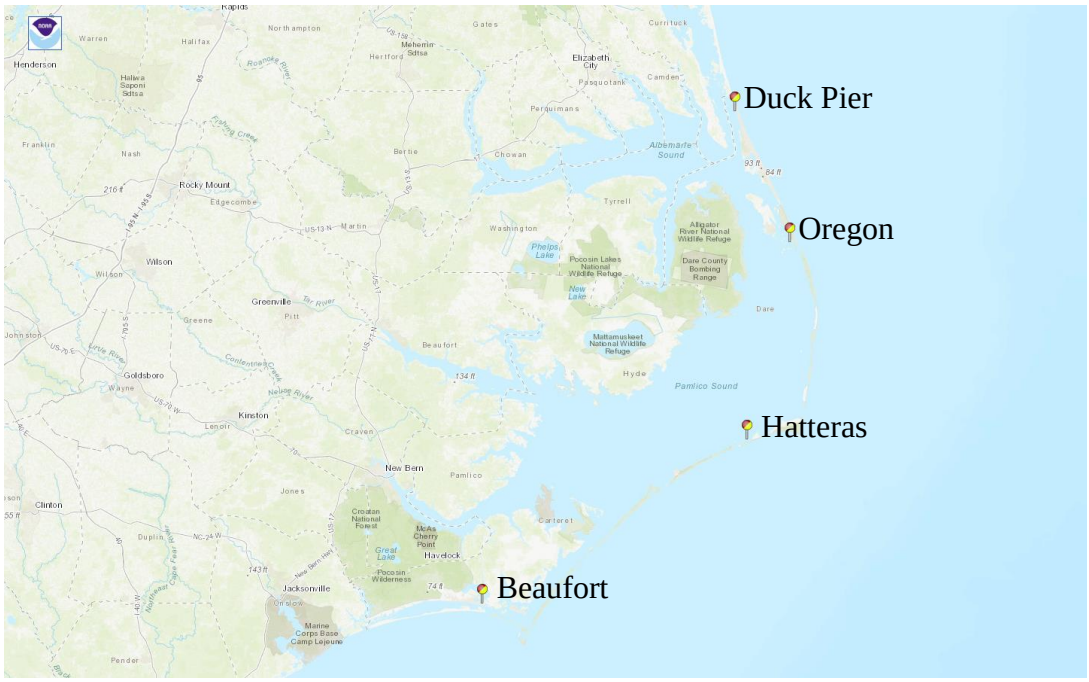

Figure C-1 - NOS Gauge Locations (NOAA/NOS/CO-OPS, 2013)

Hindcast results from the fully-resolved oceanic model, including river flow boundary conditions, are presented below without commentary. Red lines indicate model results, while black dots indicate recorded observations.

APRIL, 2003 VALIDATION

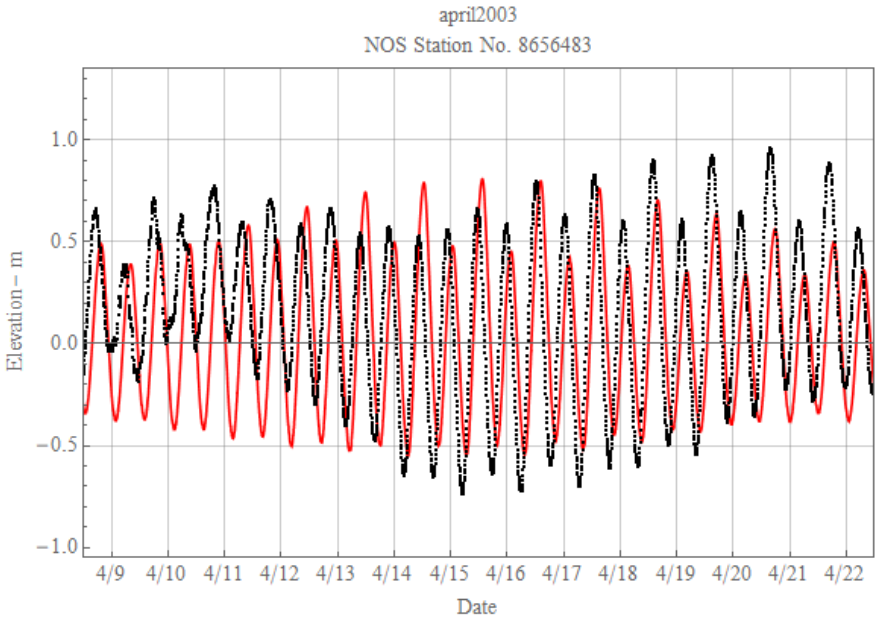

BEAUFORT

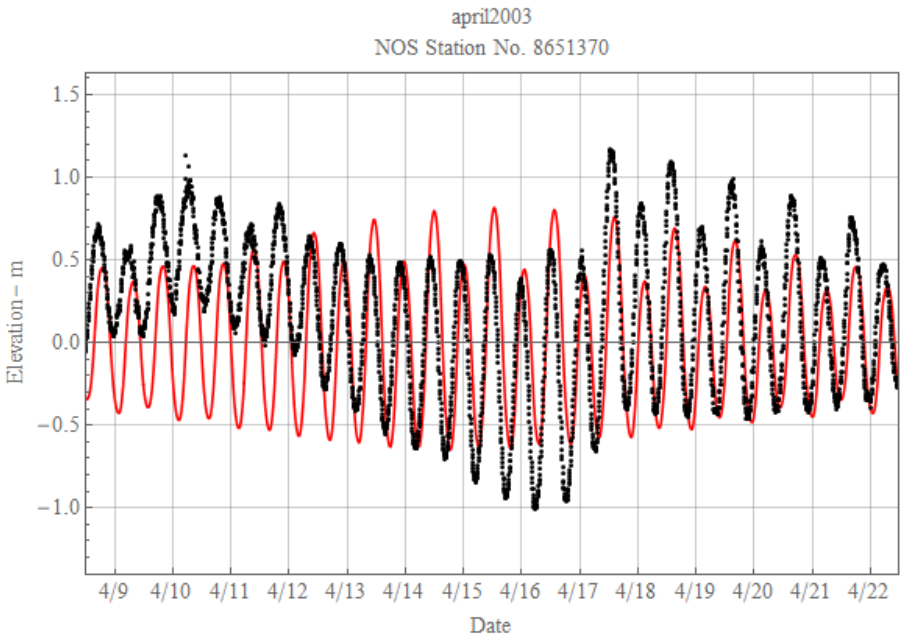

DUCK PIER

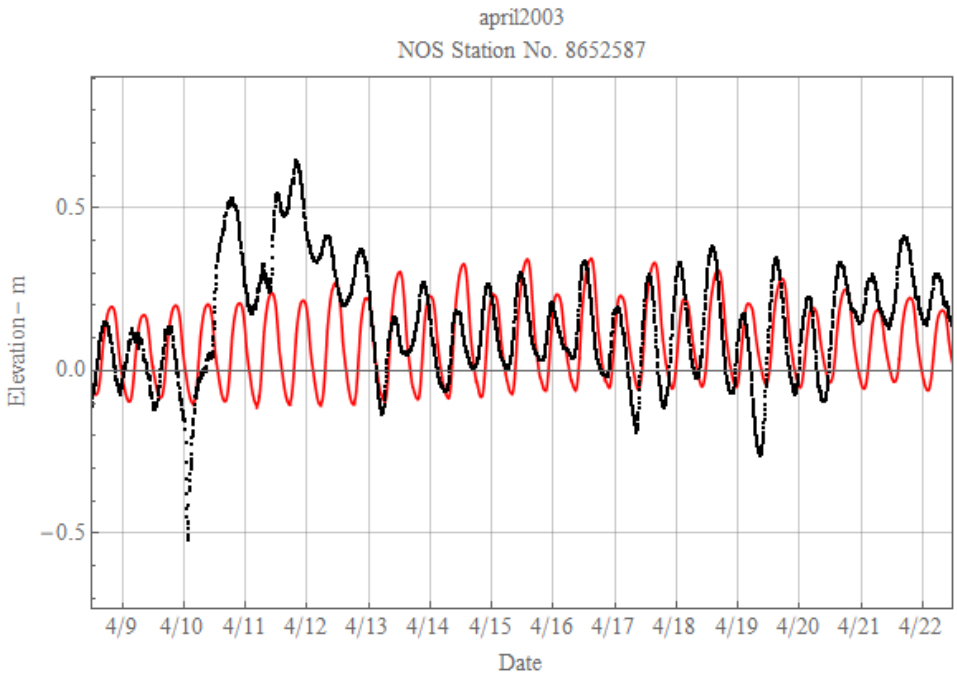

OREGON INLET

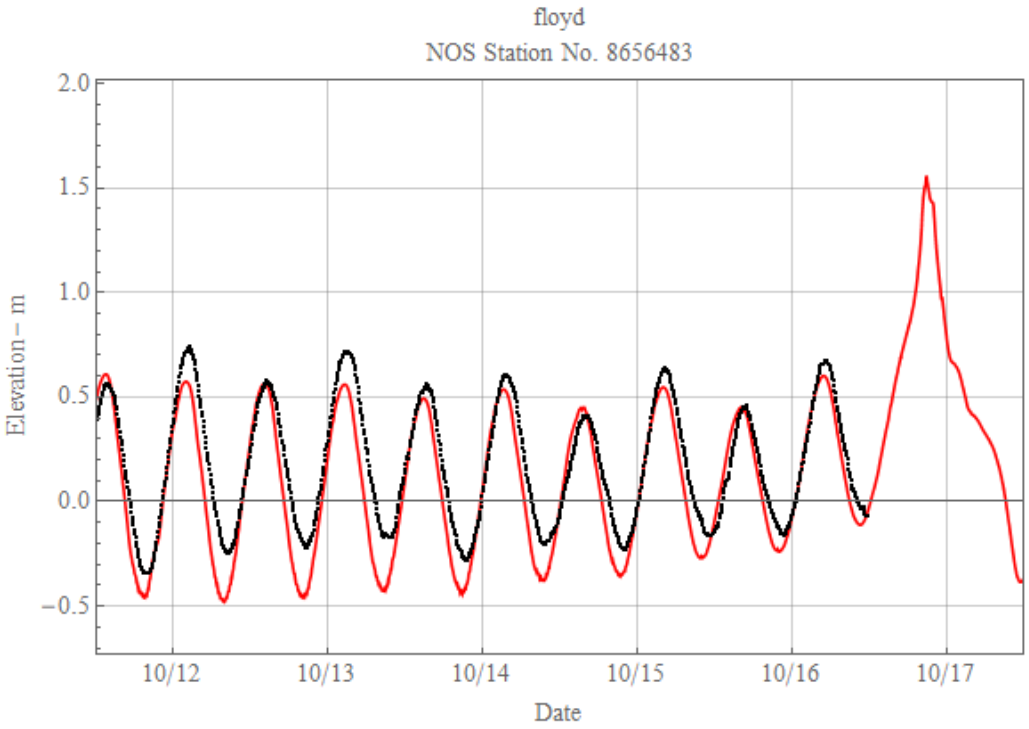

BEAUFORT

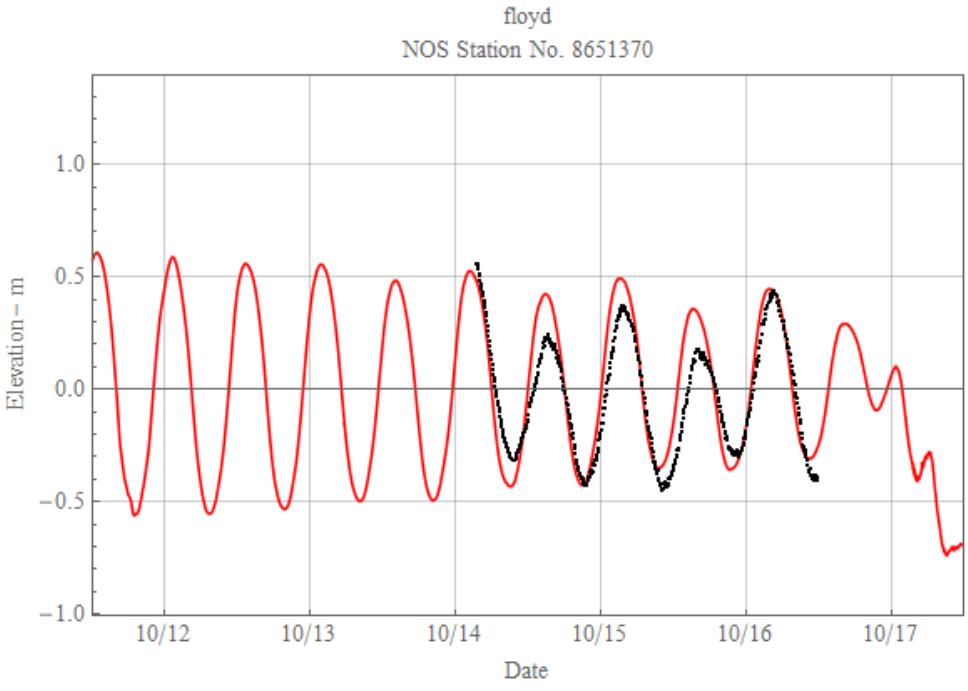

DUCK PIER

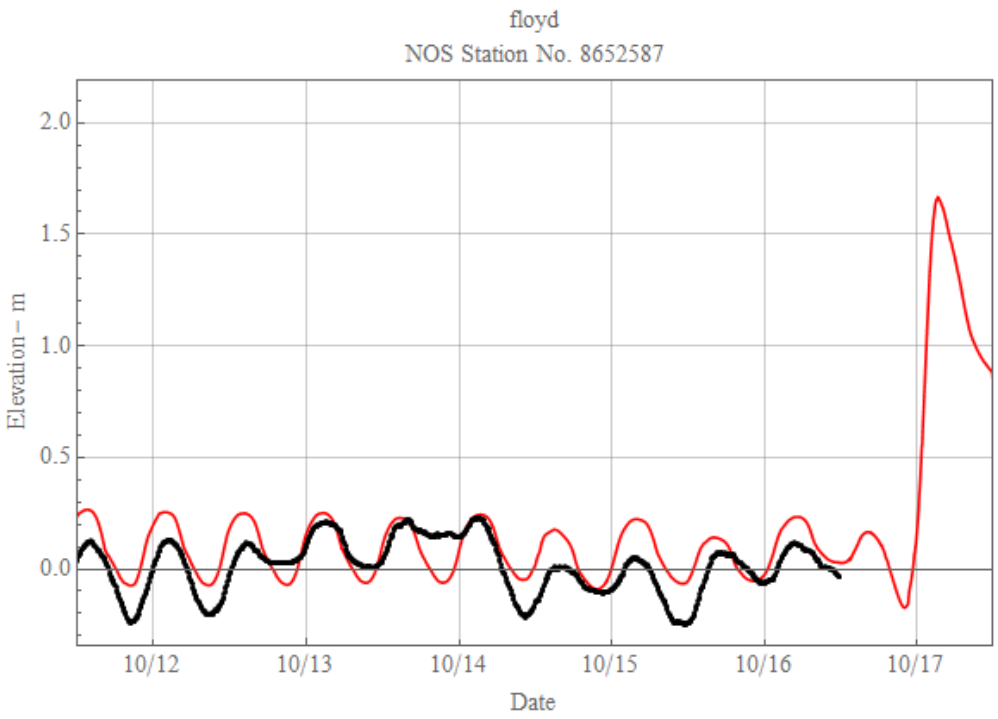

OREGON INLET

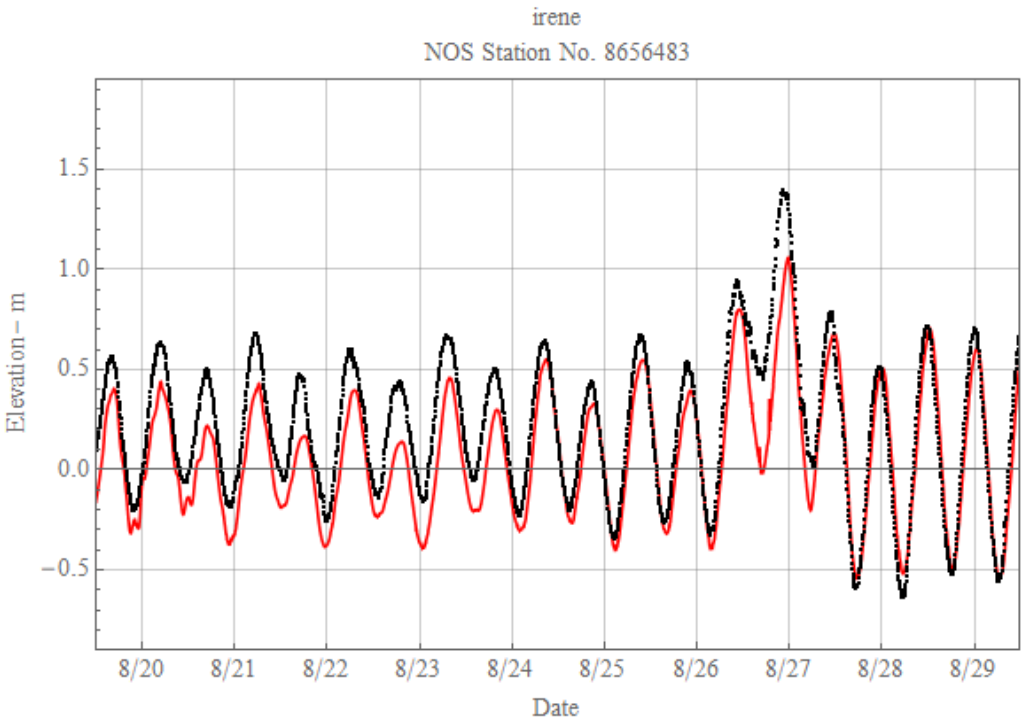

BEAUFORT

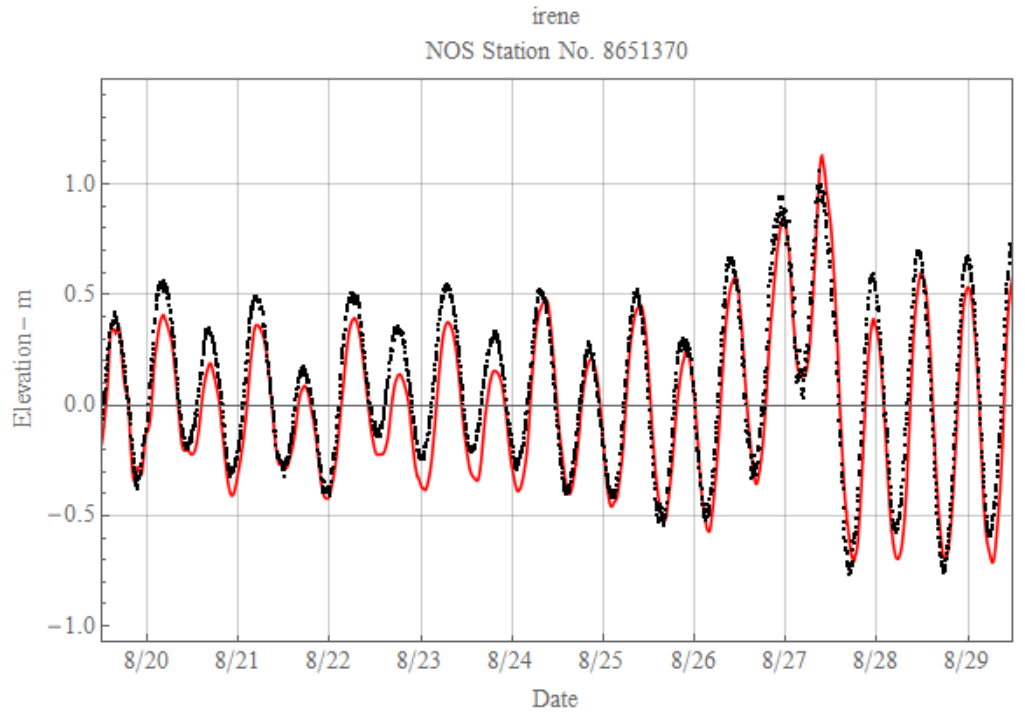

DUCK PIER

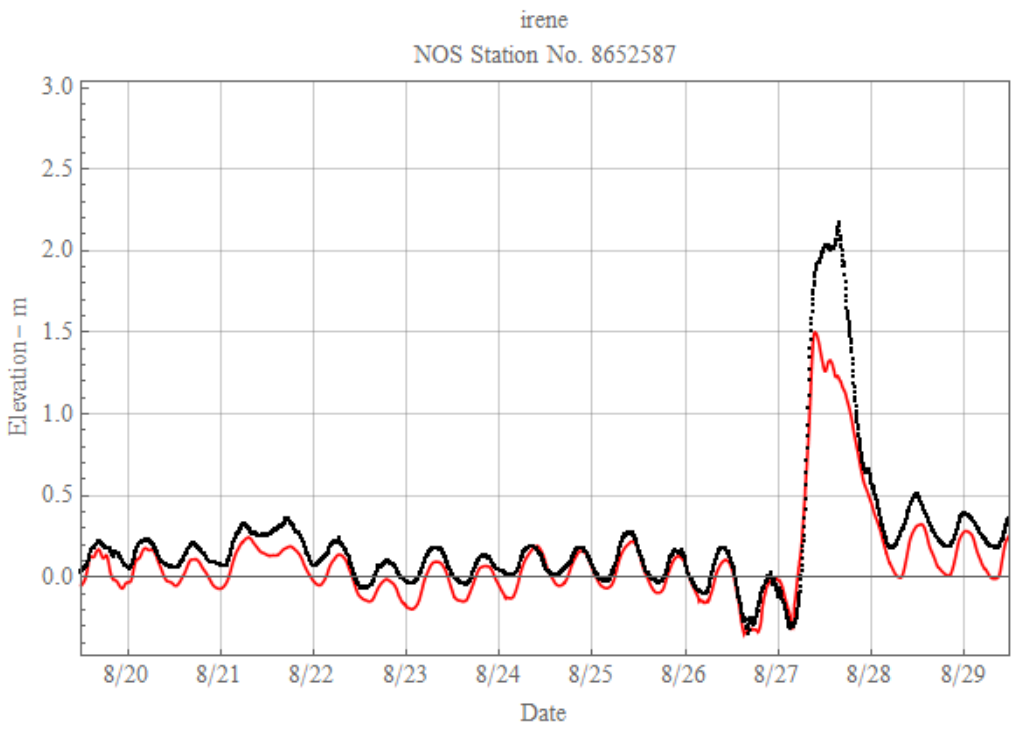

OREGON INLET

12. APPENDIX D – INUNDATION MAPPING METHODS

This thesis involves a novel ADCIRC inundation mapping technique, in which ADCIRC inundations are mapped onto a DEM using methods similar to those employed by Abshire (2012) to map HEC-RAS results. To validate this method, results from Hurricane Irene were mapped. Methods and results of each inundation method are included below. Color scales show relative depth, but the ultimate result of the mapping is the extent of the inundated domain.

INUNDATED AREA IN TARGET DOMAIN – ADCIRC NATIVE

Inundated area is an important predictive output of any flood model. ADCIRC calculates the water surface elevation at each point in the grid automatically, along with maximum water surface elevation during the course of the simulation. Because inundation below the grid's terrain elevations result in dry nodes, this result then "natively" gives an inundation extent with no further post-processing. This method preserves the model's calculated inundation depth – if the model calculated that the water surface would be 14m above terrain, the final inundation maps will reflect this. This section discusses inundation results for Hurricane Irene using this method.

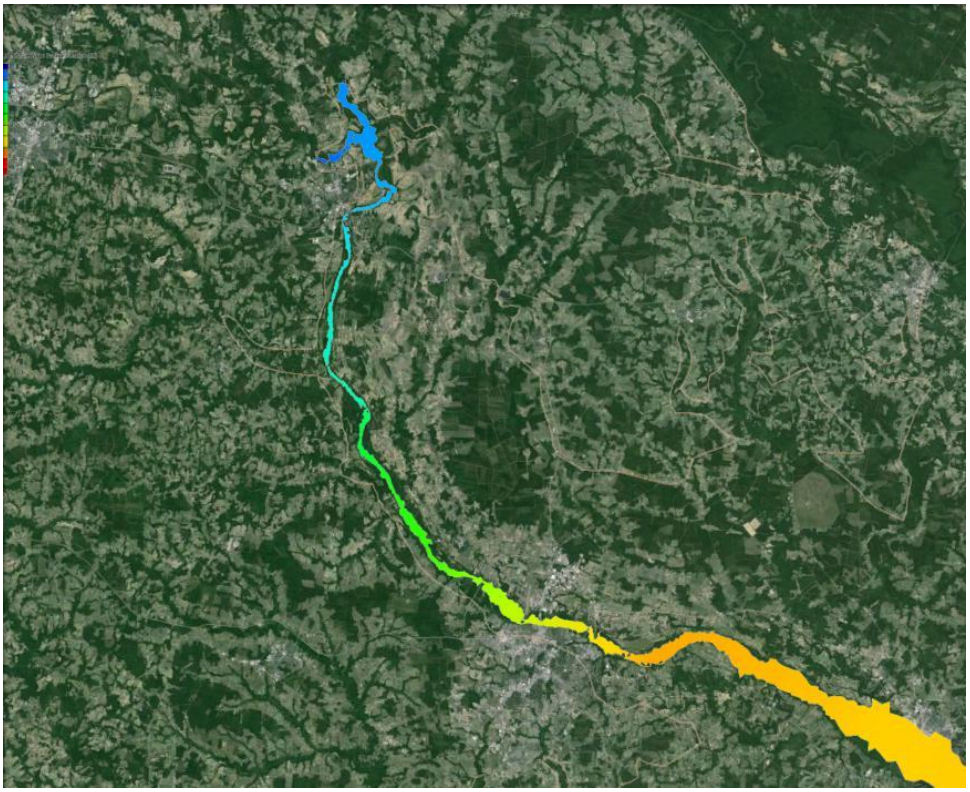

Figure D-1 - Inundation of Tar River Above Tar At Pamlico Station During Hurricane Irene

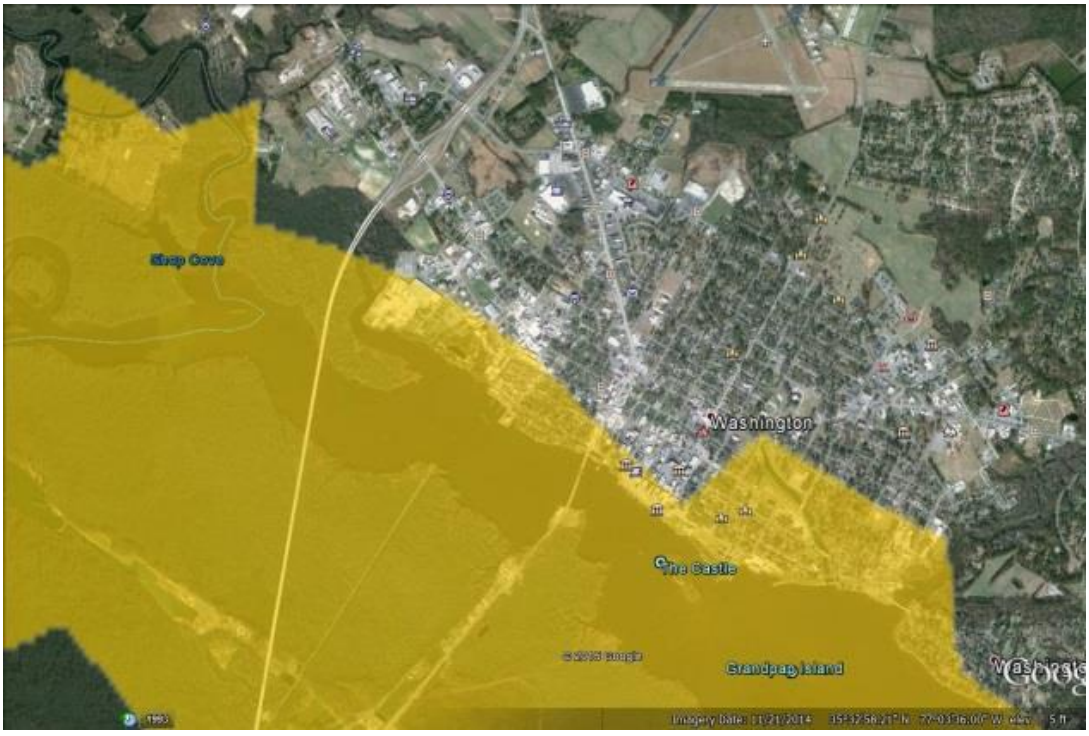

Figure D-2 - Irene Inundation at Greenville

Figure D-3 - Irene Inundation at Washington

Figure 12 shows predicted inundation for the entire comparison domain. Figure D-2 shows that inundation near Greenville, NC was predicted to be relatively mild, with possible overtopping of bridges and flooding of low-lying areas, but no significant inundation of the city center or airport indicated. Figure D-3 shows that predicted flooding in Washington, NC was predicted to be more severe, with significant inundation progressing into the city center and along multiple coastal communities in that region. This is qualitatively consistent with observed results - flooding for both areas was expected to be existent and "moderate" based on flood stage observations.

INUNDATED AREA IN HEC-RAS DOMAIN – HEC-RAS PARALLEL

Another method for calculating inundation using ADCIRC is to follow the methods recommended by HEC-GeoRAS. In that program, model results for water surface elevation at two points for each cross section are interpolated onto a convex polygon surface TIN. Then terrain elevations (taken from a 20 ft DEM obtained from the North

Carolina Flood Mapping Program (NCFMP) via the NCSU website, in this case) are subtracted from this water surface elevation TIN, giving a final inundated area. Another way to understand this visualization method is that first, the model is used to calculate a water surface profile for the river, and then that water surface elevation profile is extended to the relevant elevation contours. A detailed description of this method was cataloged by Sean Reed and Kate Abshire in (Abshire, 2012).

For this study, a similar process was followed. The primary difference is that instead of taking water surface results from HEC-RAS, the water surface elevation TIN is generated directly using ADCIRC's maxele file.

The inundated areas in the overall domain, Greenville, NC, and Washington, NC, calculated using this method are shown in Figure D-4, Figure D-5, and Figure D-6, respectively.

Figure D-4 - Inundation using GeoRAS method

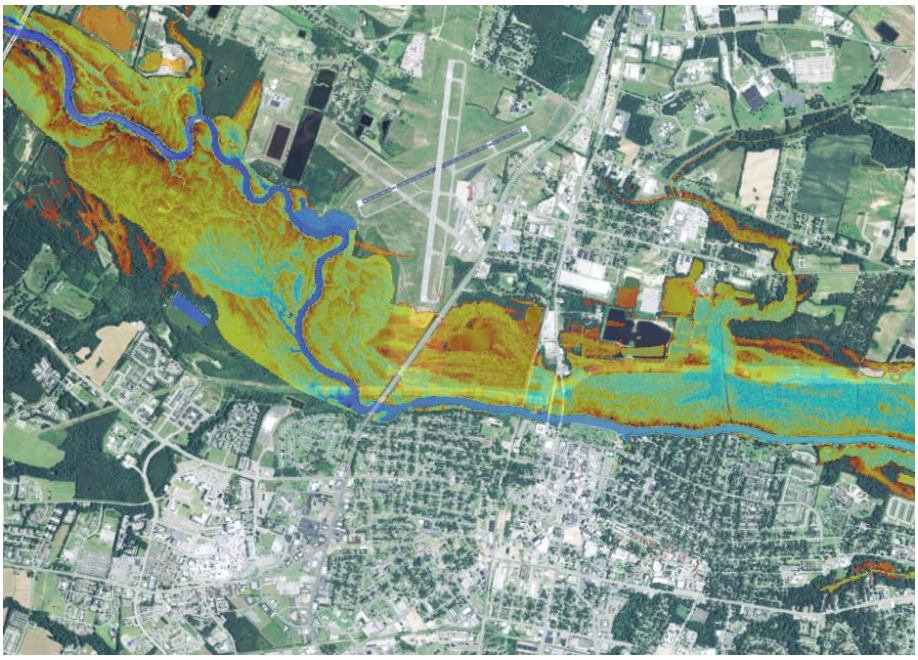

Figure D-5 - Inundation at Greenville using GeoRAS method

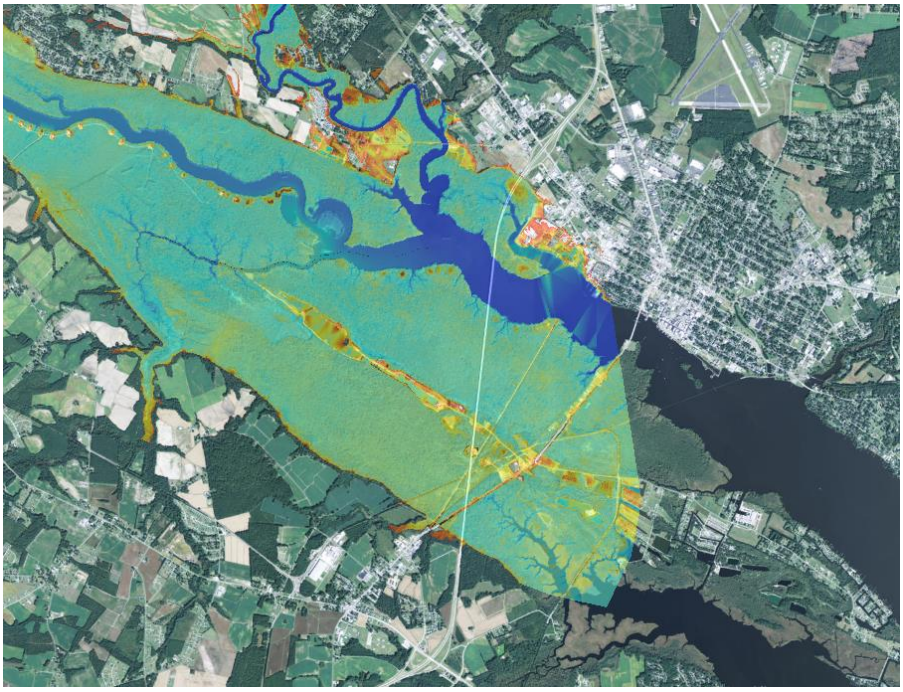

Figure D-6 - ADCIRC inundation at Washington using GeoRAS method

Qualitatively, results from this inundation method match those results found using ADCIRC's predetermined grid. For subsequent inundation maps, this method is used to provide a more direct comparison to HEC-RAS results.